A CHARACTERIZATION OF THE HUMAN G PROTEIN-COUPLED RECEPTOR, LYSOPHOSPHATIDIC ACID 1: ITS INTRACELLULAR TRAFFICKING AND SIGNALING CONSEQUENCES ON THE TUMOR SUPPRESSOR, P53

A Dissertation
Presented to
The Academic Faculty

By

Mandi Michelle Murph

In Partial Fulfillment
Of the Requirements for the Degree
Doctor of Philosophy in Biology

Georgia Institute of Technology

March 2005

A CHARACTERIZATION OF THE HUMAN G PROTEIN-COUPLED RECEPTOR, LYSOPHOSPHATIDIC ACID 1: ITS INTRACELLULAR TRAFFICKING AND SIGNALING CONSEQUENCES ON THE TUMOR SUPPRESSOR, P53

Approved by:

Harish Radhakrishna Ph.D., Advisor

Alfred H. Merrill Ph.D.

Julia Kubanek Ph. D.

Gordon B. Mills MD, Ph.D.

Nael McCarty Ph.D.

Date Approved: March 2005

ACKNOWLEDGEMENTS

Much thanks to Junken Aoki (University of Tokyo, Japan) for kindly providing an expression plasmid encoding FLAG-tagged human LPA_1, Mark McNiven (Mayo Clinic, Rochester, MN) for an expression plasmid encoding a green fluorescent protein (GFP)-tagged dynamin2 K44A mutant (Dyn-GFP2 K44A), Stephen Ferguson (Robarts Research Institute, London, Ontario) for providing expression vectors encoding GFP-Rab 5 S34N and GFP-Rab 5 Q79L, Dr. J. Silvio Gutkind (NIDCR, NIH) for the human M_2 mAChR expression vector, Gabor Tigyi (University of Tennessee, Memphis, TN) for the LPA_1 R124A expression vector and David Brindley (University of Alberta, Edmonton, CA) for the LPP-1 expression vector.

The assistance of Launa Scaccia, Victoria Newton, Giang Nguyen, Laura Volpicelli, Kelly Delaney and Lisa Brown was crucial for finishing this work. Discussions with Kymry Jones and Nikhil Urs were also helpful for completing this thesis will always be greatly appreciated.

Thanks to Julie Donaldson, Nael McCarty and members of the Radhakrishna lab for critically reading and reviewing manuscripts. Also thanks to the steering and guidance of my advisor and other committee members Harish Radhakrishna, Julia Kubanek, Alfred Merrill and Gordon Mills. Gratitude is extended to Lee and Bud Suddath and those who selected me for the Suddath award which helped facilitate my research and future immensely.

This work was supported in part through an American Heart Association Beginning Grant-in-aid 00602758, National Institutes of Health Grant HL 67134, National Institutes of Health Grant 32066AE and the Georgia Cancer Coalition Grant 32066CM.

TABLE OF CONTENTS

LIST OF FIGURES

LIST OF ABBREVIATIONS

ATX	Autotaxin
Arf	ADP-ribosylation factor
β_2AR	$_2$-adrenergic receptor
cAMP	Cyclic adenosine monophosphate
CA-125	Cancer antigen 125
DAG	1,2-diacylglycerol
DNA	Deoxyribonucleic acid
Dyn	Dynamin
EEA-1	Early endosome autoantigen-1
Edg	Endothelial differentiation gene
EGF	Epidermal growth factor
ERK	Extracellular regulated kinase
GDP	Guanosine 5' –diphosphate
GFP	Green fluorescent protein
GPCR	G protein coupled receptor
GRK	GPCR regulatory kinase
GTP	Guanine 5' –triphosphate
HA	Hemagglutinin
HeLa	Cervical cancer cells (Henrietta Lacks)
IP_3	Inositol 1,4,5-triphosphate
LDL	Low density lipoprotein
LPA	Lysophosphatidic acid (18:1; 1-oleoyl-2-hydroxy-*sn*-glycero-3-phosphate)
LPA_1, LPA_2, LPA_3	Lysophosphatidic acid receptors 1, 2, 3
LPC	Lysophosphatidylcholine
LPP-1	Lipid phosphate phosphohydrolases
mAChR	Muscarinic acetylcholine receptor

MAG	Monoacylglycerol
MAPK	Mitogen activated protein kinase
Mdm-2	Murine double-minute 2
NMS	*N*-methylscopolamine
PA	Phosphatidic acid
PBS	Phosphate-buffered saline
PC	Phosphatidylcholine
PDGF	Platelet derived growth facto
PI3-K	Phosphatidylinositol 3-kinase
PIP_2	Phosphatidylinositol 4,5-bisphosphate
PKC	Protein kinase C
PLC	Phospholipase C
PLD	Phospholipase D
PM	Plasma membrane
PPARγ	Peroxisome proliferators-activated receptor γ
PSA	Prostate-specific antigen
RNA	Ribonucleic acid
S1P	Sphingosine-1-phosphate
SRE	Serum response element
SRF	Serum response factor
USPSTF	U.S. Preventative Services Task Force
VEGF	Vascular endothelial growth factor
WT	Wild type

SUMMARY

This project was undertaken to better understand the regulation and function of the LPA_1 receptor. Two separate studies are described. In the first study, we investigated the role of LPA signaling in cell cycle regulation and its affects on the tumor suppressor, p53. In the second study we examined the internalization and trafficking of the LPA_1 receptor.

Through the binding and activation of at least four receptors, LPA_1/Edg2, LPA_2/Edg4, LPA_3/Edg7, and PPARγ, the mitogenic receptor ligand, lysophosphatidic acid (LPA), is able to enhance cancer cell growth, proliferation and motility. In the first study, we show that LPA stimulation potently inhibits the cell cycle regulator and tumor suppressor, p53. Ten μM LPA reduced the cellular levels of total p53 and p53 phosphorylated at serine 15 by approximately 50% within 1 h in A549 lung carcinoma cells and this effect was sustained for at least 6 h. This resulted in a corresponding decrease in p53-mediated transcription. Transient-transfection of the Edg-family LPA receptors, LPA_{1-3} in HepG2 hepatoma cells, which do not respond to LPA, also showed this inhibitory response. The response was specific to LPA receptors since neither G_i-coupled M_2 muscarinic acetylcholine receptors, nor a mutant LPA_1 receptor (LPA_1 R124A) which is unable to bind LPA, inhibited p53 activity. Either transient-transfection of the LPA-degrading lipid phosphate phosphatase-1 (LPP-1), or exogenous addition of phospholipase B, which decreases exogenous lysophosphatidate, reversed the LPA receptor-induced decrease in p53-mediated transcription. Although pertussis toxin did not prevent the inhibition of p53, a mutant LPA_1 receptor (LPA_1 Δ361) which lacks the C-terminal PDZ-binding domain, failed to inhibit p53 function. This establishes that, at least for LPA_1 receptors,

inhibition of p53 function requires an interaction with PDZ-containing proteins. These data establish a novel role for LPA-mediated receptor activation in diminishing p53 activity, which, in addition to LPA's well-characterized effects on growth-promoting signaling pathways, is likely to contribute to the survival and proliferation of cancer cells.

Of the Edg-family LPA receptors, the LPA_1 receptor is the most widely expressed. In the second study, we investigated the agonist-induced endocytosis of the human LPA_1 receptor, bearing an N-terminal FLAG epitope tag, in stably transfected HeLa cells. Treatment with LPA induced the rapid endocytosis of approximately 40% of surface LPA_1 within 15 minutes. Internalization was both dose dependent and LPA specific since neither lysophosphatidylcholine nor sphingosine-1-phosphate induced LPA_1 endocytosis. Removal of agonist following 30 minutes incubation resulted in recycling of LPA_1 back to the cell surface. LPA_1 internalization was strongly inhibited by dominant inhibitory mutants of both dynamin2 (K44A) and Rab5a (S34N). In addition, both dynamin2 K44A and Rab5 S34N mildly inhibited LPA_1-dependent activation of serum response factor. Finally, our results also indicate that LPA_1 exhibits basal, LPA-dependent internalization in the presence of serum-containing medium. These studies, put together, give us new insight on the function and cycle of the LPA_1 receptor in the regulation of the cell and its response to LPA.

CHAPTER 1

INTRODUCTION

Receptors

G protein-coupled receptors

Sight, smell and taste are biological sensations controlled largely by a group of proteins embedded in the plasma membrane called G protein-coupled receptors (GPCRs). Collectively, these receptors belong to a superfamily of seven-pass transmembrane proteins that respond to many different agonists such as odorants, photons, hormones, lipids, ions, amines, peptides, proteins and pheromones. Plants, yeast, insects and all eukaryotes have GPCRs and with over 1,000 members in the family, GPCRs are distinguished as the largest class of cell surface molecules in the human genome (80). These important receptors have a myriad of responsibilities in the cell including embryonic development, detecting mating pheromones, nutrient uptake, regulation of cellular homeostasis and the aforementioned sensory perception.

The serpentine-like structure of a membrane-embedded GPCR is connected by three extracellular loops, three intracellular loops and a disulfide link (Fig. 1). Depending on the receptor, conserved sequences in the second intracellular loop domain can determine GPCR internalization, ligand binding affinity, G protein coupling and receptor stability (57). Usually the critical signaling determinants of a GPCR exist within the third intracellular loop, but the amino acids located in the carboxyl-terminal tail are important in targeting and signaling as well. Peripheral ligands usually dock in an extracellular binding site, although this site can also be buried within the transmembrane regions.

Until the ligand binds to its GPCR, the receptor maintains an inactive conformation.

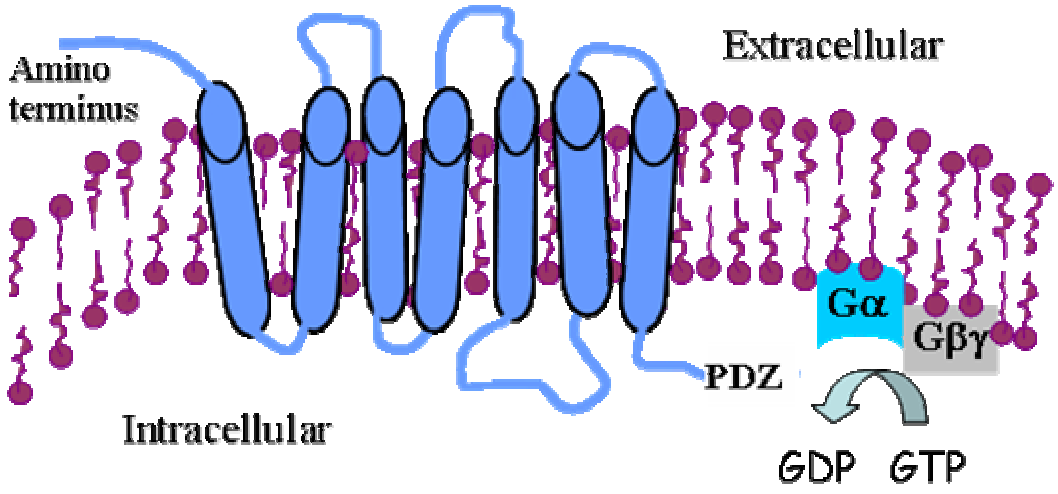

Fig. 1. A GPCR embedded in the plasma membrane. Included are the locations of the extracellular amino terminus and intracellular carboxyl terminus with the PDZ binding domain. Close by are the heterotrimeric G protein subunits α and βγ.

However, once an agonist does bind, the GPCR undergoes a conformational change, which in turn activates the receptor. The receptor is closely positioned in the membrane next to heterotrimeric G proteins composed of α and βγ subunits and the structural change allows the α subunit to couple to the GPCR. After they join together, the α subunit can exchange its GDP for GTP, thereby activating and allowing α to dissociate from its βγ partner. The α subunit is then capable of associating with other molecules, like enzymes, protein scaffolds or ion channels causing an unleashing of signaling cascades throughout the cell.

More specifically, these cascades create fluctuations in intracellular signaling from second messengers and the α subunit is primarily responsible for activating these influential molecules. For example, the G protein α subclass, G_s, causes an increase in adenylyl cyclase activity and calcium channel activity, but a decrease in sodium channel activity which can change membrane potential. In contrast, G_i activation results in a

decrease in adenylyl cyclase activity and calcium, but an increase in potassium. The activation of other G proteins, like G_q, generates second messengers by causing phospholipase C (PLC) to cleave phosphatidylinositol 4,5-bisphosphate (PIP_2) into the second messengers inositol 1,4,5-trisphosphate (IP_3) and 1,2-diacylglycerol (DAG).

Second messengers are crucial to intracellular signaling because they allow the cell to rapidly amplify a signal from an activated GPCR. These molecules can also activate protein kinases which will further transduce the original signal. An illustration of this process can be seen in the previously mentioned G_q signaling pathway whereby IP_3 binds to calcium-permeable channels on the endoplasmic reticulum membrane, which respond by opening and allowing calcium to flow into the cytoplasm. Additional proteins become activated in response to calcium, such as protein kinase C (PKC), which can phosphorylate the original signal-inducer GPCR to terminate signaling. Thus, ligand binding and GPCR activation has a variety of signaling consequences.

In order to help regulate GPCR-mediated signaling, several mechanisms (rapid receptor phosphorylation or receptor endocytosis) have been established to physically terminate the response (57). In this way, prolonged agonist exposure can culminate with either GPCR desensitization or receptor down-regulation. At a future point signal resensitization will again occur and the endocytosed receptors will then be recycled or resynthesized and sent back to the surface to receive new agonist. Through these mechanisms the cell is able to regulate the activity of a GPCR, thereby controlling cellular signaling.

If after extended signaling receptor desensitization is necessary, GPCR regulatory kinases (GRKs) can phosphorylate intracellular residues on the GPCR to induce its

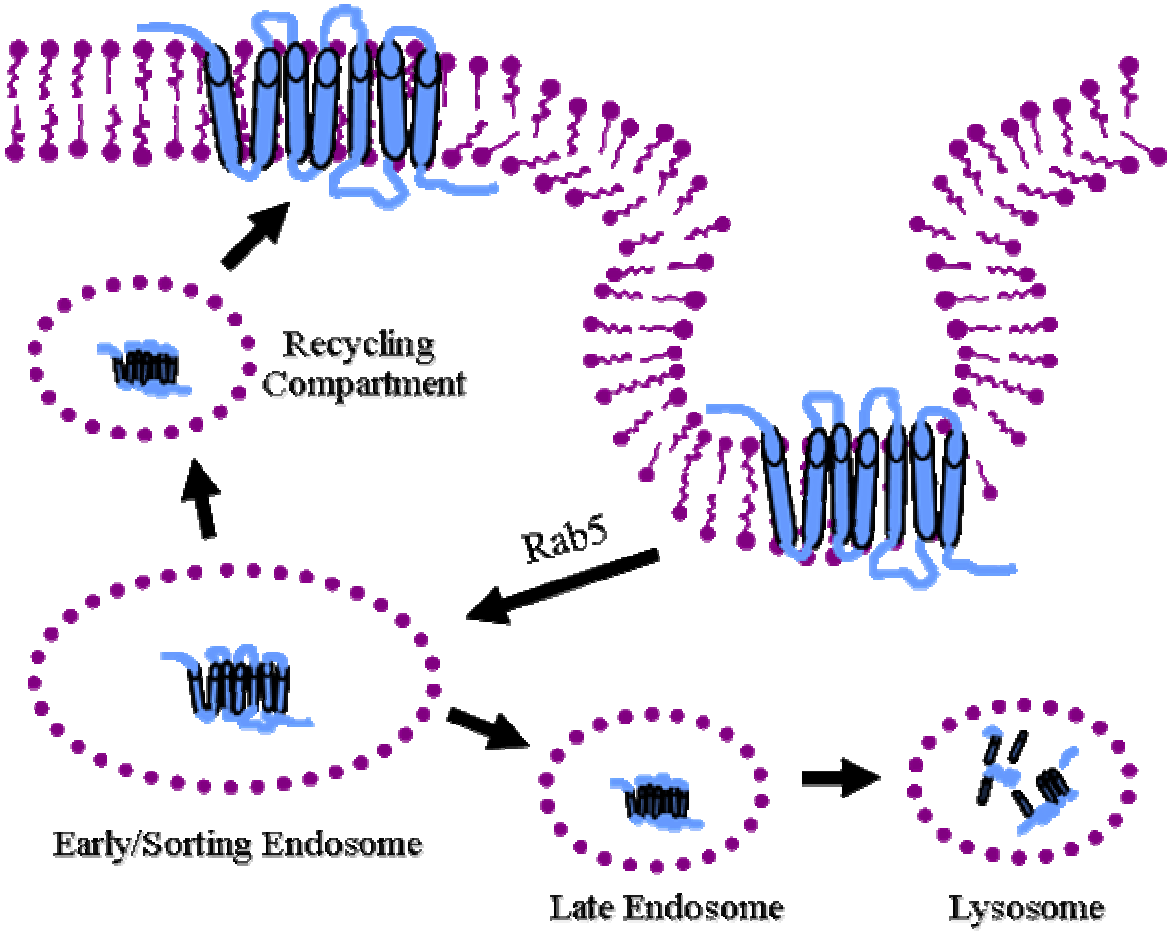

Fig. 2. Schematic of GPCR endocytosis and trafficking through the cell. Internalization begins with plasma membrane invagination and subsequent targeting to the early endosome by Rab5. From this endosome, the GPCR can either be sent to the late endosome and lysosome for degradation or it can be recycled back to the membrane.

functional desensitization. Arrestin proteins are then capable of binding specifically to these phosphorylated GPCR amino acid residues on the intracellular loops of the receptor. Arrestin binding will also physically disrupt the interaction between the receptor and its G proteins, preventing further signaling. As previously mentioned, PKC is also capable of phosphorylating the GPCR to initiate desensitization.

Another option to the cell after continual ligand stimulation of the GPCR is to degrade it in a process called downregulation. After GPCR activation, endocytosis occurs whereby, in one method, the plasma membrane invaginates and the protein dynamin pinches off and releases the clathrin-coated vesicle from the membrane (124). Once the vesicle is formed, the sequestered receptor is internalized for trafficking inside the cell with assistance from Rab proteins, V-snares, T-snares and other proteins. The first stop for the newly-formed vesicle is the early or sorting endosome where its escort, Rab5, has taken it (Fig. 2). From there the internalized GPCR can either be sent to a recycling endosome which will traffic it back to the plasma membrane or the GPCR is targeted to the lysosome for degradation (à la downregulation). Proteins that bind to sequences in the carboxyl-terminal tail of a GPCR (such as the GPCR-associated sorting protein or GASP) are thought to be responsible for the sorting process that ultimately decides a receptor's fate (220). Another factor that determines whether or not the receptor will be degraded is the amount of ubiquitin it has attached to it. Components called E3 ligases covalently attach ubiquitin molecules onto a protein. Once the protein has accumulated extensive ubiquitin attachments it will be targeted for degradation; however, the receptor may be degraded in either the proteasome or the lysosome (120, 186). In order for the cell to

begin receiving this response again, it must recycle internalized GPCRs and start resynthesizing a new pool of receptors.

Before publishing the study, *Agonist-induced endocytosis of lysophosphatidic acid-coupled LPA1/EDG-2 receptors via a dynamin2- and Rab5-dependent pathway* in 2003, nothing was known about the trafficking or intracellular destinations of any LPA-coupled receptor. To gain further insight into how cells regulate the activity of specific LPA receptors, we investigated the agonist-induced trafficking of the human LPA_1 receptor in HeLa cells. Our results indicated that LPA_1 is rapidly internalized into cells via dynamin2- and Rab5-dependent mechanisms in an LPA-specific and LPA dose-dependent manner and will be further presented in this thesis (Chapters 6-9).

GPCR PDZ domains

The phrase "G protein-coupled receptor" insinuates the sole interaction for a GPCR is the G protein it couples to at the membrane. To the contrary, receptors are unfaithful to any single partner and some GPCRs will also couple with PDZ domain-containing proteins (17). PDZ domains are approximately 80 to 90 amino acid residues of a protein folded together that contain repeated PDZ-binding residues. These proteins recognize and bind motifs containing 3 to 5 amino acid consensus sequences in the carboxyl-terminal of either a GPCR (Fig. 1) or an ion channel. The PDZ peptide-motif that is contained in GPCR tails is recognized with high specificity by PDZ-containing cellular proteins (92). The name "PDZ" comes from the first three proteins discovered that were involved in these interactions: PSD-95, DLG and ZO-1. Some examples of GPCRs with PDZ-binding domains are the β-adrenergic receptor and platelet-derived growth factor receptor (42, 78). These terminal PDZ motifs are important for protein binding and scaffold

formation; thus, the interaction provides a link between transmembrane receptors and assembly complexes which can mediate signal transduction.

The carboxyl-terminal tails of both LPA_1 and LPA_2 receptors contain a consensus PDZ docking motif (X-(S/T)-X-(V/L)). The PDZ consensus binding sequence often requires a terminal hydrophobic residue like Val or Leu, while the second and third PDZ residues indicate specificity. The terminal peptide sequence of LPA_1 is: DHSVV and the terminal sequence for LPA_2 is: DSTL. Recently it was shown that the Na+/H+ exchanger-regulating factor 2 (NHERF2) contains PDZ domains that interact with LPA_2 (along with the motifs DSLL, DSFL and DTRL present in other GPCRs), but not LPA_1 or LPA_3 (31, 141). In another report, the carboxyl terminal tail of LPA_2 was also shown to bind a focal adhesion molecule, TRIP6 (225), which again was unique to that LPA receptor. An exclusive protein that binds to the tail of only one LPA receptor is not surprising considering the identity between cytoplasmic tails of LPA_1 and LPA_2 is 27% and between LPA_2 and LPA_3 is only 17% (225). To date there has not yet been a report demonstrating any PDZ-binding interaction between a specific cellular protein and the LPA_1 receptor.

Target: GPCRs

Since they are fundamental to the regulation of many diverse cellular processes, promising pharmacological targets have always included GPCRs. In the year 2000, 26 of the top 100 pharmacological drugs targeted a GPCR and 39 affected at least one part of a mechanism mediated by a GPCR (15). In 2003, it was reported that approximately 50% of all prescribed drugs were targeting a GPCR (107).

Drugs that are directed at these receptors include the widely used pain relievers. Although its natural ligands are endorphins, the μ opioid receptor will also bind morphine and heroin. Having a similar molecular structure, the analgesic hydrocodone also binds to the μ opioid receptor and is one of the most widely prescribed drugs in the U.S. The desensitization of this receptor to its pain-relieving ligands is why a persistent increase in medicinal dosage is required for a consistent feeling of well-being or "tolerance," in more general terms (60) (recall GPCR desensitization and receptor down-regulation).

Because of their continued successes as drug targets and the driving ambition of pharmaceutical companies to quickly produce a marketable drug, GPCRs will likely remain a top research priority for the industry. High-throughput assays are making the task of screening potential GPCR antagonists more effective which allows the research to proliferate. Name-brand drugs like Schering-Plough's Clarinex and GlaxoSmithKline's Zantac are competitive antagonists that block the histamine H_1 receptor. Eli Lilly's Zyprexa and Novartis's Zelnorm both inhibit the serotonin receptor. (60) Angiotensin receptors have also been targets for many years because of their association with diabetes, hypertension, cardiac hypertrophy and other afflictions.

Lysophosphatidic acid (LPA) receptors and LPA

LPA receptors

Extracellular lysophosphatidic acid (LPA) is presented to the cell bound to serum albumin (201) where its diverse actions are mediated through GPCRs. To date there are at least five LPA receptors, including the original three endothelial differentiation gene

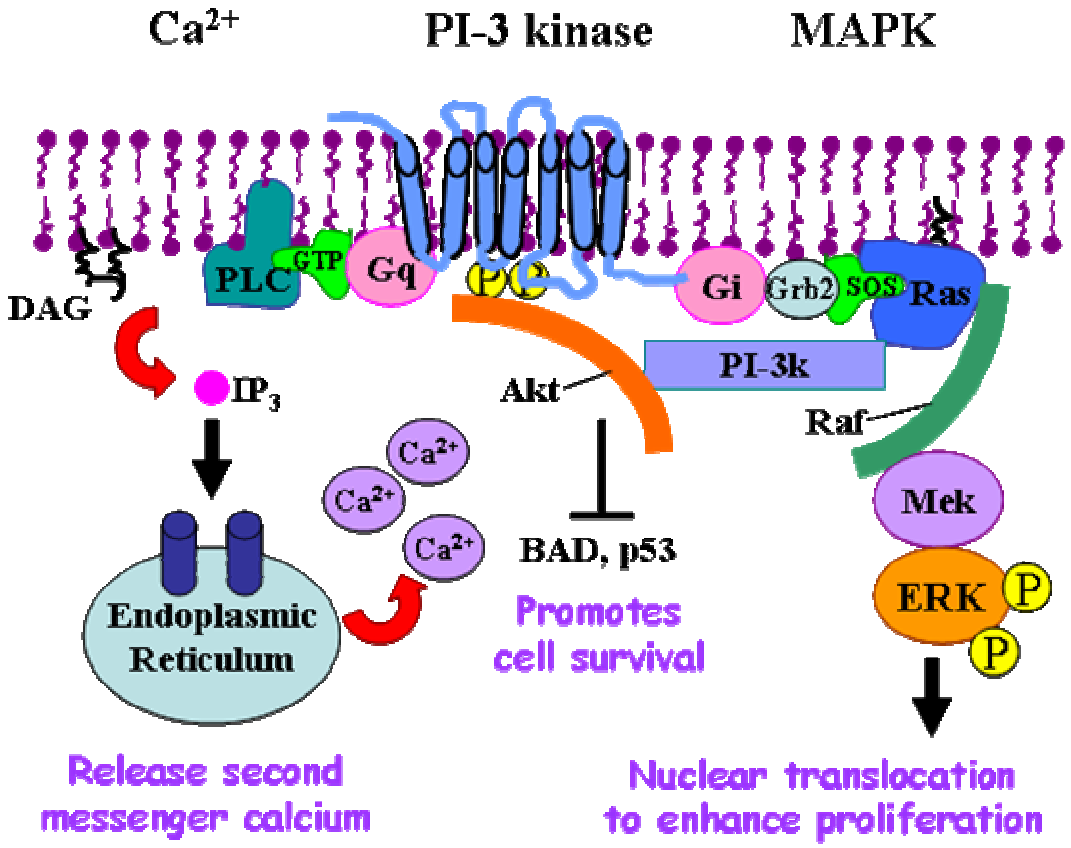

Fig. 3. GPCR signaling through G_i and G_q pathways. The leftmost signaling cascade begins with G_q activation of PLC, which cleaves PIP_2 into DAG and IP_3. This signaling pathway ultimately leads to an increase in calcium and activation of PKC via DAG. The G_i protein is shown signaling through Akt (center) to enhance cell survival. In this pathway, Ras activates PI-3 kinase which causes Akt to become phosphorylated by kinases embedded in the membrane (not on the GPCR). Akt inhibits apoptosis-promoting proteins like BAD. On the far right the MAPK pathway is activated by G_i to induce the MAPK signaling pathway components Ras, Raf, Mek and Erk which will cause an increase in cell proliferation and survival.

(Edg) family GPCRs having high amino acid sequence similarities, that reportedly bind LPA: LPA_1/Edg2, LPA_2/Edg4, LPA_3/Edg7, LPA_4/GPR23 (tentatively) and the metabolic, nuclear hormone transcription factor receptor, PPAR-γ, expressed mainly in adipocytes to control energy homeostasis (4, 7, 11, 122, 138). The G alpha proteins that couple to LPA receptors are G_i (LPA_1, LPA_2) (65), G_q (LPA_1, LPA_3), $G_{12/13}$ (LPA_1, LPA_2) and G_s (LPA_4) (138, 153).

Before describing each LPA receptor individually, it is important to understand their signaling abilities collectively since many cell types express multiple receptors. Together the Edg-family LPA receptors, LPA_1, LPA_2 and LPA_3, are capable of activating G_i, G_q and $G_{12/13}$ (65, 138, 153). As previously mentioned, LPA stimulation of G_q induces PLC activation which causes a rise in the second messengers IP_3, DAG and calcium. The response after stimulation of $G_{12/13}$ leads to an activation of Rho and stress fiber formation in the cell which is involved in cell migration. The responses to G_i include an inhibition of adenylyl cyclase, an activation of the phosphatidylinositol 3-kinase (PI-3K)-Akt cell survival pathway and an activation of the MAPK pathway (Fig. 3) (44). The latter pathway is used by the cell to signal migration, proliferation, differentiation, survival, and apoptosis and not surprisingly includes proto-oncogenes, like the highly oncogenic member Ras. The components that activate MAPK involves the G protein Ras and three kinases: Raf (MAPK kinase kinase), MEK 1/2 (MAPK kinase) and ERK 1/2 (MAPK) as the business end of the pathway which can translocate into the nucleus and phosphorylate over 50 substrates, including transcription factors. (102)

The human Edg2 protein, now referred to exclusively as LPA_1, was the first LPA receptor cloned from a human lung cDNA library in 1997 after the tedious task of

screening half a million colonies to generate a few positive clones (5). Prior to its discovery, it was hypothesized that LPA was acting through a GPCR, but later studies would suggest multiple GPCRs existed to mediate LPA-induced signals. Once the newcomer LPA_1 was cloned, a search through the 1996 Genbank database yielded a 60% sequence similarity to human Edg1 (now called SIP1), although at the time this was considered an orphan receptor since its ligand, sphingosine 1-phosphate, had not been positively associated with SIP_1/Edg1 yet (5).

Multiple studies, both current and years older, point to LPA_1 as the causative-signaler amid the LPA receptors for various affects: physiological cell migration, pathophysiological motility, activation by ascites in cancer, enhancement of metastatic potential and cell adhesion to collagen (81, 187, 232). LPA_1 is endogenously expressed in most cell types in the body, stimulates the closure of epithelial cells involved in wound healing (109) and is involved in the embryonic development of neurons (66). LPA_1 has a disease link to pathophysiological processes like ovarian cancer, but is not the only LPA receptor that seems to be a contributing factor.

The second LPA receptor identified, LPA_2, contributes to cancer metastasis because by itself it enhances cell proliferation and the secretion of angiogenic factors (187). Although LPA_2 has a 72% amino acid sequence identity to LPA_1 (4), the phenotypic differences between these two receptors are still emerging. One of the first studies on LPA_1 and LPA_2 receptors pointed out their ability to transduce calcium signaling differently (LPA_2 uses G_i alone while LPA_1 uses G_i and G_q (6)). The expression patterns vary markedly between the two receptors. While LPA_1 is endogenously expressed in most cell types, with the exception of liver cells, LPA_2 is the only LPA receptor represented in

certain breast, colorectal, ovary and lung cancer cells (81). More notably, LPA_2 is overexpressed in between 15-30% of ovarian cancers (54). The tail of LPA_2 is also enigmatic because the length and amino acid sequence differ between receptors from cell type to cell type. Nevertheless, of the LPA receptors, only the LPA_2 tail has demonstrated protein binding (previously mentioned in the PDZ-domain section).

The LPA_3 receptor was cloned in 1999 and has a sequence similarity to both LPA_1 and LPA_2 of approximately 50% (11). An interesting difference between LPA_3 and LPA_2 is the lack of LPA_3 signaling to MAPK by LPA (11) and this receptor does not couple to $G_{12/13}$. The expression pattern of LPA_3 is not nearly as ubiquitous as LPA_1 or LPA_2, but it can abundantly appear in prostate and ovarian cancer cells (81), has been reported in kidney (142) and to a lesser extent in pancreatic cancer cells (232). Conspicuously, LPA_3 is overexpressed in between 44-49% of ovarian cancers (67).

A 'de-orphaning project' resulted in the 2003 discovery of LPA_4, a G protein-coupled receptor that tentatively binds LPA. This receptor was previously referred to as p2y9/GPR23 and is closely related to the orphan receptor p2y5 and nucleotide receptors p2y1, p2y4 and p2y6 (138). A broad RT-PCR analysis demonstrated that LPA_4 only appears in a few select cell lines, including glioblastoma and melanoma cells (81). The LPA research community has not yet embraced LPA_4 as a bona-fide LPA receptor because they have not been able to independently substantiate the original claim that LPA_4 binds LPA and transduces LPA-mediated signals, even when provided with the original cell-line and plasmid constructs. To date there has not been a publication from an independent lab verifying the original results about LPA_4. Recently, LPA was referred to as a "putative agonist of the GPR23 [receptor]" and the authors curiously neglected to use

the designation LPA_4 when discussing it (44). Further research demonstrating the efficacy of p2y9/GPR23 as a legitimate LPA-receptor is needed before future endeavors evaluating LPA_4 are undertaken.

Also in early 2003, a previously recognized internal lipid receptor belonging to a larger group of nuclear hormone receptors was identified as capable of binding LPA (122). The peroxisome proliferators-activated receptor γ (PPARγ) is a nuclear transcription factor receptor that regulates genes which control energy metabolism (9). Several lipid ligands can activate PPARγ, but unlike LPA, these are all low-affinity ligands and prior to its relationship with LPA, it was presumed that the authentic ligand had not yet emerged (122). Unlike the controversy surrounding LPA_4, the claims of its status as an LPA receptor have been duplicated and substantiated by several independent labs in the past year and a half. In this way, PPARγ has been shown to be both necessary and sufficient for the formation and accumulation of cells within arterial walls through mildly oxidized low density lipoprotein (LDL) (236) and will be discussed in further detail during the disease section of this introduction.

LPA Abundance

The ligand for the aforementioned LPA receptors is LPA: a mitogenic, albumin-bound, lipid component of serum that elicits a wide range of effects on the cell including proliferation, migration, morphological changes, neointima formation and cell survival (43, 45, 56, 66, 74, 95, 113, 158, 218, 236). It is simple and unique from other lysophospholipids because it lacks a head group attached to its phosphate moiety, such as the choline head group in lysophosphatidylcholine (193). LPA in human serum is produced and secreted by activated platelets in response to either coagulation or wound

healing and as such is a normal serum component (109, 197, 227). LPA can also be produced by fibroblasts, adipocytes, ovarian cancer cells and prostate cancer cells (206). Extracellular lipoprotein oxidation of LDL can also produce LPA (190).

LPA has been dubbed both an "extracellular mediator and intracellular messenger"(75) because a distinct source of LPA exists in the cellular cytosol which is produced from the phospholipid biosynthesis of phosphatidic acid (PA) (203, 230). A debate in the field exists surrounding whether the plasma membrane separates charged LPA from metabolic LPA or how and whether this lipid manages to cross the membrane bilayer. Fueling this quandary is a series of reports suggesting LPA binds to and activates intracellular receptors. Notably, the previously discussed receptor PPAR-γ is located exclusively inside the cell and binds LPA with high-affinity (122). Reports have suggested that the nuclear membrane contains functional LPA_1 receptors (71, 134), but supportive work is needed before this is widely accepted.

Nevertheless, LPA can be manufactured starting with PA and vice versa, it also functions intracellularly as a precursor to the formation and production of PA and more-complex lipids (129). In this intricate loop of lipid biosynthesis with PA, LPA is able to regulate membrane curvature and the formation of caveoli (104, 178, 206). Under normal conditions, the highest concentration of LPA found in rat tissue is in the brain (40) and this concentration increases following brain injury (200) just as the concentration will likewise increase on a much smaller scale during the body's normal wound healing processes.

The amount of LPA found in the plasma of healthy volunteers is around 1 μM, while the amount in serum from the same group ranged from approximately 0.1-10 μM (10). A

different study suggested LPA is present in serum at concentrations ranging between 2-20 μM (49). Plasma concentrations of LPA are being investigated as a potential biomarker for ovarian cancer with one study reporting levels elevated more than 30 units in 29 of 35 cancer patients (53, 197). Similar studies have indicated that the amount of LPA found in the ascites of ovarian cancer patients can reach up to 80 μM (53, 199).

A Matter of Life or Death

Cells depend on extracellular signaling factors to maintain homeostasis and prevent apoptosis. Multiple sources indicate LPA is a genuine protective factor, although the explanation as to how it affects survival varies widely. Several examples from reports illustrate a wide diversity among the cell types affected. In rat mesangial cells, 30 μM LPA was able to increase survival after concurrent treatment with PDGF (95). In T-cells, LPA concentrations at and below 1 μM decreased the apoptosis-promoting protein Bax (74). Renal proximal tubular cells remained viable and confluent after 10 days when grown in serum-free media supplemented only with 12 μM LPA (113). The intestinal epithelial cells of mice treated orally with 1 mM/L LPA 2 hr after radiation showed fewer apoptotic cells than untreated controls (43). Finally, in HEY ovarian cancer cells, LPA decreased the killing ability of an effective chemotherapeutic agent (63).

For LPA to induce cell survival, it was first suggested this effect was mediated through a PI-3K-independent, G_i–dependent activation of MAPK (56). In contrast, it has also been proposed that LPA acts through a PI3K-dependent pathway since both survival and proliferation were blocked by wortmannin or LY-294002, drugs which inhibits this

pathway (113). Another study proposed that both G_i and PI3K were fundamental to LPA-induced Schwann cell survival (218).

The list continues with more explanations of how LPA increases cell survival. A study involving intestinal epithelial cells proposed that LPA actually inhibits the apoptotic mitochondrial pathway (45). Interestingly, a recent report suggested that LPA-mediated survival was not dependent on transactivation of either EGF, ErbB2 or PDGF receptors (44), implying that activated LPA receptors are directly mediating survival signals. The complete list for how LPA mediates survival is exhausting. It might be that LPA has many different pathways to influence cell survival and perhaps these events differ among cell lines.

Extracellular environment of LPA

If the regulation of cell survival does ultimately depend on the activation of LPA receptors, then understanding the regulation of extracellular LPA levels is essential.

LPA is produced externally from lysophosphatidylcholine (LPC), a component of lipoprotein particles found in human plasma and circulation at relatively abundant levels exceeding 100 μM (206). The precursor to LPC, phosphatidylcholine (PC), is also found at high levels of approximately 1 mM (206). Therefore, the progenitor ingredients to manufacture LPA are copious in the external medium.

The generation of extracellular LPA is catalyzed from LPC by the enzyme autotaxin (ATX) (Fig. 4), a transmembrane, ecto-nucleotide pyrophosphatase/phosphodiesterase, formerly known in relation to LPA only as lysophospholipase D (lysoPLD) (203, 205). ATX was identified in 1992 from melanoma cells as a tumor motility-stimulating protein that induced both random and directed cell migration (196). Until a few years ago, it was

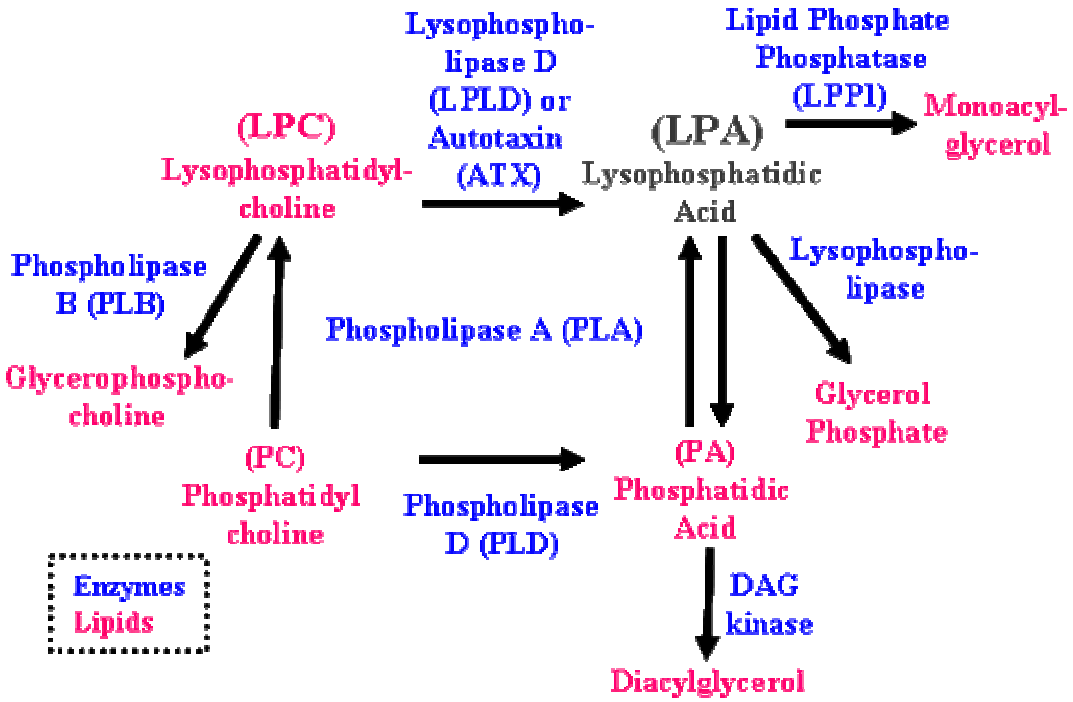

Fig. 4. The metabolic pathway of LPA. This diagram shows a complex network linking LPA to a variety of lipids (pink) and enzymes (blue) both intracellularly and extracellularly. LPA is positioned at the top right of the diagram. Intracellularly, both PLA1 and PLA2 can hydrolyze PA (at different sites) to give LPA. Alternatively, ATX can remove the choline headgroup from LPC for LPA production extracellularly. LPC can also be hydrolyzed to form glycerophosphocholine by the actions of PLB.

thought that lysoPLD and ATX were two different, unrelated enzymes. Then in 2002 it was discovered that lysoPLD, an obscure enzyme catalyzing the production of LPA, was actually identical to the better-known ATX (203, 205). Research since then has shown ATX is strikingly elevated in a number of cancer cell types, including kidney, prostate, ovary, lung and hepatocyte tissues (195, 196, 205, 234).

Many cancer cell lines are capable of releasing large amounts of LPC into the culture medium (237); furthermore, hepatocyte cells in particular are known for their ability to synthesize abundant PC (212). Using these cells as an example, the presence of both ATX and LPA-precursors in hepatocyte-conditioned medium would be enough to generate and maintain a constant, abundant pool of LPA. It is important to consider even serum-starved hepatocytes in culture may not have had all traces of LPA removed from the medium, exposing them to LPA before it is manually added to treat the cells, especially if the cells have had time to condition the medium over several days. The presence of external LPA comes without the mammalian cell having to manufacture its own source of LPA internally and then maneuver it through the lipid bilayer (an idea which is still not clear and remains unproven). Because of this, it has been hypothesized that LPA acts as both an autocrine and paracrine mediator (222). Furthermore, ATX stimulates motility in a pertussis-toxin sensitive manner, indicating that a G protein signaling pathway is directly responsible (and implicating LPA and LPA receptors) for mediating the migratory response of ATX (110, 196).

Also affecting the extracellular pool of LPA molecules are lipid phosphate phosphohydrolases (LPPs), a class of phosphatidate phosphohydrolase homologues which includes the isoform LPP-1. This isoform and its relatives LPP-2 and LPP-3 are

six transmembrane domain proteins that can localize to the cell-surface or be retained in the endoplasmic reticulum. These hydrolytic ecto-enzymes expose their active sites on the exterior surface of the plasma membrane and are capable of increasing the dephosphorylation of exogenous LPA to monoacylglycerol by two-fold (Fig. 5) (51, 98, 112).

Even though LPP-1 is non-selective for its lipid phosphate substrate, settling for LPA, PA or S1P along with others, it has been believed to negatively regulate LPA signaling (179, 216). One study suggested that in cancer cells, 95% of the hydrolysis of LPA occurs by LPPs (94). Through its hydrolysis of LPA, LPPs are preventing receptor activation, attenuating signal transduction, decreasing the amount of extracellular LPA available and thus having an indirect effect on major cell processes. The signaling responses diminished by overexpression of LPP-1 are MAPK, cAMP, calcium, DNA synthesis and cell division (148). The overexpression of LPP-1 even causes an increased rate of cellular apoptosis in ovarian cancer cells (98, 199) and the increase in LPA found in the ascites of ovarian cancer patients is thought to result at least in part from a decrease in mRNA activity of LPP-1 expression (199). In summary, the degradative consequence of LPP-1 on LPA appears to be a key pathway to LPA-mediated signal termination.

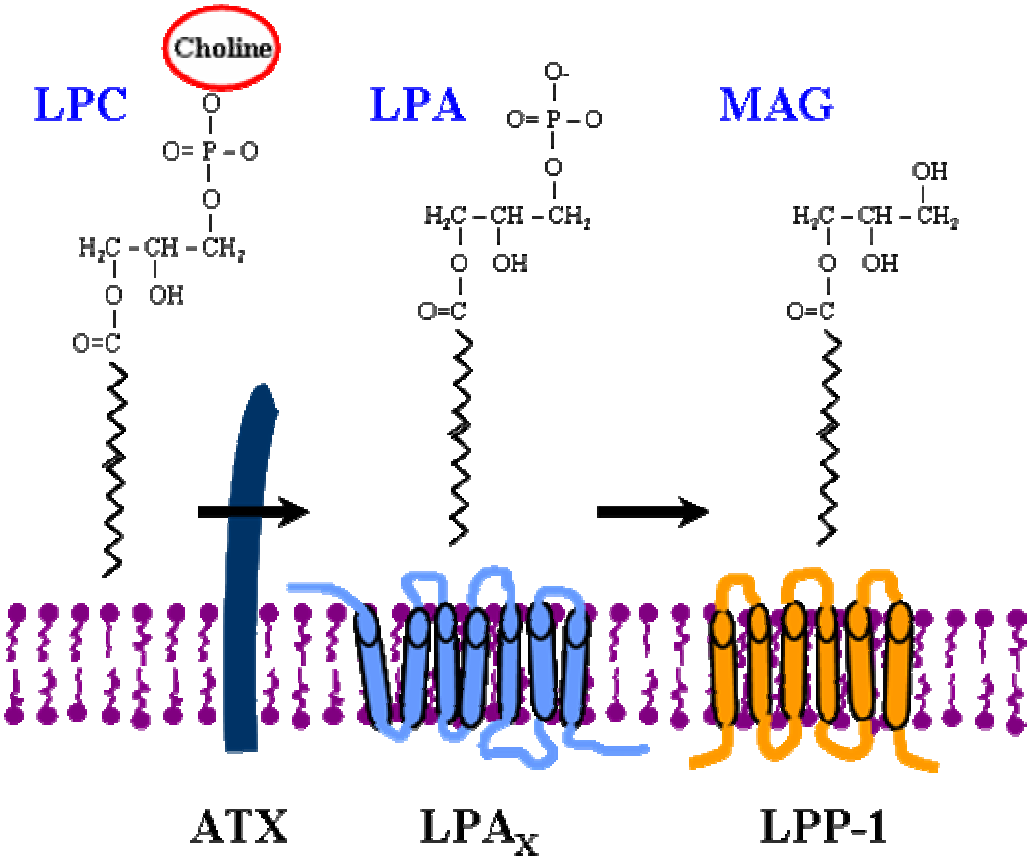

Fig.5. The extracellular metabolic pathway of LPA. This diagram gives a closer look at the cell-surface enzymatic actions that produce and degrade LPA along with the chemical structures of the lipids involved. Note the synthesis from LPC by ATX to yield LPA and LPA's degradation by LPP-1 to MAG at the plasma membrane.

Disease

LPA's role in Disease

Recent studies have suggested that LPA might contribute to a multitude of undesirable health consequences like cancer, atherosclerosis and ischemia reperfusion injury (142, 202, 206). If indeed these studies are correct, they implicate LPA as a factor in the two leading causes of death in the Western world: heart disease and cancer (8, 202). It will remain important to study the biology of LPA because of this uncertainty and for the hope that new treatment strategies will be developed from LPA research.

Athclerosclerosis

The American Heart Association defines atherosclerosis as the process where deposits of cholesterol, waste, calcium and other factors build up in the inner lining of an artery, forming a plaque. These plaques become increasingly more dangerous as they grow and reduce blood flow through the artery. If they rupture, blood clots and blockage can follow which may lead to a stroke or heart attack, depending on the location of the ruptured artery.

Intriguingly, LPA and other platelet agonists accumulate in the lipid core of human atherosclerotic plaques, at elevated concentrations 13 times above normal (52, 229). The LPA that accumulates is probably generated by mild oxidation of LDL (190) and produced from the macrophages and smooth muscle cells present (193). When the lipid-rich core of human carotid plaques was isolated, it was capable of directly activating platelets through aggregation and shape change; furthermore, these effects could be inhibited completely using an LPA receptor antagonist, implicating LPA receptor

specificity (167). LPA has also been shown to mediate vascular remodeling; it induces the accumulation of cells within the arterial walls, called neointimal lesions, and the de-differentiation of smooth muscle cells through the LPA receptor, PPARγ (75, 236).

The implications here are threefold: that LPA in atherosclerotic plaques exists and has the potential to trigger platelet activation through LPA receptors (167). Second, treating patients who have a ruptured plaque with LPA receptor inhibitors might help prevent the formation of blood clots (167, 193). Finally, it has also been suggested that regular treatment with LPA receptor inhibitors might benefit people with hypertension and cardiovascular disease (229).

Ovarian cancer

The American Cancer Society lists ovarian cancer as the fifth most common cancer in women and the fourth largest cause of cancer death in women. They estimate there will be about 25,580 new diagnosed cases of ovarian cancer in the United States in 2004 and approximately 16,090 women will die from the disease that same year. Unfortunately, at the time of initial diagnosis, two-thirds of patients already have a late-stage of the disease which drops their chances of survival down to 20-30% over 5 years (197).

A consequence of cancer forming in the peritoneal body cavity is the accumulation of abnormal fluid in the abdomen, called ascites. A gross amount of abnormal fluid buildup causes severe abdominal distention and discomfort. This uncomfortable ascetic fluid in ovarian cancer contains abundant tumor cells, lymphocytes and even LPA (68). The levels of LPA measured in the ascites of women with ovarian cancer are elevated and can reach up to 80 μM (53, 199), while normal levels are approximately 0.1-20 μM (10, 49). In gynelogical patients with stage I ovarian cancer, 80% had elevated levels of LPA with

a false positive rate of 5% (206, 227, 228). Similar increases are also seen in the blood of patient samples with cervical and endometrial cancer (173, 174, 206).

In approximately 15-30% of ovarian cancer cells, the LPA_2 receptor and LPA_2 mRNA are elevated (53, 54). Similarly, the LPA_3 receptor is overexpressed in between 44-49% of ovarian cancer cells (54). Adding LPA to ovarian cancer cells in culture causes an activation of the proliferative signaling pathway, MAPK (226) and an increase in the concentration of urokinase plasminogen activator which contributes to metastasis and cell migration (152). Thus, LPA contributes to the growth, proliferation and metastasis of ovarian cancer cells through the LPA receptors.

Even with this new knowledge about the changes associated with LPA and ovarian cancer, there is still no regular, reliable screening performed in women. This is in contrast to prostate cancer screening where regular physical exams monitor the fluctuations in a man's prostate-specific antigen (PSA) levels. Women who have yearly gynecological exams are usually limited to one routine screening test to monitor their reproductive health, a pap smear, which screens for cervical dysplasia, not ovarian cancer. The diagnostic test available for ovarian cancer is looking for a protein released from damaged cells called cancer-antigen 125 (CA-125) but it is rarely performed for screening. The CA-125 diagnostic test is also criticized for having a 3-7% false positive rate, although the National Cancer Institute claims that only 25-30% of men with elevated PSA levels actually have prostate cancer (1). Nevertheless, more reliable tests for ovarian cancer are needed.

Much discussion surrounding CA-125 has occurred in the past few years due to a widely-circulated e-mail from an anonymous source encouraging all women to demand

their doctors to perform a CA-125 test. In response to the increased demand for tests, a statement from the U.S. Preventative Services Task Force (USPSTF) recommended against routine screening for ovarian cancer (1). The USPSTF defended their position listing several reasons: first, they found no evidence that earlier diagnosis of ovarian cancer reduced mortality; second, there is only a 1:70 incidence of ovarian cancer in the overall population; finally, the USPSTF felt that false-positives would lead to harm (i.e. "potential distress and anxiety in otherwise healthy women") (1). Instead they recommended the position previously held by the American College of Obstetricians and Gynecologists which is to "remain vigilant for the early signs and symptoms of ovarian cancer, such as abdominal or pelvic pain and unexplained weight loss (1)."

Unfortunately, it is not always the case that this utopian vigilance by doctors exists; furthermore, moderate weight loss would typically not be the kind of "symptom" a woman sadly reports to her doctor during their one-minute, once-a-year exchange. Oftentimes, the initial misdiagnosis of ovarian cancer is irritable bowl syndrome (IBS) or other gastrointestinal problems because the symptoms are not specific. Only later when a woman's abdomen size competes with that of a woman who is pregnant does it become obvious the cause is not IBS. By that time, it could be too late for successful treatment. Cancer in the abdominal area has the unpleasant ease of metastasizing to organs in the peritoneal cavity which makes treatment more difficult. To reemphasize this point again, the high mortality associated with ovarian cancer is often from late-stage detection (197). This is why studying LPA and LPA receptors is so important for this disease; better screening and diagnostic tests for women are desperately needed and fluctuations in LPA could become an early disease biomarker.

Secretion of mediating factors

A discussion surrounding the involvement of LPA in cancer would not be complete without also mentioning the release of paracrine signaling molecules. LPA stimulation can cause the cell to produce TGF-beta (147), insulin-like growth factor II (72, 73), IL-6, IL-8 (55, 192) and vascular endothelial growth factor, VEGF (93). These effects may be specific to cancer cells as one report indicated that LPA stimulated the expression of IL-6 in ovarian cancer cell lines, but not in the normal ovarian surface epithelial cells (29).

The anti-inflammatory cytokine IL-6 is induced by the immune system under alarming conditions to aid the induction of an acute phase reaction along with controlling the level of proinflammatory cytokines (223). Interleukin-6 is also capable of acting as an autocrine growth factor in malignancy; furthermore, the survival rate of ovarian cancer patients declines with increasing levels of IL-6 (16). Similarly, IL-8 and VEGF are both negatively linked to ovarian cancer and they contribute to the progression of ovarian cancer possibly by promoting metastases (54). IL-8 expression is also associated with a higher invasiveness potential of cancer cells *in vitro* ((64 Vignon, Lazennec 2003)Testing the IL-8 produced by cancer cells revealed the cytokine was identical to that normally produced by a monocyte (64). VEGF is an angiogenic factor that stimulates vascular endothelial cells to develop new blood vessels and it is often elevated in human cancers as tumors strive to maintain a supply of nutrients critical for their survival (93). This and other research suggests that LPA probably contributes to and exacerbates tumorigenesis through a paracrine function.

Obesity, cancer and LPA

It is rapidly becoming common knowledge that obesity is a contributing factor in a variety of ailments such as high blood pressure, high cholesterol, heart disease, diabetes, sleep apnea, depression, asthma and even cancer of the uterus, gall bladder, breast, colon, and kidney (171). According to a recent survey by the National Health Policy Forum, obesity is becoming the fastest growing health crisis in the U.S. (171). In 1991, approximately 12% of the U.S. population was considered obese. Today, nearly 30% are obese and an additional 34% are overweight (171); thus, the majority of people in the U.S. have a serious weight problem. Fast food and sedentary lifestyles threaten to consume many lives because of the health risks being overweight has on the rest of the body.

The previous list of cancers associated with obesity did not include ovarian cancer, but a variety of studies suggest there may be a correlation. The American Cancer Society conducted an epidemiological survey of over 300,000 women in the U.S. and Puerto Rico and concluded that obesity resulted in an increase of 36% for the risk of ovarian cancer mortality in postmenopausal women (163). Japan, an Asian country often idealized for a healthier diet and lifestyle than the West, has seen an rise in ovarian cancer in the past decade and has hypothesized that the reason is a marked increase in obesity (133).

Obesity is linked to the etiology of many cancers because as the ratio of body mass index and body fat increases, so does the risk, prognosis and mortality from cancer due to the changes in endocrine function, hormones, receptors and growth factors (176). More specifically, fat cells or adipocytes secrete causative agents in hormone-related cancers:

estrogen, progesterone, androgens and testosterone (163, 164). Besides hormones, adipocytes also secrete abundant fatty acids, eicosanoids and even LPA (59, 207). In genetic obesity and adipocyte differentiation, fat cells are capable of up-regulating ATX expression which would result in even more LPA production (59). Also interesting is that the secretion of these paracrine factors controls adipocyte growth and recruits new fat cells to the tissue, increasing overall tissue mass(59). Therefore, as fat cells produce factors like LPA, they cause an increase in fat and unwanted cell proliferation, perhaps contributing to the etiology of ovarian cancer.

The tumor suppressor p53

Twenty-six years ago in 1979, a new molecule named after its molecular weight of 53 kDa, p53, was discovered. The initial description of p53 was a protein that accumulated in the nuclei of cancer cells (114). At the time researchers didn't realize what they had stumbled upon was actually a mutant form of p53, a common denominator in 50% of all human cancers (13, 18, 157, 162, 169, 175, 235). Damage to the p53 gene is the most frequently observed alteration involved in tumorigenesis (191). Today a Pubmed literature search for "p53" retrieves over 33,500 articles, demonstrating the enormous amount of research that has occurred on this important protein since its discovery.

The p53 protein is critical to the cell because it is a tumor-suppressor and transcription factor that affects DNA repair, apoptosis and cell cycle progression. Checkpoint controls in the cell's replication cycle prevent the reproduction of mutant cells. One of p53's cellular-gatekeeping functions is to halt the progression of cell replication in G1 and G2 phase if there has been damage to the DNA from drugs, UV light, etc. Normally, p53 is kept at relatively low concentrations in the cell because the half-life is only around 30

minutes (119). After DNA damage p53 accumulates in the nucleus, becomes stabilized and phosphorylated. The p53 protein can then upregulate genes involved in cell cycle arrest. One example of this is the increase in the cyclin-kinase inhibitor, p21, which blocks cyclin-kinase complexes necessary for cell-cycle progression. An arrest after DNA damage is critical to the cell because it allows time to repair the problem before replication proceeds (88).

Apoptosis is another process controlled largely by p53 under stress-induced conditions. If the cellular damage is well beyond the repair that would occur during cell-cycle arrest, a buildup of p53 can induce the death pathway. A cell has two components influencing apoptosis: extrinsic signals from cell surface "death" receptors and intrinsic signaling mainly from the mitochondria (47). Remarkably, p53 is involved in both processes. For the extrinsic involvement, p53 is capable of increasing the expression of death receptors (88). For its intrinsic involvement, p53 activation can modulate protein expression involved in mitochondrial membrane permeability (128).

Surprisingly for a transcription factor, p53 has been microscopically observed localized to the mitochondria. There p53 directly forms complexes with the anti-apoptotic protein Bcl-2 to inhibit its protection; this in turn causes an interaction with apoptotic-promoting proteins and ultimately releases cytochrome c from the mitochondria (128). The release of cytochrome c initiates a death signal by activating proteins such as caspase 3 and caspase 9 to begin apoptosis. Caspases belong to a larger family of cysteine proteases that are capable of cleaving proteins along nuclear lamina, for example, which is terminal to the life of a cell.

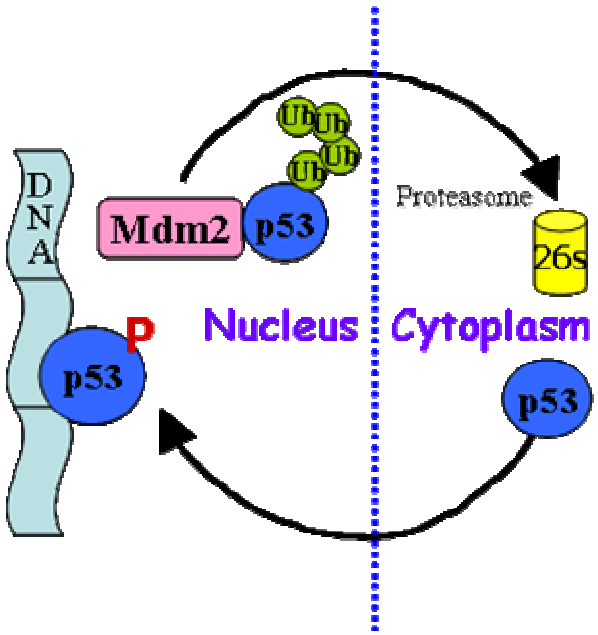

Fig. 6. The degradative pathway of p53 shows ubiquitination by Mdm2 and subsequent delivery to the proteasome. Phosphorylated p53 in the nucleus binds to DNA to upregulate genes.

The regulation of p53 is largely influenced by the protein murine double-minute 2, Mdm2 (also referred to by its human counterpart, Hdm2). To target a protein for destruction in the proteasome, at least four or more 76 amino-acid ubiquitin proteins must be covalently attached in tandem to the lysine residues on a protein for an adequate degradation signal. The Mdm2 protein is an E3 ubiquitin ligase that promotes the ubiquitination and degradation of p53 in an autoregulatory feedback loop.

Activating p53 will cause it to induce the transcription of Mdm2, which then binds p53 and inhibits its further activity. In other words, p53 positively regulates Mdm2 and Mdm2 negatively regulates p53. The negative regulation of p53 occurs threefold: first by Mdm2 binding to p53's N-terminal domain to block transcriptional activation (130, 143); second, by conjugating ubiquitin to the Lys residues on p53 which target it to the

proteasome for degradation (90); finally, Mdm2 simultaneously directs the nuclear export of p53 and delivery to the cytosolic proteasome (21, 70).

Damage to the DNA is one catalyst for the disruption of Mdm2 binding and would then be follow with p53 phosphorylation, stabilization, activation and accumulation. More specifically, within minutes after DNA damage, p53 is phosphorylated at serine 15 along its N-terminus which induces a conformational change in p53 and prevents its interaction with Mdm2 (188, 189). The association of p53 and Mdm2 is so critical, altering the integrity of Mdm2 or affecting the regulatory pathway of Mdm2 will functionally inactivate p53 (69, 233).

Because a strong link between LPA and cell survival has been established and since LPA is a well-known mitogen, we were curious what regulatory effects the LPA receptors might have on the cell cycle. The p53 tumor suppressor was of particular interest because it is modulated by LPA and aberrantly expressed in many cancers. Previously, no research has documented any connection between Edg-family LPA receptors and p53. The majority of findings that support a role for LPA mediating cellular apoptosis suggest that this occurs through the G_i signaling pathway (45, 56, 95, 113), making LPA-mediated signal transduction through a receptor PDZ-binding domain a unique find. In addition, to date there has not been a direct correlation with ecto-enzymes modulating the LPA signaling through these receptors. This subsequent chapters presented in this thesis will answer some of these questions and highlight the importance of studying these GPCRs and how they transduce LPA-induced signals.

PART I:

ACTIVATION OF LYSOPHOSPHATIDIC ACID RECEPTORS INHIBITS THE TUMOR SUPPRESSOR, P53, THROUGH INTERACTIONS OF THE PDZ BINDING DOMAIN

CHAPTER 2

INHIBTION OF THE P53 TUMOR SUPPRESSOR BY LYSOPHOSPHATIDIC ACID RECEPTORS

INTRODUCTION

Lysophosphatidic acid (LPA) is a mitogenic lipid found in bodily fluids that elicits a wide range of effects on the cell including: proliferation, migration, morphological changes, neointima formation and survival (30, 45, 56, 66, 74, 95, 236). LPA is produced in blood by activated platelets in response to wound healing (109, 227) and is also produced by a variety of cancer cells (48, 185). The diverse actions of LPA are primarily mediated through one of three seven-transmembrane, G protein-coupled receptors (GPCRs): LPA_1/Edg2, LPA_2/Edg4, LPA_3/Edg7, and by the metabolic receptor, PPAR-γ (4, 7, 11, 122, 138). Recent studies suggest that the orphan receptor GPR23 is also a high affinity LPA receptor (138). The LPA-binding GPCRs can collectively activate the following classes of G alpha proteins: G_i, G_q, and $G_{12/13}$ (96, 138, 153). The resultant effects of LPA are mediated through the activation of downstream signaling pathways controlled by the balance of these G alpha proteins (208).

LPA potently stimulates the growth, survival and motility of a variety of cancer cells, which can produce and release LPA themselves (129). A variety of cancer cells have been shown to secrete an ecto-lysophospholipase D enzyme known as autotaxin (ATX), which can use extracellular lysophosphatidylcholine as a substrate to produce LPA (196, 203, 205). ATX stimulates motility in an LPA-dependent and pertussis-toxin sensitive manner (110, 196). LPA signaling leads to the activation of both cell-proliferative

signaling pathways, such as the Ras/MAP kinase pathway, and cell survival pathways, such as the phosphatidylinositol-3 kinase (PI-3K)/Akt pathway (218). These effectors are primarily activated via pertussis toxin-sensitive, G_i signaling.

Although much is known about the effects of LPA signaling on cancer cell growth and motility, relatively little is known about LPA's effects on cell cycle regulators, such as the p53 tumor suppressor. p53 is a transcription factor that controls the expression of genes encoding proteins that effect apoptosis and cell cycle progression (161, 184, 198). DNA damage causes phosphorylation-induced stabilization of p53 which then up-regulates cyclin kinase inhibitors to block cyclin-kinase complexes that are necessary for cell-cycle progression (50, 170, 224). If the damage is irreparable, then p53 up-regulates the expression of genes that promote apoptosis, such as Bax (181, 182). Although human cancers differ in a multitude of factors, a common denominator that is consistently seen throughout numerous types of cancer is inactivation of p53 function in about 50% of all cancers (77).

Given the strong mitogenic effects of LPA and the commonly observed loss of p53 function in cancer cells, we investigated whether LPA signaling affected the function of the p53 tumor suppressor. We found that signaling initiated by all three Edg-family LPA receptors (LPA_1, LPA_2, and LPA_3) potently inhibited p53-mediated transcription and promoted the loss of p53 protein in both A549 lung cancer cells and HepG2 hepatoma cells. In the case of LPA_1, we found that inhibition of p53 is likely mediated through a novel mechanism: interaction with PDZ domain containing proteins via its PDZ-binding domain in the cytoplasmic tail.

CHAPTER 3

MATERIALS AND METHODS

Cell culture

HepG2 cells were obtained from Dr. Athanassios Sambanis (Georgia Institute of Technology, Atlanta) and maintained as described previously (137). A549 cells were purchased from the American Type Culture Collection (Manassas, VA) and grown at 37°C and 5% CO2 in F12K Kaighn's modification medium (Mediatech, Herndon, VA) supplemented with 10% fetal bovine serum, 100 I.U./ml penicillin, 100 µg/ml streptomycin (HyClone, Logan, UT) and 1.5 g/liter sodium bicarbonate (Biosource International, Camarillo, CA). The HeLa cells were maintained in Dulbecco's modified Eagle's medium (DMEM) supplemented with 10% FBS, 100 I.U./ml penicillin, and 100 mg/ml streptomycin (complete medium) at 37°C with 5% CO2.

Reagents

Lysophosphatidic acid (18:1 LPA; 1-oleoyl-2-hydroxy-*sn*-glycero-3-phosphate) (Avanti Polar Lipids, Alabaster, AL) was stored in chloroform at -20°C and dried down immediately before use under a stream of nitrogen. LPA was then reconstituted in 1% fatty-acid free, charcoal-stripped BSA as previously described (111, 152). Mouse anti-p53 antibody (DO-1), which detects total p53, and mouse anti-β-actin antibody, which was used to monitor loading accuracy, were obtained from Santa Cruz Biotechnology Inc (Santa Cruz, CA). Phosphorylated p53 at serine 15 (Pp53[S15]) was detected with affinity-purified rabbit anti-Phospho-p53[S15] antibodies from Cellular Signaling

Technology (Beverly, MA) and Santa Cruz Biotechnology. The FLAG epitope tag was visualized using primary mouse anti-FLAG antibodies obtained from Sigma (St. Louis, MO) followed by fluorescent secondary antibodies. Carbamoylcholine chloride (carbachol) and actinomycin D were also purchased from Sigma. Pifithrin-alpha (PFT-α) was obtained from EMD Biosciences, Inc. (San Diego, CA). Pertussis toxin was obtained from BIOMOL (Plymouth, MA). All other reagents were from Sigma Chemical Co.

Plasmids

The original plasmid encoding the human FLAG-LPA_1 receptor was a kind gift from Junken Aoki (University of Tokyo, Japan) and the modified construction of the FLAG-LPA_1 plasmid has been reported (154). To enhance the cell-surface expression of LPA_2 and LPA_3, PCR was used to attach a signal leader sequence from the influenza hemaglutinin protein onto the amino terminus of the plasmid preceding the FLAG epitope tag. The FLAG-LPA_2 vector was constructed using the primers 5'-ATGCGGATCCATGGACTACAAAGACGAT –3' and 5' –GATCTCAGTCCTGTTGG TTGGG-3'. The FLAG-LPA_3 vector was constructed by isolating total RNA from OVCAR-3 cultured cells with a GenElute Direct mRNA Miniprep kit (Sigma). Following isolation, RT-PCR was performed using the following oligonucleotides: 5'-GATCATGAAGACCATCATCGCCCTGAGCTACATCTTCTGCCTGGTGTTCGCCG ACTACAAGGACGATGATGACAAGATGAATGAGTGTCAC-3' and 5'-CGATTTAG GAAGTGCTTTTA-3'. The RT-PCR reaction included 10 ng RNA, 10 μM sense and anti-sense primers, deoxynucleotides, reaction buffer, and 0.5 U of *Taq* DNA polymerase (Invitrogen, Carlsbad, CA) in a final volume of 50 μl. The mixes were first incubated at

50°C for 30 min to allow mRNA to be copied into cDNA, followed by a 2 min hold at 94°C and 40 cycles of 94°C for 15 s, 55°C for 30 s and 72°C for 2 min. After the PCR reaction, a single 1062 bp band was observed, which was purified and subcloned into pcDNA3.1 V5/His mammalian expression vector (Invitrogen). LPA_1-Δ361 was constructed using wild-type LPA1 plasmid as the template and modifications were made as follows: 5'- GATCATGAAGACCATCATCGCCCTGAGCTACATCTTCTGCCTG GTGTTCGCCGACTACAAAGACGATGACGATAAA-3' and 5'-AGCTAGCTCGAG CTAGTGGTCATTGCTGTGAAC-3'. The PCR cycle began with a 2 min hold at 94°C, followed by 25 cycles of 1.5 min 94°C, 1.5 min 55°C and 3 min 72°C before a 72°C hold for 10 min. The PCR products were purified and inserted into pcDNA3.1/V5-His using a TOPO TA Cloning Kit (Invitrogen). All of the DNA sequences were confirmed by DNA sequencing (Georgia Tech DNA Sequencing Facility, Atlanta). The LPA_1-R124A expression plasmid was the kind gift of Dr. Gabor Tigyi (University of Tennessee, Memphis, TN).

Transfections

For indirect immunofluorescence studies in HepG2 cells, Exgen 500 reagent (Fermentas, Hanover, MD) was used for transient transfection in complete media and the control comparison was made using the plasmid, pEGFP-N2 (BD Biosciences Clontech, Palo Alto, CA). For all other studies, HepG2 and A549 cells were transfected using Lipofectamine or Lipofectin (Invitrogen), respectively, according to the Manufacturer's guidelines.

Preparation of whole-cell lysates

A549 cells were grown in 150 mm dishes for 24 h before washing with serum-free medium (SFM) and starved in SFM for 12-16 h prior to the treatments indicated above and in figure legends. Cells were rinsed with ice-cold PBS supplemented with phosphatase inhibitors (Active Motif, Carlsbad, CA), detached by scraping and collected by centrifugation. Pellets were then solubilized on ice for 30 min with intermittent agitation in lysis buffer (10 mM Tris pH 7.4, 100 mM NaCl, 1 mM EDTA, 1 mM EGTA, 1 mM NaF, 20 mM $Na_4P_2O_7$, 2 mM Na_3VO_4, 1% Triton X-100, 10% glycerol, 0.1% SDS and 0.5% deoxycholate, (Biosource International) supplemented with 1 mM PMSF from a 0.3 M stock and protease inhibitor cocktail (1:10 dilution; Sigma). Protein concentration was quantified using a BCA protein assay (Pierce, Rockford, IL).

Indirect Immunofluorescence and Quantitation

Immunofluorescence staining was performed as previously described (36). Briefly, cells were grown on glass coverslips and fixed in 2% formaldehyde in PBS before rinsing in PBS supplemented with 10% fetal calf serum (PBSserum) and incubation with primary antibodies. Coverslips were subsequently rinsed three times with PBS-serum and incubated with fluorescently-labeled secondary antibodies. During the last wash, Hoechst 33342 dye (Molecular Probes, Eugene, OR) was added to label the DNA. Samples were mounted onto glass slides and observed with an Olympus BX40 epifluorescence microscope equipped with a 60X plan-apochromat lens and digital photomicrographs were obtained with a MagnaFire SP digital camera. All photographs were obtained using the same exposure time.

For quantitation of fluorescence intensity, photomicrographs of 25 cells per time point or experimental treatment were obtained from each experiment that was repeated at least three independent times. The fluorescence intensity of the nuclear-localized p53 was measured in each cell using Metamorph Imaging Software (Universal Imaging Corporation, Downington, PA). The fluorescence intensity produced by p53 was normalized by first subtracting the background and then dividing that value by the fluorescence intensity of DNA labeled with Hoechst dye for each cell. Normalized data averages of each photomicrograph from all experiments were combined to obtain a grand average throughout. The data are presented as the mean ± S.E.M.

ELISA for p53

Whole cell lysates were collected and processed as described in the methods above. Twenty-five micrograms of whole cell protein was used to determine total p53 and Pp53[S15] levels at each experimental point. Analysis for these determinations was performed using p53-specific ELISA kits (Biosource) following the Manufacturer's protocol. The final protein concentrations obtained were calculated by comparing the absorbance of triplicate samples to a standard curve from control p53 samples provided in the kit. Graphs of standard curves must have met the following criteria: R_2 values >0.98 and readings equivalent to Manufacturer's OD listed values for experiments to be considered acceptable. The amount of protein from the experimental samples was controlled so that the measured absorbance fell within the limits of the standard curve and no values were extrapolated. The data shown are presented as percent of control (untreated sample) combined from three independent experiments of triplicate samples represented as normalized mean ± S.E.M.

Luciferase reporter gene assay

Both firefly luciferase and *Renilla* (pRL-TK) luciferase activities were measured 36 h post-transfection using a dual luciferase assay kit (Promega, Madison, WI) as previously described (35,36). The construct pSRE-luc (BD Biosciences Clontech) expresses firefly luciferase and is stimulated by serum response factor (SRF) activation. The pp53-TA-luc vector contains a p53-response element, where p53 binds, that is upstream of the luciferase reporter (BD Biosciences Clontech). The plasmid, pRL-TK, which constitutively expresses *Renilla* luciferase (Promega), was used to normalize for differences in transfection efficiency. The normalized value is defined as the ratio of the (SRE, or p53-induced) firefly luciferase activity to *Renilla* luciferase. The data are presented as percent of control and were compared to untreated controls. They are shown as the mean ± S.E.M. of triplicate measurements from a representative experiment that was repeated at least three times.

Statistical analysis

The data was analyzed using either a single-factor or two-factor ANOVA followed by a Tukey's statistical test. A P value of <0.05 was considered significant.

CHAPTER 4

RESULTS

We were interested in determining whether the mitogenic lipid, LPA, affected the function of cell cycle regulators in cancer cells. Of particular interest was the tumor suppressor p53 since it can arrest damaged cells in G1 (184) and cause apoptosis once nuclear threshold levels are reached (116, 168). To address this question, we investigated the effects of LPA stimulation on the level of p53 protein present in A549 human lung carcinoma cells since these cells rapidly proliferate, express wild-type p53, and endogenously express LPA receptors (81, 117). In addition, we also used human epithelial liver hepatocellular carcinoma HepG2 cells as a comparative model because they are unresponsive to LPA and also express wild-type p53 (61, 91, 137).

First, we compared the relative expression of p53 protein in HepG2 cells, A549 cells and OVCAR-3 cells, which express high levels of mutant p53 (159, 231). The results indicate that A549 cells express approximately twice as much p53 when compared to HepG2 cells (Fig. 7A), which express very low amounts of endogenous p53. OVCAR-3 cells express much higher levels of non-functional, endogenous p53 compared to either A549 cells, or HepG2 cells.

To determine whether LPA had any effect on p53 levels, A549 cells were treated with a physiological concentration of 10 μM LPA for 1-24 h and whole cell extracts were prepared and analyzed by ELISA (Fig. 7B). Treatment of A549 cells with 10 μM LPA for 1 h led to a 50% reduction in the levels of both total and active, serine15-phosphorylated p53 (Pp53[S15]), which remained at this level for up to 6 h. The levels of

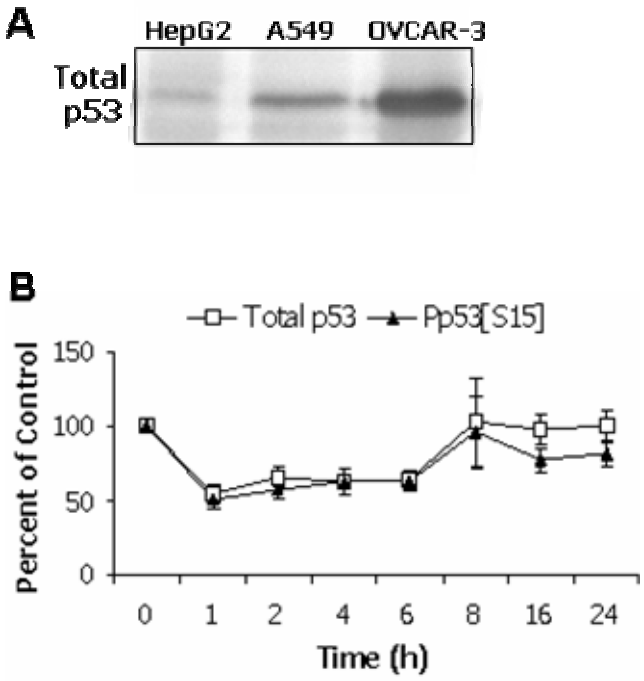

Fig. 7. LPA treatment reduces the level of p53 tumor suppressor protein in A549 lung carcinoma cells. (A) HepG2, A549 and OVCAR-3 cells were grown in 10 cm dishes in complete media for 48 h prior to preparation of whole-cell lysates and immunoblotting with mouse anti-p53 (DO-1) antibody. (B) After growing A549 cells in 150 mm dishes, cells were rinsed and serum-starved overnight before treatment with 10 μM LPA for the times indicated. Whole cell extracts were analyzed for total p53 (white boxes) and phosphorylated Pp53[S15] (black triangles) by ELISA. The level of p53 (total or phosphorylated) protein in LPA-treated samples was normalized to that observed in untreated cells. The data represent the mean ± S.E.M. of three independent experiments performed in triplicate.

total and phosphorylated p53 began to increase after 6 h of LPA treatment and returned to control levels after 8 h. Independent quantitation using indirect immunofluorescence microscopy yielded identical results (data not shown).

We also examined the effects of LPA stimulation on the intracellular distribution of endogenous p53 protein (Fig. 8). In control cells, p53 was localized primarily to the nucleus and was also present in punctate spots that were dispersed throughout the cytoplasm (Fig. 8A). These cytoplasmic p53 spots co-localized with anti-ubiquitin antibodies suggesting that the p53 in these spots was ubiquitylated. Treatment with 1 μM LPA for 1 h led to a significant reduction in labeling of nuclear p53 and labeling of the cytoplasmic structures was also greatly diminished (Fig. 8B, 1 μM LPA). For comparison, we examined the effects of a known p53 inhibitor, pifithrin-α, which blocks p53-dependent transcriptional activation and apoptosis (103).

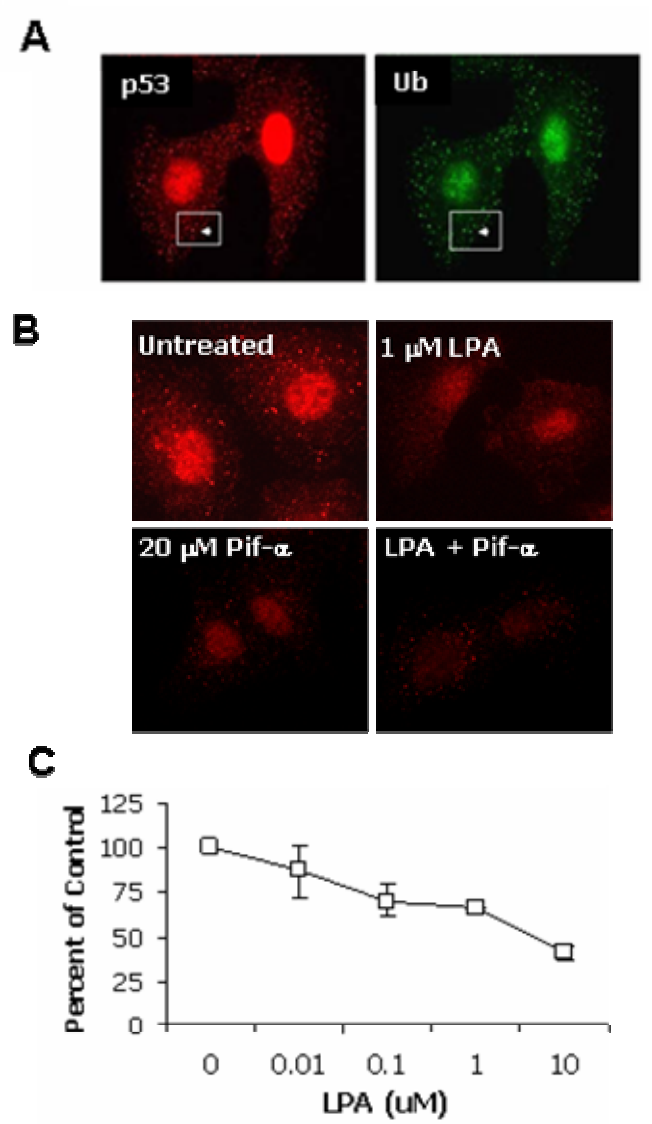

Fig. 8. Sustained LPA treatment decreases nuclear localization of p53. (A) A549 cells were plated onto glass coverslips prior incubation for 8 h in SFM. The cells were fixed and incubated with mouse anti-p53 antibody (DO-1) and rabbit anti-ubiquitin antibody followed by fluorescently-labeled secondary antibodies. (B) Approximately 2 x 10^5 A549 cells were plated. After 16 h of serum-starvation, cells were then either left untreated (*Untreated*), treated with 1 μM LPA for 1 h (*1 μM LPA*), treated with 20 μM pifithrin-α for 16 h (*20 μM Pif-α*), or with both 20 μM pifithrin-α and 1 μM LPA for 16 h (*LPA+Pif-α*). (C) A549 cells grown on glass coverslips were serum-starved for 16 h prior to treatment with the indicated concentrations of LPA for 6 h. Total p53 was localized by indirect immunofluorescence microscopy using mouse anti-p53 (DO-1) primary antibody followed by anti-mouse Cy3 secondary antibody. The fluorescence intensity of nuclear p53 staining was normalized to DNA labeled Hoechst dye and was quantified by image analysis as described in METHODS. The data represent the mean ± S.E.M. of the fluorescence intensity of nuclear p53 in LPA-treated cells relative to that observed in untreated cells and are from a representative experiment that was repeated at least three times with similar results.

Treatment of A549 cells with 20 μM pifithrin-α for 16 h strongly reduced both nuclear and cytoplasmic labeling of p53 and was similar to the effects of LPA (Fig. 8B, 20 μM Pif-α). Interestingly, concurrent treatment of cells with both LPA and pifithrin-α, for 16 h, resulted in a synergistic reduction in p53 staining (Fig. 8B, LPA + Pif-α). A549 cells were also incubated with various concentrations of LPA for 6 h and the LPA dose-dependent loss of nuclear p53 staining was quantified using Metamorph image analysis software (Fig. 8C). We observed a progressive reduction in nuclear p53 labeling as the concentration of LPA was increased through the physiological range. Reduction in nuclear p53 staining was first apparent at 0.01 μM and was the greatest at 10 μM LPA (~ 50% of control). In conclusion, the loss of nuclear p53 labeling paralleled the reduction in cellular p53 protein levels observed by ELISA (Fig. 7B).

Next, we determined the effects of LPA stimulation on p53-mediated transcription by using a p53-stimulated luciferase reporter gene assay. For these experiments we examined both A549 cells, which express endogenous LPA receptors, and HepG2 cells (LPA unresponsive cells) after expression of individual LPA receptors. A549 and HepG2 cells were transiently co-transfected with a plasmid encoding a firefly luciferase reporter gene, whose expression is driven by a basal promoter and an upstream p53 response element, and with the plasmid pRL-TK, which constitutively expresses *Renilla* luciferase and serves to control for variations in transfection efficiency. The results in Fig. 9A show that LPA stimulation of native A549 cells led to a 60% reduction in p53-mediated transcription of the luciferase reporter gene (Control, black bar). In contrast, LPA stimulation of native HepG2 did not affect p53-mediated transcription, which is

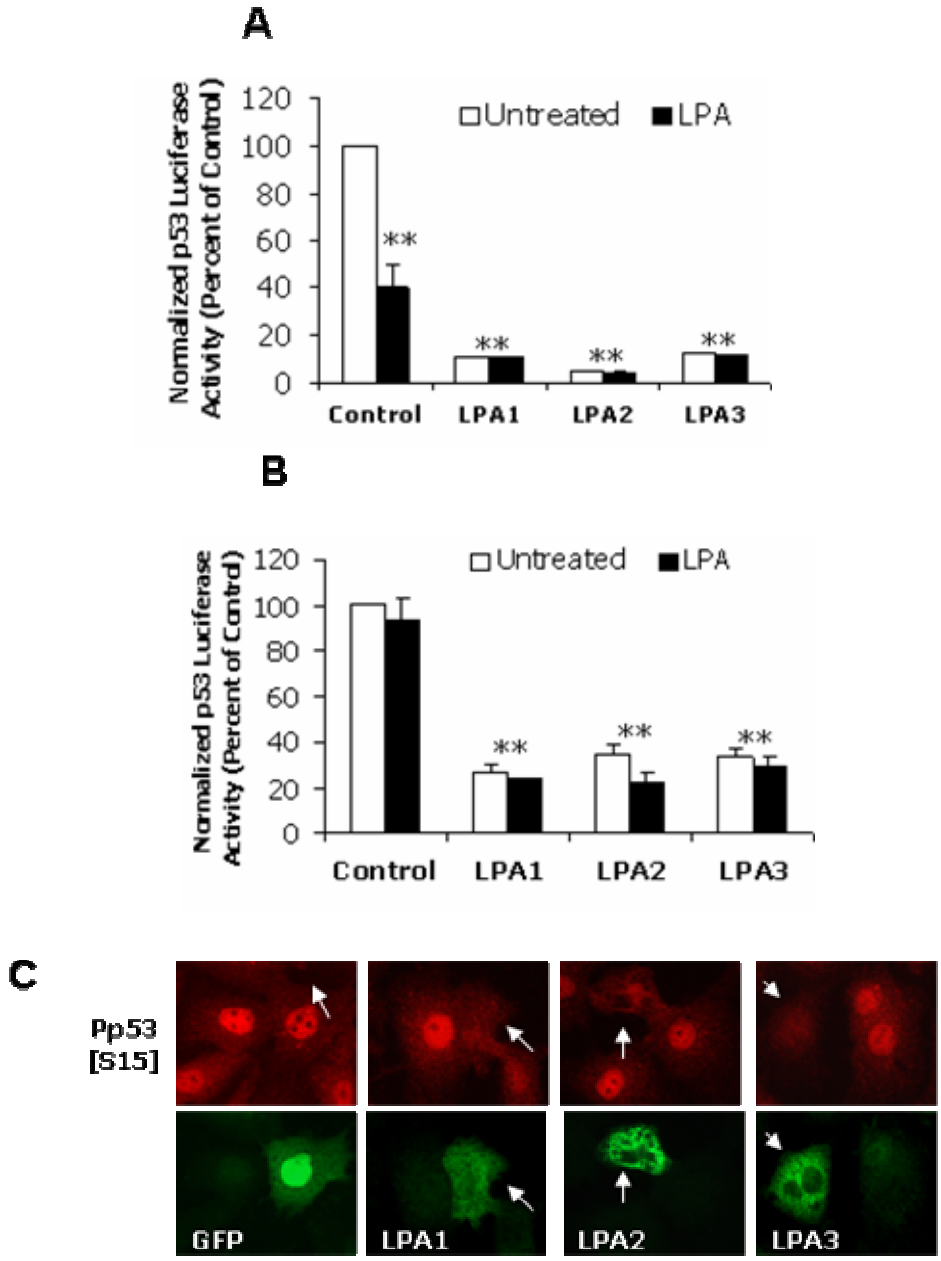

Fig. 9. Overexpression of the Edg-family LPA receptors inhibits the transcriptional activation of p53. A549 cells (A) or HepG2 cells (B) seeded in 24-well dishes were transiently transfected with the indicated plasmids along with p53 luciferase reporter and pRL-TK (*Renilla* luciferase) construct. Transient expression levels of FLAG-LPA receptors were kept within 10% of each other. Twenty-four h post-transfection, cells were incubated overnight with 10 μM LPA before measuring both firefly and *Renilla* luciferase. The data are presented here as percent of control (mean ± S.E.M. of triplicate samples) and the graphs are from a representative experiment, which was repeated at least three times with similar results. **P<0.01, comparison of cells treated with or without LPA to untreated, control cells. (C) HepG2 cells were transiently transfected with pEGFP (control) or FLAG-tagged LPA receptors before processing for indirect immunofluorescence. Primary antibody staining to determine the localization of LPA receptors was performed using mouse anti-FLAG antibodies and Ser15 phosphorylated p53 using rabbit anti-Pp53[S15] antibodies in the presence of 10% saponin.

91, 137). Over-expression of any of the three Edg-family encoded LPA receptors, LPA_1, LPA_2, or LPA_3, strongly reduced p53-mediated transcription in both A549 and HepG2 cells to approximately 10- 35% of that observed in the corresponding control, untransfected cells. Additionally, indirect immunofluorescence studies showed that over-expression of LPA_1, LPA_2, or LPA_3 strongly reduced the nuclear localization of active p53[S15] in HepG2 cells (Fig. 9C) even in the absence of added LPA.

Neither the inhibition of p53-mediated transcription, nor the loss of nuclear p53 localization by over-expression of LPA receptors required the addition of exogenous LPA. We hypothesized that these cells produced LPA themselves, which in turn would activate the transfected receptors. To test this, we examined the effects of a mutant LPA_1 receptor, LPA_1 R124A, which cannot bind and be activated by LPA (172, 217). The data in Fig. 10A indicate that, unlike wild type LPA_1 receptors, over-expression of the LPA_1 R124A receptor in HepG2 cells does not inhibit p53-mediated transcription supporting the hypothesis that the transfected LPA receptor must be capable of binding LPA in order to inhibit p53 function. We also speculated that if these cells produced LPA to activate the transfected receptors, then over-expression of lysophospatidate phosphatase 1 (LPP1), an enzyme that degrades LPA (98, 148), should prevent the inhibition of p53. We observed that transient transfection of LPP1 alone significantly elevated the transcriptional activity of endogenous p53 in A549 cells (Fig. 10B) and that co-expression of LPP1 with wild type LPA_1 receptors prevented the inhibition of p53-mediated transcription, which was readily observed in cells transfected with LPA_1 receptor plasmids alone. Similar results were also observed in HepG2 cells (data not shown). As our first alternative approach, we determined the effects, on p53-mediated

transcription, of exogenously adding phospholipase B (PLB) to A549 cells transfected with LPA_1-encoding plasmids (Fig. 10C). Addition of PLB to adipocytes inhibits LPA signaling by degrading either extracellular lysophosphatidylcholine (LPC), which is a substrate for LPA production via phospholipase D, or LPA itself (207). Addition of exogenous PLB prevented the inhibition of p53-mediated transcription by overexpressed LPA_1 receptors in A549 cells. For another alternative approach, we determined the effects, on p53-mediated transcription, of adding a commercially-available inhibitor of LPP-1 activity to HepG2 cells transfected with either LPA_1 or LPA_1 and LPP-1 together. The LPP-1 inhibitor decreased p53-mediated transcription, likely because it affects the exogenous pool of LPP-1 and increases available LPA in the medium. Taken together, these results indicate that the inhibition of p53-mediated transcription observed in cells transiently transfected with LPA receptors requires receptor activation and that the transfected cells are likely to provide the LPA that is required to activate the transfected receptors.

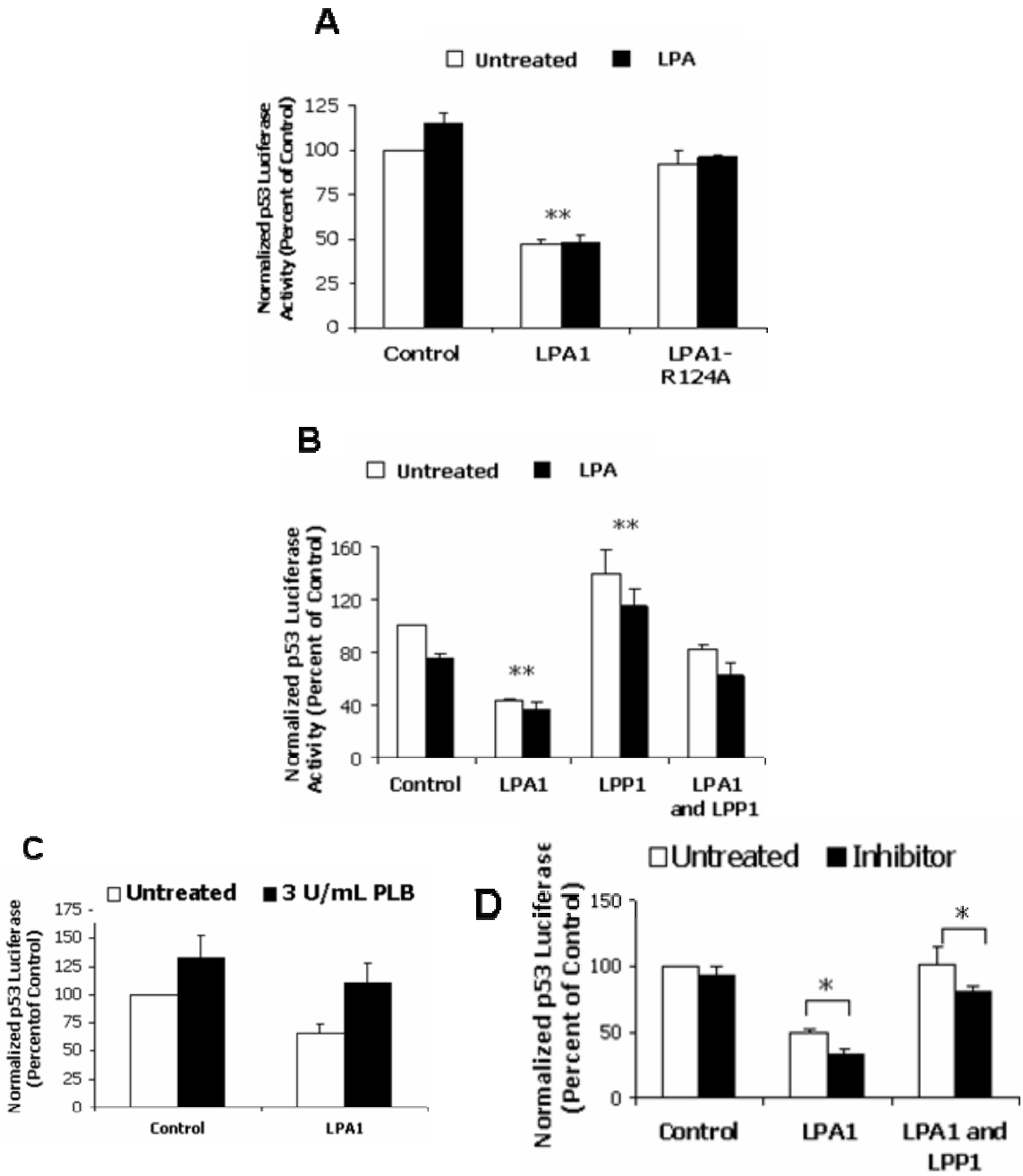

Fig. 10. The inhibition of p53-mediated transcription requires LPA receptor activation and is prevented by LPP1. (A) Transient transfection of HepG2 cells or (B) A549 cells were performed using plasmids indicated in the figures along with p53 luciferase and pRL-TK plasmids. Twenty-four h posttransfection, the cells were treated overnight with 10 μM LPA, followed with quantitation of luciferase activities. The data are presented here as a percent of control and are from a representative experiment that was repeated at least three times with similar results. **P<0.01, comparing p53 luciferase activity in LPA receptor-transfected cells compared to control, untransfected (control) cells. (C) A549 cells were transiently transfected prior to treatment overnight with 3 U/mL phospholipase B. (D) HepG2 cells were transfected as indicated and treated for 16 h with 1 μM of an LPP-1 inhibitor. *P<0.05, comparing transfected pairs either untreated or treated with the inhibitor.

Transcriptional inhibitors such as actinomycin D (ActD) greatly enhance the stability and nuclear accumulation of p53, which ultimately leads to the induction of apoptosis (28, 100, 101). To determine whether LPA would still inhibit p53 in the presence of ActD, we compared the effects of these two compounds, administered alone or in combination, on both the nuclear accumulation of p53 and on p53-mediated transcription in A549 cells (Fig. 11). Whereas LPA treatment (10 μM, 1 h) reduced the nuclear accumulation of both total p53 and Pp53[S15], ActD treatment (2 μg/ml for 2 h) increased both total and phosphorylated p53 levels in the nucleus (Fig. 11A and B). In contrast, treatment of A549 cells with both LPA and ActD prevented the decrease in nuclear p53 levels observed in cells treated with LPA alone. This established that the ActD-induced p53 stabilization is dominant to the LPA-induced decrease in p53. In addition, we also found that ActD reversed the inhibition of p53-mediated transcription in HepG2 cells overexpressing LPA_1, LPA_2, and LPA_3 receptors (Fig. 11C).

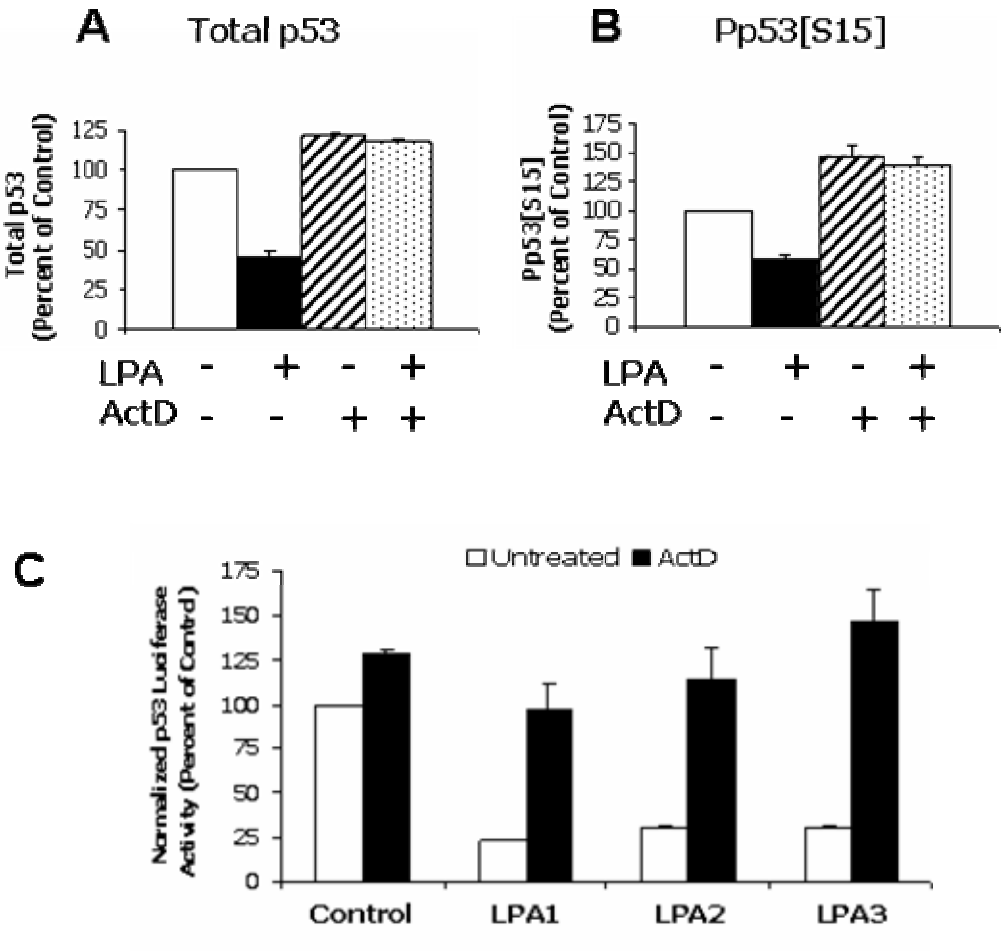

Fig. 11. Inhibitors of transcription prevent the LPA-mediated decrease of nuclear p53. (A and B) Serum-starved A549 cells were treated with either 10 μM LPA for 1 h, 2 μg/ml actinomycin D for 2 h, or with 2 μg/ml actinomycin D (2 h) followed by 10 μM LPA for an additional 1 h. Total p53 (A) was localized using mouse anti-p53 (DO-1) antibody and phosphorylated p53[S15] (B) was localized using rabbit anti-p53 and fluorescently labeled secondary Cy antibodies. The fluorescence intensity of nuclear p53 staining was normalized to DNA labeled with Hoechst dye and was quantified as described in METHODS. The data represent the mean ± S.E.M. of the fluorescence intensity of nuclear p53 in LPA-treated cells relative to that observed in untreated cells and are from a representative experiment that was repeated at least three times with similar results. (C) HepG2 cells were transiently transfected in SFM with the indicated plasmids along with p53 luciferase reporter and pRL-TK (*Renilla* luciferase) construct. Twenty-four hours posttransfection, cells were incubated overnight with 2 μg/ml actinomycin D before measuring luciferase. The data are presented as a percent of control, untreated cells (mean ± S.E.M. of triplicate samples) from a representative experiment that was repeated three times with similar results.

The Edg-family of LPA receptors are coupled to multiple classes of G proteins including: G_i, G_q, and $G_{12/13}$ (96) and the LPA-induced stimulation of cell survival is mediated in many cases through the stimulation of G_i and βγ signaling pathways (45, 56, 74). To investigate whether overexpression of other GPCRs which couple specifically to G_i might also inhibit p53 function, we examined the effects of over-expression of the muscarinic acetylcholine type 2 receptor (M_2 mAChR) on p53-mediated transcription in HepG2 cells (Fig. 12A). In contrast to LPA_1 receptor transfected cells, over-expression of the G_i-coupled M_2 mAChR and stimulation with its agonist, carbachol (1 mM), did not reduce p53-mediated transcriptional activation of the p53 luciferase reporter gene. Rather, we observed an enhancement in p53-mediated transcription in cells expressing M_2 mAChRs.

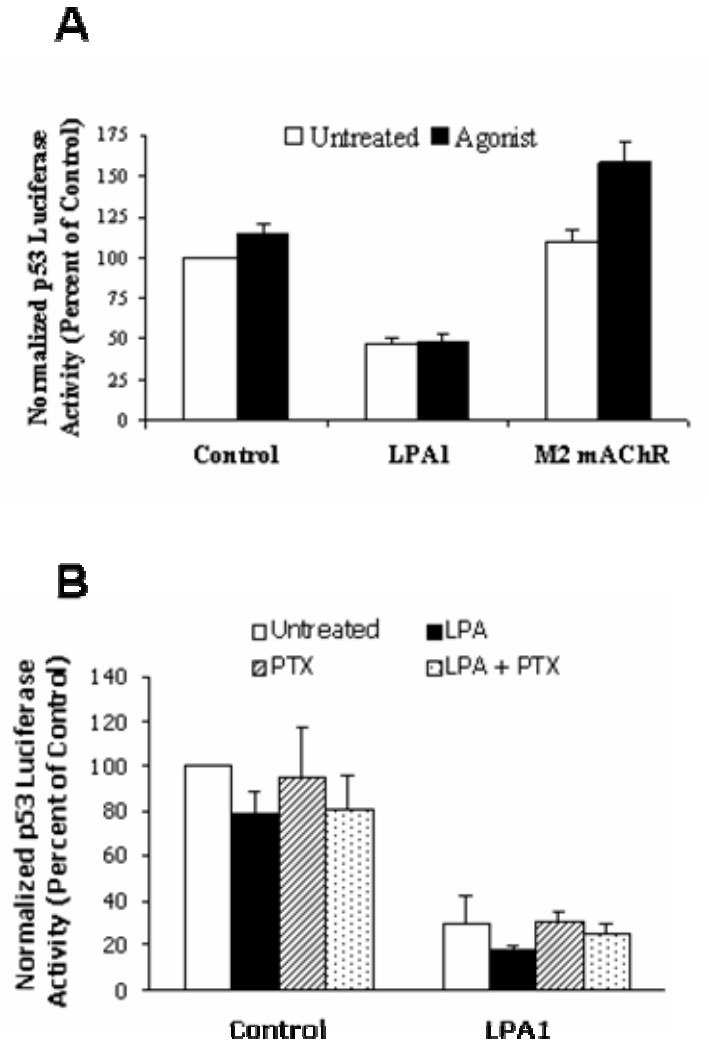

Fig. 12. LPA-mediated p53 suppression is not dependent on G_i signaling. (A) HepG2 cells were transiently transfected with either pBluescript plasmid, plasmid encoding LPA_1 or plasmid encoding M_2 muscarinic acetylcholine receptor (M_2 mAChR) in addition to the p53 luciferase and pRL-TK plasmids as described in METHODS. The control and FLAG-LPA_1 transfected cells were treated overnight with 10 μM LPA and the M_2 mAChR cells were treated overnight with 1 mM carbachol. Luciferase activities were measured as described in METHODS and then normalized to untreated, control cells. **P<0.01 comparing p53 luciferase activity in either LPA_1- or M_2 mAChR-transfected cells to control, untreated cells. (B) HepG2 cells, transfected with pBluescript or LPA_1 plasmids, were treated overnight with either 10 μM LPA, 25 ng/ml pertussis toxin or both before measuring firefly and *Renilla* luciferase as described in METHODS.

We also tested the G_i signaling inhibitor, pertussis toxin, and found that it had no effect on the LPA_1-induced inhibition of p53 (Fig. 12B) suggesting that the mechanism of LPA-mediated inhibition of p53 was not mediated through G_i-dependent signaling pathways. Further experiments that tested the effects of constitutively-active and dominant-negative mutants for G_i, G_q, and $G_{12/13}$ proteins neither mimicked nor inhibited, respectively, the LPA receptor-induced inhibition of p53 (data not shown). Taken together, these data suggested that the inhibition of p53 function by LPA receptors was not mediated by traditional G-protein-dependent signaling pathways and so we investigated another possibility.

We noted that both the LPA_1 and LPA_2 receptors, but not LPA_3 receptors, contain consensus PDZ-binding domains (S/T-X-V/L) in their cytoplasmic tails (Fig 13A), which would permit them to associate with PDZ domain-containing proteins. To test whether interaction of an LPA receptor with a putative PDZ domain-containing protein might be important for the inhibition of p53 function, we generated a truncation mutant of the LPA_1 receptor (LPA_1 Δ361) where the final three cytoplasmic amino acids (SVV) that comprise the PDZ-binding domain were deleted. Indirect immunofluorescence studies indicated that this receptor localized to the plasma membrane and underwent agonist-induced internalization into punctate endosomal structures like wild type LPA_1 receptors (Fig. 13B). To assess signaling, we determined the ability of this mutant receptor to stimulate the $G_{12/13}$- and Rho GTPase-dependent activation of the serum response factor transcription factor in HepG2 cells. The data in Fig. 13C indicated that LPA_1 Δ361 receptor promoted the LPA-induced activation of an SRE-luciferase reporter gene plasmid similar to wild type LPA_1 receptors. In contrast to SRF stimulation, LPA_1 Δ361

receptors failed to inhibit p53-mediated transcription (Fig. 13D). These data suggested that, at least for LPA_1 receptors, the inhibition of p53 function depends upon the association with an as yet unidentified PDZ-containing protein.

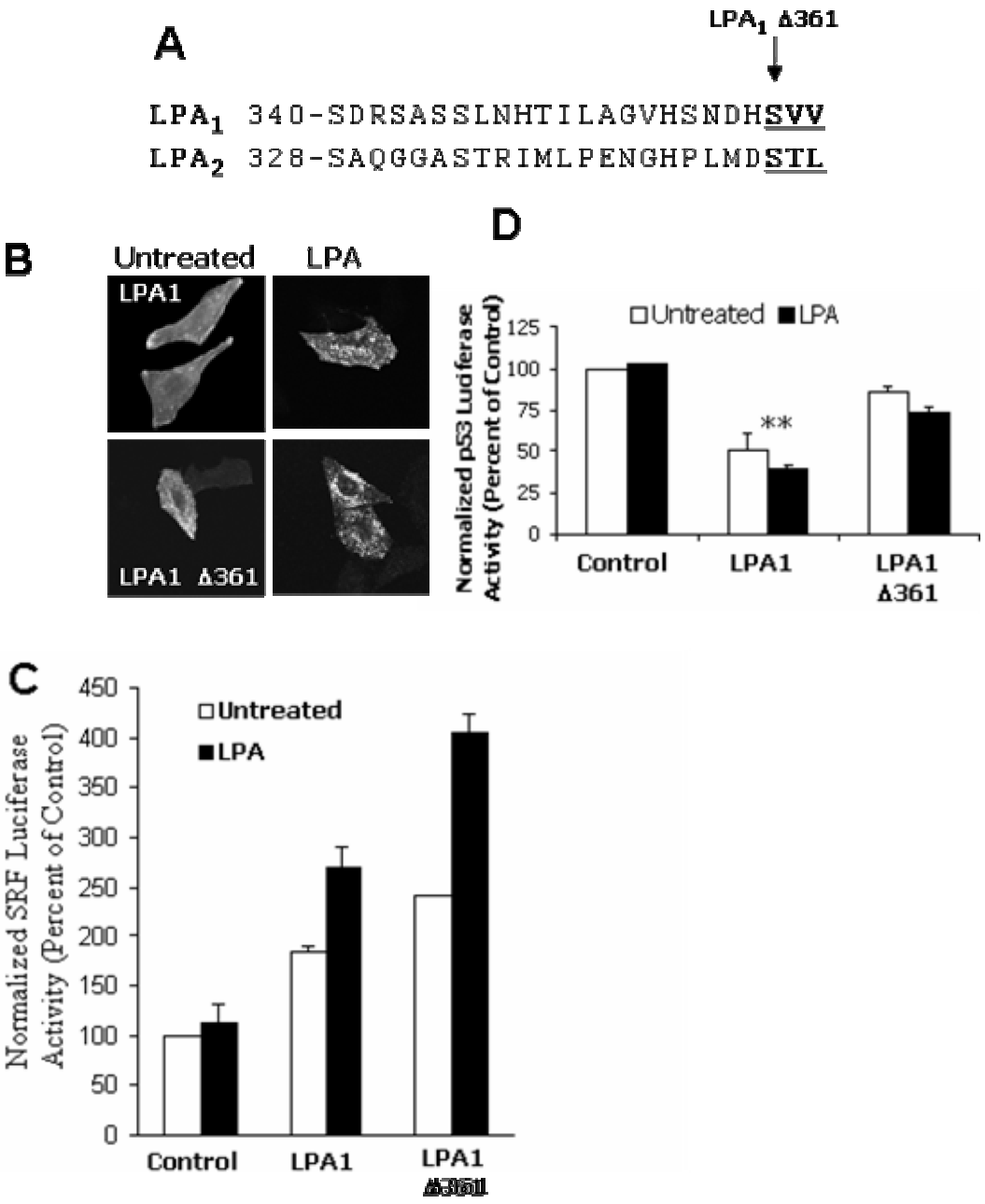

Fig. 13. The PDZ-binding domain of the LPA1 receptor is required for inhibition p53- mediated transcription. (A) Schematic representation of the C-terminus of wild type LPA1, LPA2 and the site of truncation of the LPA1-Δ361 mutant. (B) HeLa cells were transfected and after 36 hours, the cells were incubated in the absence (Untreated) or presence of 10 μM LPA for 30 min before processing for indirect immunofluorescence localization of LPA1. (C and D) HepG2 cells were transfected with plasmids encoding either SRE-luciferase (C) or p53- luciferase (D) along with pRL-TK and either pBluescript (control), wild-type FLAG -LPA1 or FLAG-LPA1-Δ361 in SFM. After 24 h posttransfection, cells were incubated in the absence or presence of 10 μM LPA for 16 h prior to determination of luciferase activity. The data (mean ± S.E.M.) are shown as a percent of control and are from a representative experiment repeated at least three times **P<0.01, compared to untreated cells.

CHAPTER 5

DISCUSSION

LPA signaling inhibited p53-mediated transcription and promoted a rapid decrease in the levels of p53 protein present in A549 lung carcinoma cells and LPA receptor-transfected HepG2 hepatoma cells. In the case of LPA_1 receptors, the inhibition of p53-mediated transcription depended upon the presence of an intact C-terminal PDZ-binding domain. Overexpression of LPA receptors strongly inhibited p53 function even in the absence of exogenously added LPA. This inhibition was prevented upon co-expression of the lipid phosphate phosphatase, LPP1, which can degrade exogenous LPA, or lipid phosphates that are produced downstream of LPA receptor activation (22). Furthermore, addition of exogenous phospholipase B, which decreases the accumulation of exogenous LPA, also blocked the inhibition of p53 function. This suggests that production of extracellular LPA may activate the transfected receptors. Consistent with this hypothesis, transfection of cells with mutant LPA_1 R124A receptors, which cannot bind LPA, failed to inhibit p53 activity indicating that the observed inhibition of p53 requires LPA receptor activation.

LPA stimulation of A549 lung carcinoma cells led to a rapid loss of p53 protein from the nucleus of these cells (Fig. 8) and a concurrent decrease in the cellular levels of total p53 and Pp53[S15] (Fig. 7). The p53 protein contains several nuclear import signals (NLS) as well as multiple nuclear export signals (NES) (127, 139, 239). In non-tumorigenic cells, association of p53 with the E3 ubiquitin ligase, MDM2, promotes

ubiquitylation and nuclear export of p53 with subsequent degradation of the protein by cytoplasmic proteasomes (83, 106, 221). Previous studies have also shown that serine 15 lies within an N-terminal NES and that phosphorylation of this residue prevents nuclear export of p53 (239). Our data demonstrate that stimulation of endogenous LPA receptors in A549 cells (Fig. 8) and transient transfection of any of the three Edg-family LPA receptors into either A549 cells, or HepG2 cells decreased Pp53[S15] in the nucleus (Fig. 9C). These results are consistent with a model where LPA signaling lowers the abundance of cellular protein of Ser15-phosphorylated p53, which in turn promotes the nuclear export of p53. Our immunofluorescence studies also showed that p53 localized to numerous punctate structures in the cytoplasm, which co-localized with anti-ubiquitin antibodies (Fig. 8A). The decrease in Ser15-phosphorylated p53 could result from either LPA-mediated inhibition of kinases that phosphorylate p53 at this site (e.g., ATM or ERK) (12, 183), or by enhancement of serine/threonine phosphatases that dephosphorylate p53 at this site (e.g., PP5) (240).

Consistent with the loss of nuclear p53 protein, we observed a decrease in p53-mediated transcription in LPA stimulated cells (Fig. 9). It was intriguing that over-expression of LPA receptors alone was sufficient to promote the inhibition of p53-mediated transcription. However, several lines of evidence support the specificity of this response. First and most important, stimulation of native, untransfected A549 cells with LPA inhibited p53-mediated transcription (Fig. 9A, control cells). Second, transfection of HepG2 cells with the LPA_1 R124A receptor mutant did not inhibit p53-mediated transcription (Fig.10A). Arginine 124 is located in the extracellular domain of the LPA_1 receptor and is critical for binding to LPA; mutation of this residue to alanine inhibits

LPA binding and activation of the receptor (172, 217). Third, coexpression of LPA_1 and the lipid phosphate phosphatase, LPP-1, prevented the inhibition of p53- mediated transfection (Fig. 10B). Over-expression of LPP-1 attenuates the stimulation of MAP kinases, phospholipase D, and cell division by exogenously added LPA (98, 148). Finally, we also observed that LPA inhibition of p53-mediated transcription is prevented by treatment of A549 cells with exogenous phospholipase B, which degrades lysophosphatidylcholine and LPA and inhibits LPA signaling (207) (Fig. 10B). These data indicate that LPA produced by the A549 and HepG2 cells is sufficient to activate the transfected LPA receptors. To further support the specificity of LPA-induced inhibition of p53, we observed that over-expression of the M_2 mAChR, another G_i-coupled receptor did not inhibit p53-mediated transcription (Fig. 12A), but rather it increased p53-mediated transcription. Together with the finding that pertussis toxin did not rescue the LPA-induced inhibition of p53 activity; our data suggests that the inhibition of p53 is independent of LPA receptor stimulation of G_i-mediated signaling pathways.

How do LPA receptors inhibit p53 activity? At least in the case of the LPA_1 receptor, the mechanism of p53 inhibition is likely to involve association with a PDZ-containing protein. This hypothesis is based on the finding that a mutant LPA_1 receptor, which lacks the C-terminal PDZbinding domain (LPA_1 Δ361), is unable to inhibit p53-mediated transcription (Fig. 13). However, this mutant LPA receptor is functional in LPA-mediated signaling since it was able to undergo agonist-induced internalization. The mutant also stimulated SRF-mediated transcription which is Rho- and $G_{12/13}$ dependent (Fig. 13B and C). This suggests that the lack of inhibition of p53-mediated transcription by LPA_1 Δ361

is specific to this signaling event and not due to a global defect in LPA signaling by this receptor.

Many GPCRs, such as β-adrenergic receptors contain C-terminal PDZ-binding domains and associate with a variety of PDZ-containing proteins such as PSD-95 (92) and the Na/H exchanger regulatory factor (NHERF) 1 and 2 (78, 79). Although several proteins that interact with the C-terminal tail of the LPA_2 receptor have recently been reported (141, 225), thus far no LPA_1 interacting proteins have been reported. Of particular interest is the recent finding that NHERF2 binds to the PDZ-binding domain of the LPA_2 receptor to promote phospholipase C β3 activation (141). We are currently investigating whether the LPA_2-induced inhibition of p53 activity requires its PDZ-binding domain. It is intriguing that over-expression of LPA_3 also inhibits p53-mediated transcription and yet this receptor does not contain a consensus PDZ-binding domain raising the possibility that LPA_3 may inhibit p53 activity through a distinct mechanism from LPA_1.

LPA is a potent mitogen for a variety of normal and tumorigenic cells and is known to promote both cell proliferative and anti-apoptotic signaling pathways (129). Studies on the cellular mechanisms involved in mediating the pro-growth effects of LPA have focused on the activation of Ras/MAP kinase and Rho GTPase signaling pathways as well as stimulation of the serine/threonine kinase, Akt. However, relatively little is known about the effects of LPA signaling on cell cycle regulators such as the p53 tumor suppressor. Our studies highlight a previously unappreciated effect of LPA signaling, namely that it potently inhibits transcriptional activation of p53 and enhances p53 degradation. In normal cells, activated p53 promotes G_1 cell cycle arrest and/or apoptosis

in response to DNA damage (88). p53 is either mutated or inactivated in 50% of all cancers, which enhances the ability of cancer cells to evade cell cycle arrest and apoptosis. In tumor cells that contain wild type p53 protein key down-stream effectors such as the cyclin kinase inhibitor, $p21^{CIP1}$, are often mutationally inactivated. We propose that LPA receptor-mediated inhibition of p53 activity in cells that express wild type p53, such as A549 cells, may enhance cancer cell survival by preventing the activation of apoptosis. The combined effects of LPA on cancer cells to promote cell proliferative signaling, while inhibiting p53-mediated transcription are likely to contribute to the potent mitogenic effect of this lipid growth factor on cancer cells.

PART II:

CHARACTERIZATION OF THE AGONIST-INDUCED ENDOCYTOSIS OF THE LYSOPHOSPHATIDIC ACID (LPA_1) RECEPTORS THROUGH A DYNAMIN2- AND RAB5-DEPENDENT INTERNALIZATION PATHWAY

CHAPTER 6

INTRODUCTION

LPA is a major serum phospholipid that exhibits growth factor-like properties towards a variety of cells (131). Some of the pleiotropic cellular effects exerted by LPA include the stimulation of cell migration (135), tumor cell invasion (194) and neurite retraction (97), as well as growth stimulation of a variety of normal and tumorigenic cells (209). Most of these effects are mediated by the binding of LPA to cell-surface serpentine receptors that couple to and activate heterotrimeric G proteins of the G_i, G_q and $G_{12/13}$ families (218). LPA stimulation of cells via these G-protein pathways has been shown to inhibit adenylyl cyclase, induce intracellular calcium release, activate rho GTPases, stimulate transcription of serum responsive genes, and activate the ERK1/2 mitogen-activated protein kinases (86, 96, 132, 209).

Molecular cloning studies have identified three mammalian receptors that belong to the endothelial differentiation gene (EDG) family of G-protein-coupled receptors (GPCRs) that are activated by LPA: LPA_1/EDG-2, LPA_2/EDG-4 and LPA_3/EDG-7 (30). These receptors were initially termed EDG receptors since they share sequence homology with the sphingosine-1-phosphate (S1P)-specific $S1P_1$/EDG-1 receptor (87). Heterologous expression studies have shown that all three receptors can activate Gi- and Gq-coupled signaling pathways (96). LPA_1 and LPA_2, but not LPA_3, can additionally stimulate G12/13-coupled pathways. Recent studies have also indicated that LPA is a potent mitogen for ovarian cancer epithelial cells and that increased LPA concentrations

in the serum and ascites might serve as a useful biomarker for ovarian cancer (53, 131, 227).

These studies also suggest that expression of LPA_2 or LPA_3, which are not expressed in normal ovarian epithelial cells, is upregulated in ovarian cancer epithelial cells (53). Interestingly, LPA_1 has been shown to be a negative regulator of ovarian cancer cell growth (67). Of the three known LPA receptors, LPA_1 shows the widest tissue distribution. Human LPA_1 is expressed in adult organs such as brain, heart, ovary, testes, colon, prostate and spleen, but is not detectably expressed in liver, thymus or lung (35, 84).

Agonist binding and activation of most GPCRs usually results in the rapid phosphorylation and endocytosis of the receptor (57). GPCR endocytosis serves as an entry point for targeting activated GPCRs into a variety of intracellular compartments including endosomes and lysosomes. Dephosphorylation of receptors in endosomes and subsequent recycling back to the cell surface constitutes GPCR resensitization, whereas targeting receptors to lysosomes for degradation is used for GPCR downregulation. Thus far, nothing is known about the trafficking or intracellular destinations of any LPA-coupled receptor.

To gain further insight into how cells regulate the activity of specific LPA receptors, we investigated the agonist-induced trafficking of the human LPA_1 receptor in HeLa cells. Our results indicate that LPA_1 is rapidly internalized into cells via dynamin2- and Rab5-dependent mechanisms in an LPA specific and LPA dose-dependent manner. Interestingly, we find that LPA_1 is internalized and recycled at a low basal level when

cells are cultured in medium that contained 10% FBS, which suggested that LPA levels in serum are sufficient to induce LPA_1 activation and endocytosis.

CHAPTER 7

MATERIALS AND METHODS

Cells, reagents and antibodies

HeLa cells were maintained in Dulbecco's modified Eagle's medium (DMEM) supplemented with 10% FBS, 100 I.U./ml penicillin, and 100 mg/ml streptomycin (complete medium) at 37°C with 5% CO2. Mouse monoclonal antibodies against the FLAG epitope tag were purchased from Sigma, mouse antibodies against the early endosomal marker EEA1 were obtained from Transduction Laboratories (Lexington, KY), mouse antibodies to the human transferrin receptor B3/25 were from Roche Molecular Biochemicals (Indianapolis, IN), and mouse anti-LAMP-2 IgG (H4B4), developed by J. T. August and J. E. K. Hildreth, was obtained from the Developmental Hybridoma Bank developed under the auspices of the NICHD and maintained by the University of Iowa, Department of Biological Sciences (Iowa City, IA). Alexa594- and Alexa488-conjugated goat anti-mouse and goat anti-rabbit IgG was purchased from Molecular Probes (Eugene, OR). Lysophosphatidic acid (1-Oleoyl-2-hydroxy-sn-glycerol-3-phosphate; LPA) and D-erythro sphingosine-1-phosphate (S1P) were purchased from BIOMOL Research Laboratories (Plymouth Meeting, PA). L-alpha-lysophosphatidylcholine (LPC), fatty acid-free BSA, and all other chemicals were purchased from Sigma. Stock solutions of LPA and LPC were prepared by dissolving in dH2O and sonication, whereas S1P was prepared by dissolving in methanol, followed by

evaporation under a stream of nitrogen gas. The dried S1P was then dissolved in 4 mg/ml fatty acid-free BSA (Sigma) in dH2O. For lipid stimulation, cells were grown on glass coverslips for 16-24 hours at 37°C in complete medium and then incubated in serum-free DMEM (SF-DMEM) for an additional 16 hours at 37°C prior to incubation with the appropriate lipid in SF-DMEM.

DNA manipulations and transfections

An expression plasmid encoding the human LPA_1 receptor containing an amino terminal FLAG epitope tag (11) was the kind gift of Junken Aoki (University of Tokyo, Japan). The FLAG epitope tag in this receptor is exposed to the extracellular environment when LPA_1 is at the cell surface. To enhance cell-surface expression of LPA_1, PCR was used to attach a signal leader sequence from the influenza hemaglutinin protein onto the amino terminus of FLAGtagged LPA_1 cDNA using the following primers: 5'-ATCATGAAGACCATCATCGCCCTGAGCTACATCTTCTGCCTGGTGTTCGCCGA CTACAAAGACGATGACGATAAA-3'and 5'-GATCTCAAACCACAGAGTGATC-3'. Following PCR amplification, the cDNA product was subcloned into the eukaryotic expression vector pcDNA 3.1/V5-His using a TOPO TA Cloning Kit (Invitrogen, Carlsbad, CA) All DNA sequences were confirmed by DNA sequencing (Emory DNA Sequencing Core Facility, Atlanta, GA).

To generate stable HeLa cell transfectants, wild-type (WT) LPA_1 was transfected into HeLa cells using the calcium phosphate coprecipitation method (Radhakrishna and Donaldson, 1997). At 36 hours after transfection, cells were detached and re-plated at a

1:25 dilution into complete medium containing 600 μg/ml G418 (Life Technologies, Gaithersburg, MD). Approximately two weeks later, G418-resistant clones were amplified and tested for LPA_1 expression by indirect immunofluorescence microscopy. For immunolocalization studies, HeLa cells were grown on glass coverslips to approximately 50% confluency and transfected in six-well dishes using the calcium phosphate method. The cells were transiently co-transfected with either WT and mutant plasmids encoding green fluorescent protein (GFP)-Rab5 along with plasmids for FLAG-tagged LPA_1 into six-well dishes using 5 μg of Rab5 DNA or WT and mutant dynamin plasmids (10 μg of dynamin plasmid per well) with FLAG-tagged LPA_1.

Indirect immunofluorescence

At 22 hours after transfection, the cells were rinsed with SF-DMEM and incubated in the same medium for 16-24 hours before further treatments. Cells were treated as described in the figure legends, fixed in 2% formaldehyde in PBS for 10 minutes, and rinsed with 10% FBS and 0.02% azide in PBS (PBS-serum). The cells were permeabilized by treating with ice-cold methanol for 30 seconds at –20°C, rinsing with ice-cold PBS twice and incubating in PBS-serum for 5 minutes. Fixed cells were incubated with primary antibodies diluted in PBSserum containing 0.2% saponin for 45 minutes, and then washed (three times, 5 minutes each) with PBS-serum. The cells were then incubated in secondary antibodies diluted in PBS-serum plus 0.2% saponin for 45 minutes, washed with PBS-serum (three times, 5 minutes each) and once with PBS, and mounted on glass slides. Samples were observed using an Olympus BX40 epifluorescence microscope equipped with a 60X Plan pro lens and photomicrographs were prepared using a Spot RT

monochrome ‘C’ digital camera (Diagnostic Instruments, Sterling Hts, MI). The fluorescence images were photographed using the same exposure time and processed identically using Adobe Photoshop 5.0.

Quantitation of LPA_1 internalization

HeLa cells expressing FLAG-tagged LPA_1 were treated as described in the figure legends and fixed as described above. The fixed cells were labeled with 10 μg/ml concentration of Alexa488-labeled conconavalin A (ConA), which was obtained from Molecular Probes in the absence of detergent permeabilization to label the plasma membrane uniformly. The cells were then washed with PBS/serum and labeled with mouse anti-FLAG antibodies (M1) and Alexa594- labeled goat anti-mouse antibodies in the presence of 0.2% saponin as described above. Photomicrographs of 24 cells per time point or experimental treatment were obtained from a total of three independent experiments using a Zeiss (Heidelberg, Germany) LSM 510 laser scanning confocal microscope equipped with a 63X̣Plan-Apochromat oil immersion lens. The percentage of cell-surface receptors was determined by measuring the extent of LPA_1 colocalization with the cell-surface marker Alexa594-labeled ConA. Quantitation of co-localization was performed as described previously using Metamorph Imaging System Software (Universal Imaging Corporation, West Chester, PA) (215). Briefly, background was substracted from unprocessed images and the percentage of LPA_1 pixels (red) overlapping ConA pixels (green) was measured. The data was normalized to untreated cells (time=0) and the percentage of internalized receptors was calculated by subtracting the percentage of cell-

surface receptors from 100%. The data is presented as mean (± s.e.m.) and statistical analysis was performed using ANOVA followed by a Dunnett's post-hoc test.

Immunoblotting

At 30-36 hours after plating, cells were detached from a T-75 flask with trypsin/EDTA or scraped from culture dishes after the indicated treatment, washed twice with ice-cold PBS, and pelleted by centrifugation at 300 *g* for 5 minutes at 4°C. The pellets were resuspended in 100-200 μl of cell lysis buffer (1% NP-40, 1% sodium deoxycholate, 0.1% SDS, 0.15 M NaCl, 0.01 M sodium phosphate pH 7.2, 2 mM EDTA, 50 mM NaF, 0.2 M sodium orthovanadate, 0.02% azide, 100 μg/ml leupeptin and 0.1 mM PMSF) and incubated on ice for 15 minutes. Detergent-insoluble material was removed by centrifugation at 13,000 *g* for 10 minutes at 4°C. The samples (30 μg of protein per lane) were then separated by SDS-PAGE on 10% gels and transferred to nitrocellulose paper. MAP kinase activation was detected using the PhosphoPlus p44/42 MAP Kinase antibody kit (Cell Signaling, Beverly, MA) and LPA_1 was detected using an affinity-purified rabbit anti-FLAG antibody (Sigma). The binding of primary antibodies was detected by enhanced chemifluorescence detection (Amersham Biosciences, Piscataway, NJ).

Measurement of serum response factor (SRF) activity

A transcriptional reporter gene assay (Clontech) was used to monitor the activity of SRF. For these studies, we used the HepG2 human hepatoma cell line since this cell does not contain functional LPA receptors (61). Approximately $7x10^4$ HepG2 cells were plated in

96-well dishes and transfected with 0.2 μg plasmid encoding FLAG- LPA_1, 0.2 μg pSRE-luc, 0.05 μg pRL-TK and either 0.2 μg of pBluescript KS+ or 0.2 μg of the GTPase (dynamin or Rab5) construct. Cells were transfected in SF-DMEM using lipofectamine (Invitrogen) at 1 μl lipofectamine per 0.4 μg DNA. pSRE-luc encodes firefly luciferase and contains three tandem copies of the serum response element upstream of a basal promoter; luciferase expression is strongly stimulated by SRF. The pRL-TK construct constitutively encodes *Renilla reniformis* luciferase whose expression is controlled by a thymidine kinase promoter; *Renilla* luciferase expression serves to monitor transfection efficiency. After incubation with the DNA complexes for 24 hours, the cells were rinsed with SF-DMEM and incubated in the same medium with either no additions or 1 μM LPA for an additional 16 hours. Both firefly luciferase and *Renilla* luciferase activity was measured using the Dual Luciferase Reporter Assay System (Promega, Madison, WI) and data were collected with a TD-20/20 luminometer (Turner Designs, Sunnyvale, CA). Normalized luciferase activity was calculated by dividing the firefly luciferase activity by the *Renilla* luciferase activity. Statistical analysis was performed using a single-factor ANOVA followed by a Tukey's statistical test.

CHAPTER 8

RESULTS

Expression and functional analysis of epitope-tagged LPA_1 receptors in HeLa cells

To investigate the consequences of agonist stimulation on the intracellular trafficking of human LPA_1, we established a stably transfected HeLa cell line expressing human LPA_1 containing an amino-terminal FLAG epitope tag. Western blotting showed that FLAG-tagged LPA_1 was expressed as a protein of approximately 43 kDa in cell extracts prepared from stably transfected HeLa cells (Fig. 14A, E2), but was not detected in extracts from untransfected HeLa cells (Fig. 14A, H). This is consistent with a molecular mass of approximately 41 kDa that was previously reported for human LPA_1 (65).

Since HeLa cells are known to express endogenous LPA_1 and LPA_2 receptors, we wanted to determine the time course of LPA-induced activation of signaling for later comparison with the time course of agonist-induced LPA_1 endocytosis. Stimulation of many cell types with LPA induces a rapid, but transient, activation of the mitogen-activated protein kinase (MAPK) pathway (van Corven et al., 1992). Thus, we examined the time course of LPA-induced activation of the endogenous MAP kinases ERK1/2 (Fig. 14B) both in stably transfected HeLa cells expressing FLAG-tagged LPA_1 and in untransfected HeLa cells. ERK1/2 activation was assessed using commercially available antibodies that recognize the dually phosphorylated, active form of ERK1/2. In cells stably expressing FLAG- LPA_1, the levels of activated ERK1/2 increased rapidly from 1 to 5 minutes following treatment with 10 μM LPA, with peak activation occurring

between 5 and 10 minutes, and then steadily decreased such that very little activated ERK1/2 could be detected after 30 minutes of LPA treatment. In the absence of LPA treatment, ERK phosphorylation was not detected. Untransfected HeLa cells also exhibited a rapid increase in activated ERK1/2; however, we consistently observed that the peak ERK activation occurred between 10 and 30 minutes. This response was slightly slower than that observed in cells over-expressing FLAG- LPA_1 and was most probably due to enhanced ERK activation through the elevated levels of LPA_1 present in the FLAG- LPA_1-expressing cells. Taken together, these results indicated that LPA stimulation induced a rapid but transient activation of MAPK in HeLa cells.

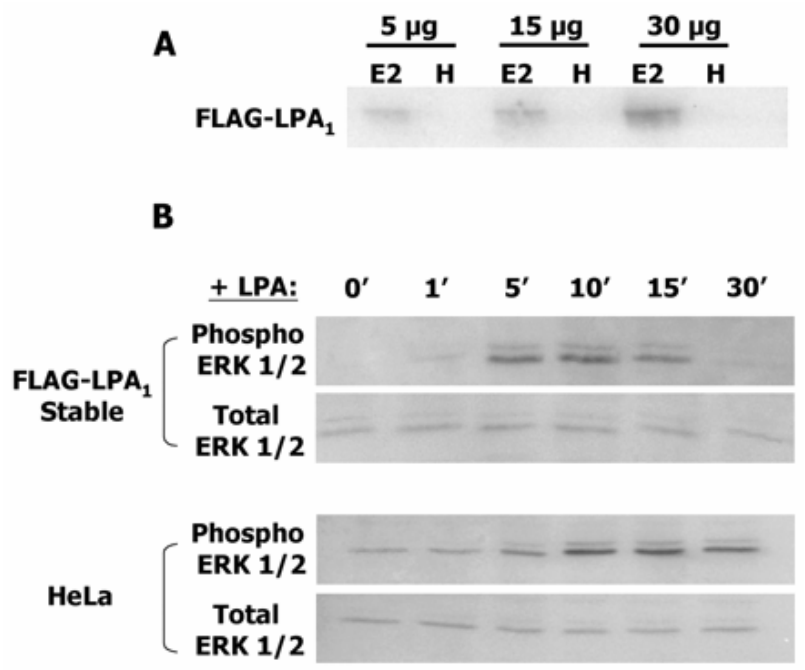

Fig. 14. Stable expression of human LPA_1 in HeLa cells and LPA stimulation of ERK1/2 activity. (A) Cell extracts were prepared from either untransfected HeLa cells (H) or from stably transfected HeLa cells expressing LPA_1 (E2). Various amounts of extracts were separated by 10% SDS-PAGE, transferred to nitrocellulose and probed with rabbit anti-FLAG antibodies and processed for chemiluminescence detection. A single band of approximately 43 kDa was detected by anti-FLAG antibodies in extracts prepared from stably transfected LPA_1-expressing cells, but not from untransfected HeLa cells. (B) Stable LPA_1-expressing HeLa cells or untransfected HeLa cells were stimulated with 10 µM LPA for the indicated times and washed at 4°C prior to detergent solubilization. Equal amounts of cell extracts (30 µg) were separated by SDS-PAGE and probed with rabbit antibodies against dually phosphorylated ERK1/2 or total ERK1/2 as described in the Materials and Methods. LPA-stimulated ERK activity is maximal between 5 and 10 minutes and then declines by 30 minutes in the FLAG-LPA_1 stable transfectants.

Agonist-dependent internalization and recycling of LPA1

We next determined the effects of LPA stimulation on the cellular distribution of LPA_1 (Fig. 15) using indirect immunofluorescence. Treatment with 10 μM LPA resulted in a time-dependent redistribution of LPA_1 from a predominantly plasma membrane (PM) localization, observed in unstimulated cells (Fig. 15, 0 min), to small punctate intracellular structures. These structures are likely to be intracellular endosomal compartments since they were not observed if immunofluorescence labeling was performed without detergent permeabilization (data not shown). In the absence of permeabilization, anti-FLAG antibodies only labeled the LPA_1 receptors at the cell surface by binding to the externally oriented FLAG epitope. Furthermore, the anti-FLAG antibodies did not label untransfected HeLa cells (data not shown). Endosomal staining was first observed within 10 minutes after LPA treatment and increased in fluorescence intensity such that, after 30 minutes of stimulation, LPA_1 localized predominantly to these vesicular structures. There was also a noticeable decrease in plasma membrane labeling after 30 minutes of LPA treatment (Fig. 15, 30 min). This pattern of localization was the same after 60 minutes of LPA treatment (Fig. 15, 60 min).

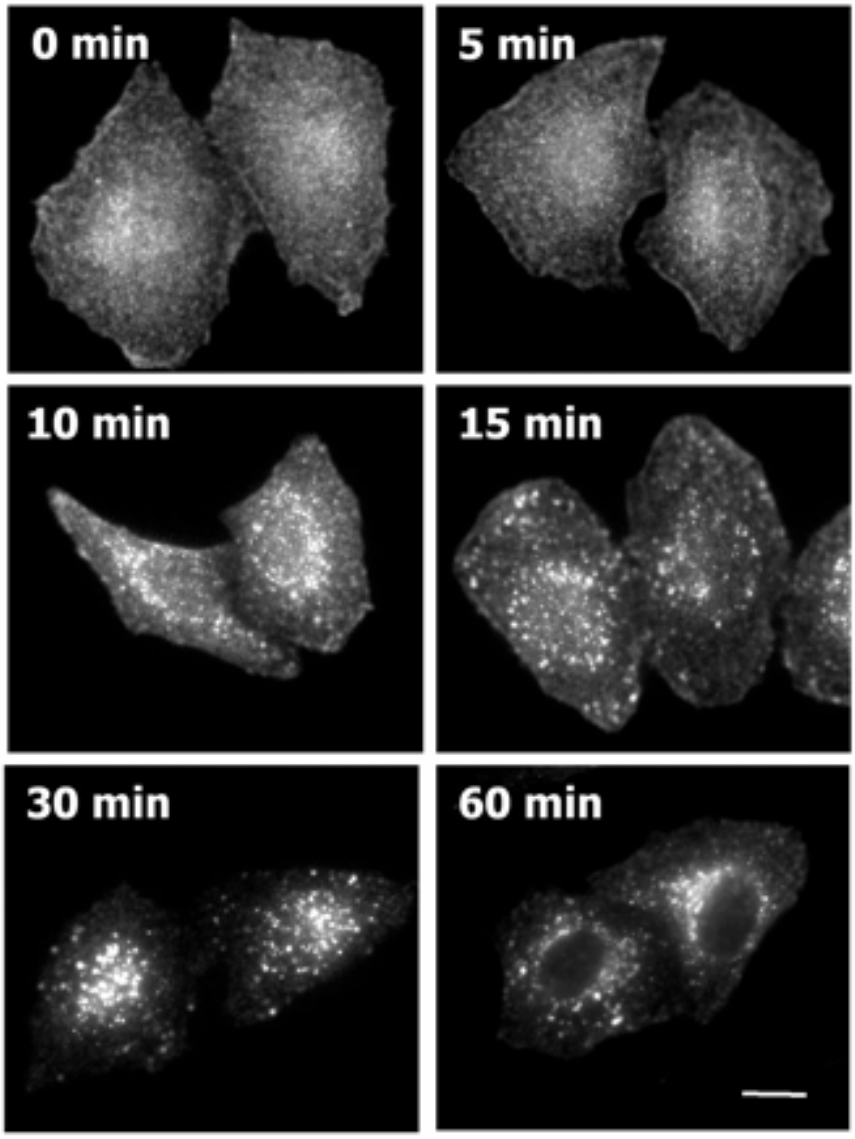

Fig. 15. LPA induces the time-dependent internalization of LPA_1 in HeLa cells. Stably transfected HeLa cells expressing LPA_1 were incubated for various times with 10 μM LPA, fixed and processed for indirect immunofluorescence localization of LPA_1 using mouse anti-FLAG antibodies and Alexa594-labeled goat anti-mouse secondary antibodies. LPA_1^+ endosomal structures are first observed after 10 minutes of LPA treatment. Bar, 10 μm.

To quantify LPA_1 internalization, we used a quantitative immunocytochemical approach that was recently used to analyze muscarinic acetylcholine receptor internalization in PC12 cells (215). This approach takes advantage of the observation that unstimulated receptors show greater co-localization with a plasma membrane marker than internalized receptors. Internalization is quantified by measuring the extent of fluorescence overlap between the receptor and plasma membrane marker using fluorescence imaging software (see Materials and Methods). In the case of the M4 muscarinic acetylcholine receptor, data obtained from the fluorescence quantitation of receptor endocytosis was indistinguishable from data obtained through radioactive ligand binding experiments (215). We measured the effects of LPA treatment on the extent of fluorescent pixel overlap and LPA_1, which was stained with mouse anti-FLAG antibodies and Alexa594-labeled secondary antibodies. Fig. 16A shows a representative panel of images, obtained by confocal microscopy, which compares the distribution of LPA_1 and Alexa488-ConA in stably transfected HeLa cells either before or after treatment with 10 μM LPA. Both Alexa488- ConA and LPA_1 are extensively co-localized at the PM in untreated cells. Following LPA treatment, there is a significant reduction in the extent of co-localization between LPA_1 and Alexa488-ConA. Quantification of the overlap in fluorescence showed that approximately 40% of surface LPA_1 receptors are internalized within 15 minutes after LPA treatment and that there is no further increase in internalization (Fig. 16B). This is comparable with the extent of internalization of β2-adrenergic receptors (β2ARs) (140, 180).

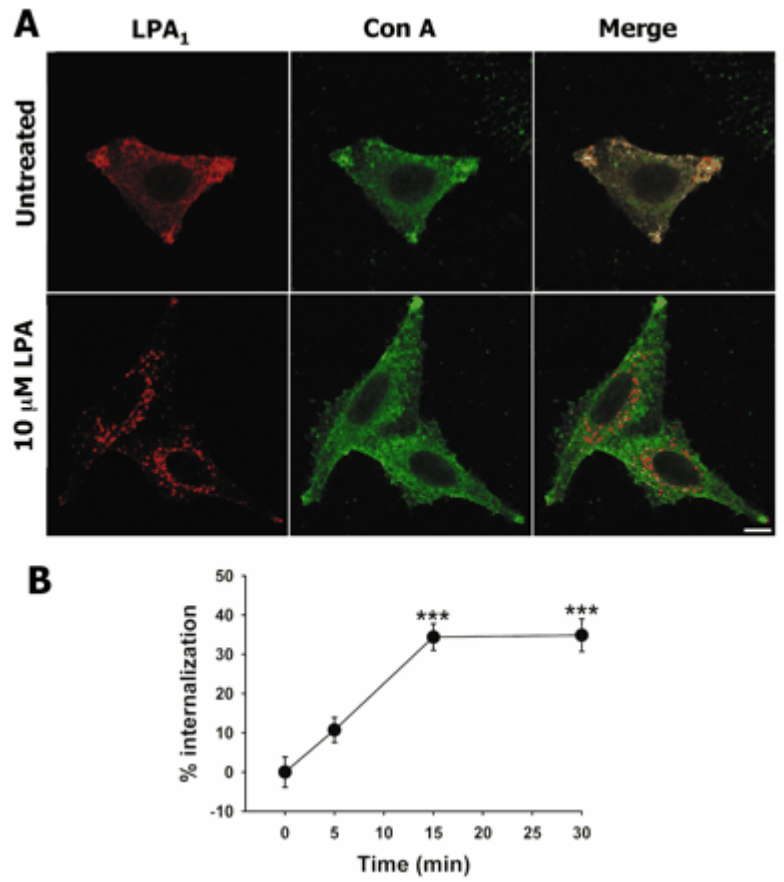

Fig. 16. Quantitation of LPA_1 internalization. LPA_1-transfected cells were incubated with 10 μM LPA for various times and then fixed and processed for quantitation of receptor internalization by laser scanning confocal microscopy as described in the Materials and Methods. (A) A representative confocal image is shown of untreated and LPA-treated cells stained with ConA to label the PM, and anti-FLAG antibodies to label FLAG-tagged LPA_1. Note that LPA_1 extensively co-localizes with ConA in untreated cells, but localizes to punctate fluorescent structures after LPA treatment. Bar, 10 μm. (B) Quantitation of internalization showed that approximately 40% of LPA_1 is internalized within 15 minutes after LPA treatment. The data is presented as the mean ± s.e.m. at each time point (n=24 cells analyzed). ***P<0.0001 compared with untreated cells.

We next sought to determine the identity of the LPA_1+ endosomal structures. We co-localized the internalized LPA_1 with different endocytic organelle markers using double-label immunofluorescence staining (Fig. 17). The internalized LPA_1 showed extensive overlap with both transferrin receptor (TfR) and the early endosomal marker EEA1. Interestingly, LPA_1 appeared to coincide more with TfR+ compartments than with EEA1+ compartments. Since TfR labeling includes small transport vesicles, sorting endosomes, as well as juxtanuclear recycling endosomes, these observations are consistent with the possibility that internalized LPA_1 traverses the same endocytic pathway as the TfR. By contrast, LPA_1 did not colocalize with the lysosomal marker LAMP-2, indicating that following short-term exposure to LPA, these receptors are not transported to lysosomes. This raised the possibility that internalized LPA_1 might recycle back to the cell surface. Internalization of other GPCRs, such as the β2AR, is thought to be required for receptor resensitization and subsequent recycling (140). Internalized β2ARs have been shown to be dephosphorylated in an early endosomal compartment prior to recycling back to the cell surface (150, 180).

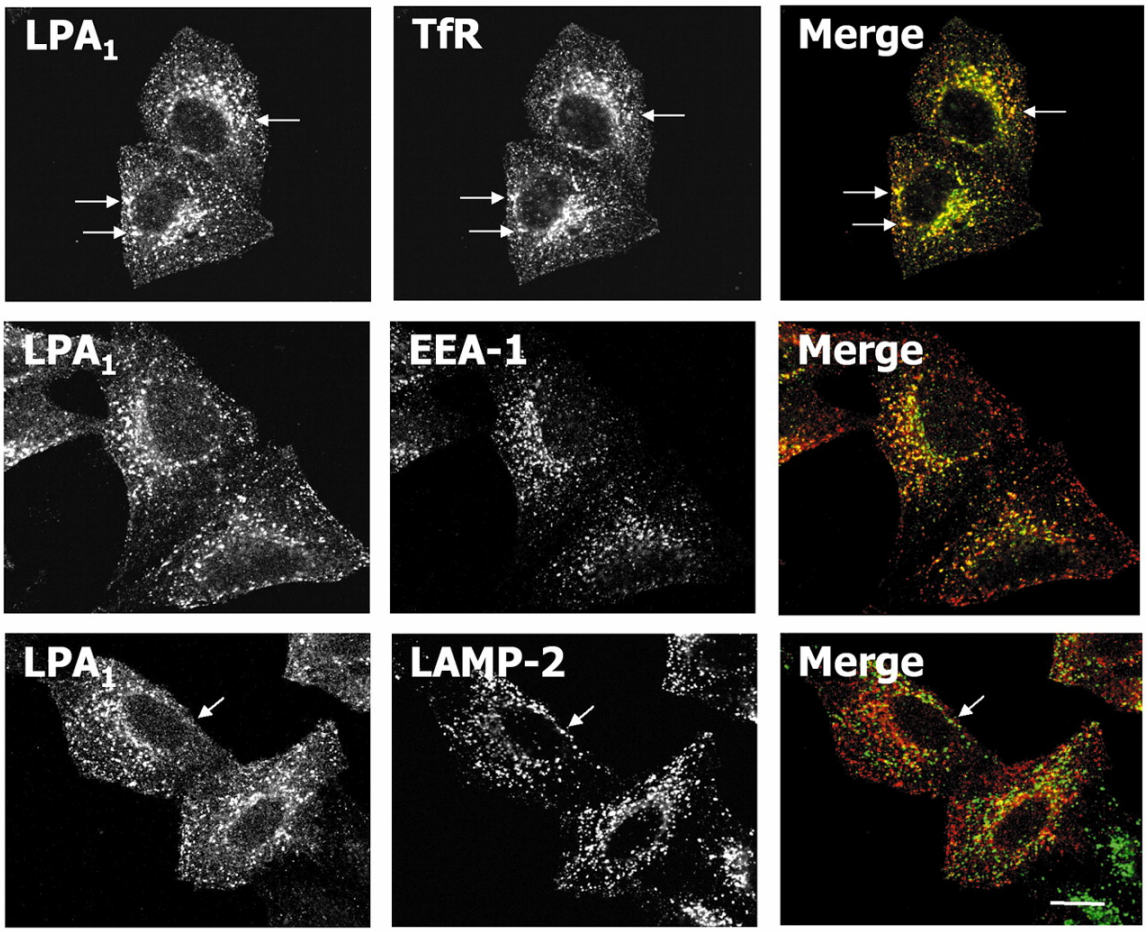

Fig. 17. Internalized LPA_1 co-localizes with the clathrin-dependent endosomal markers, EEA-1 and transferrin receptor (TfR). Stably transfected HeLa cells expressing LPA_1 were treated with 10 μM LPA for 30 minutes, fixed, processed for double-label indirect immunofluorescence and analyzed by confocal microscopy. The endosomal markers EEA-1 and TfR, and the lysosomal marker LAMP-2, were localized with mouse monoclonal antibodies followed by Alexa488-labeled goat anti-mouse secondary antibodies. LPA_1 was localized using rabbit anti-FLAG antibodies followed by Alexa594-labeled goat anti-rabbit secondary antibodies. The arrows in the upper panels indicate endosomal structures that contain both LPA_1 and TfR. The arrow in the bottom panel indicates a structure that is $LAMP2^+$, but does not contain LPA_1. Bar, 10 μm.

We investigated whether internalized LPA_1 could recycle back to the PM upon removal of LPA (Fig. 18). Cells were first treated with 10 μM LPA for 30 minutes to induce internalization of LPA_1 into LPA and then incubated at 37°C for various times prior to fixation and immunofluorescence localization of LPA_1. In the absence of LPA treatment, LPA_1 was predominantly localized to the PM (Fig. 18A, Untreated). After 30 minutes treatment with 10 μM LPA, LPA_1 localized to numerous endosomal structures (Fig. 18A, +LPA). Upon removal of agonist (Fig. 18B), LPA_1 first localized to large juxtanuclear endosomes after 5 minutes and then began to appear at the PM after 15 minutes with a corresponding decrease in endosomal labeling. Within 30 to 60 minutes after removal of agonist to prevent further stimulation and internalization, LPA_1 was predominantly localized to the PM. These observations indicated that the portion of LPA_1 receptors which previously had internalized upon LPA treatment, then rapidly recycled back to the PM upon removal of LPA while other receptors were not stimulated to internalize.

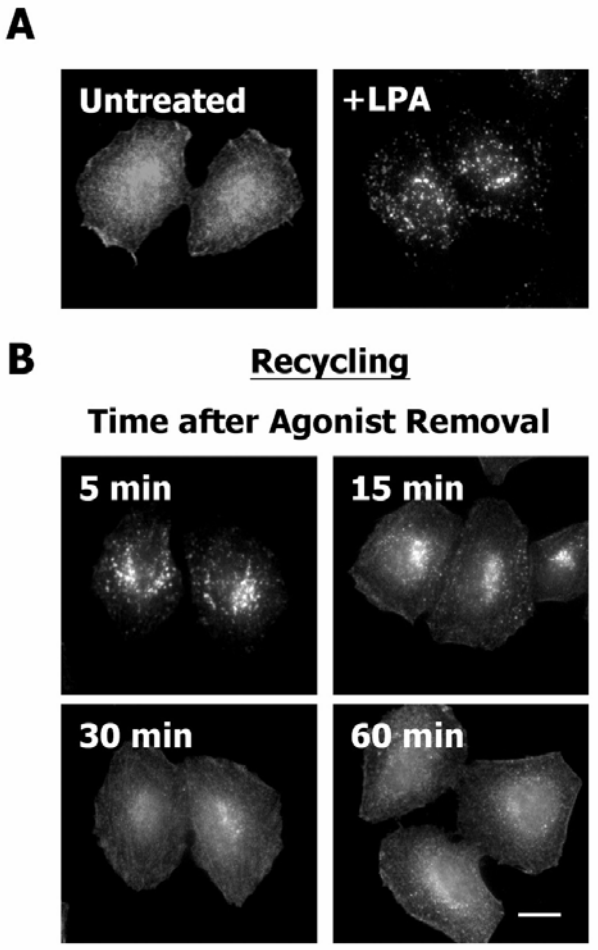

Fig. 18. Agonist removal stimulates the recycling of internalized LPA_1 back to the PM. (A) Stably transfected HeLa cells expressing LPA_1 were incubated in the absence (Untreated) or presence (+LPA) of 10 μM LPA for 30 minutes. (B) The cells were then rinsed, incubated in serum-free medium for the indicated times and processed for indirect immunofluorescence localization of LPA_1. Bar, 10 μm.

LPA_1 internalization is both dose dependent and LPA specific

To determine whether LPA-induced internalization of LPA_1 occurred at physiologically relevant concentrations of LPA, we determined the dose dependence of LPA treatment on LPA_1 internalization (Fig. 19). Concentrations of LPA in the range of 1-10 μM have been reported to be required for growth stimulation of fibroblasts (210). Following 30 minutes incubation with different concentrations of LPA, we observed that LPA_1 internalization was dose dependent and that labeling of small punctate endosomal structures was first observed after treatment with 10 nM LPA. We observed a steady increase in the number and fluorescence intensity of these endosomal structures as the concentration of LPA was increased up to 100 μM.

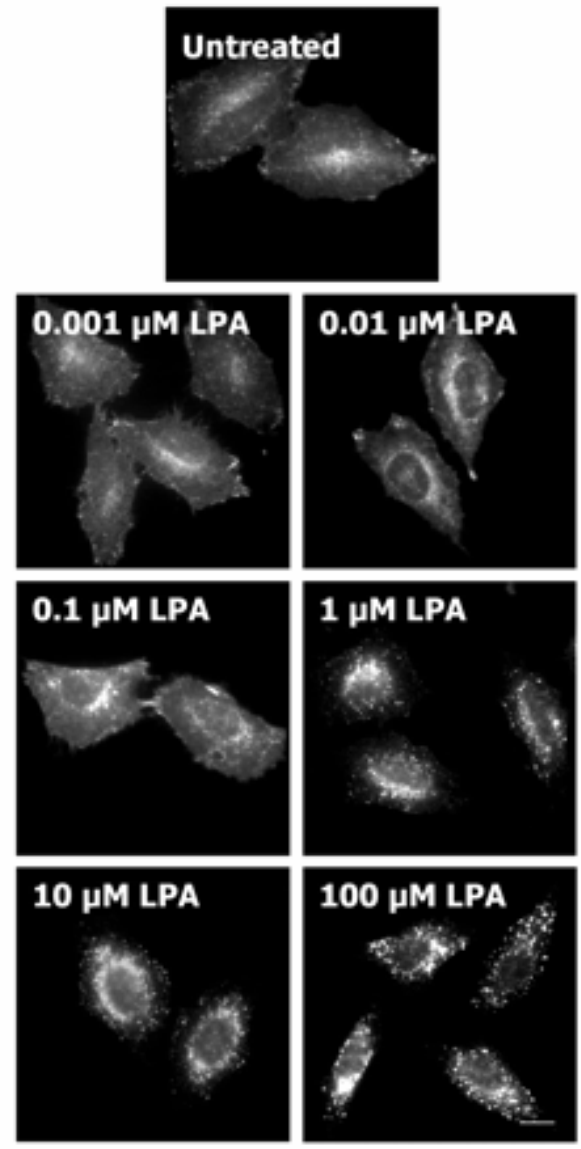

Fig. 19. Concentration dependence of LPA-induced LPA_1 internalization. Stably transfected HeLa cells expressing LPA_1 were incubated for 30 minutes with different concentrations of LPA, fixed and processed for indirect immunofluorescence localization of LPA_1. Endosomal labeling of LPA_1 can be observed even after treatment with 0.01 µM LPA. Bar, 10 µm.

To determine whether internalization of LPA_1 was specific for LPA, we examined the effects of two related bioactive lipids, S1P and LPC. S1P (100 nM) has been shown to potently and specifically activate the closely related S1P1/EDG-1, S1P3/EDG-3, S1P2/EDG-5, S1P4/EDG-6 and S1P5/EDG-8 receptors (87). Treatment of LPA_1-expressing HeLa cells with either S1P (0.1 μM or 10 μM) or LPC (1 μM) did not induce the internalization of LPA_1. Rather, LPA_1 remained at the cell surface, suggesting that neither of these related lipids stimulated LPA_1 internalization (Fig. 20). Although cells treated with S1P appeared to have larger puncta, these were not internal structures since immunofluorescence labeling in the absence of detergent permeabilization was the same as that observed in permeabilized cells (data not shown). At higher concentrations of LPC, the cells became rounded and detached from the substratum (not shown). Taken together, these results indicated that LPA_1 internalization was dependent upon LPA concentration and was specifically stimulated by LPA and not by other related lipids.

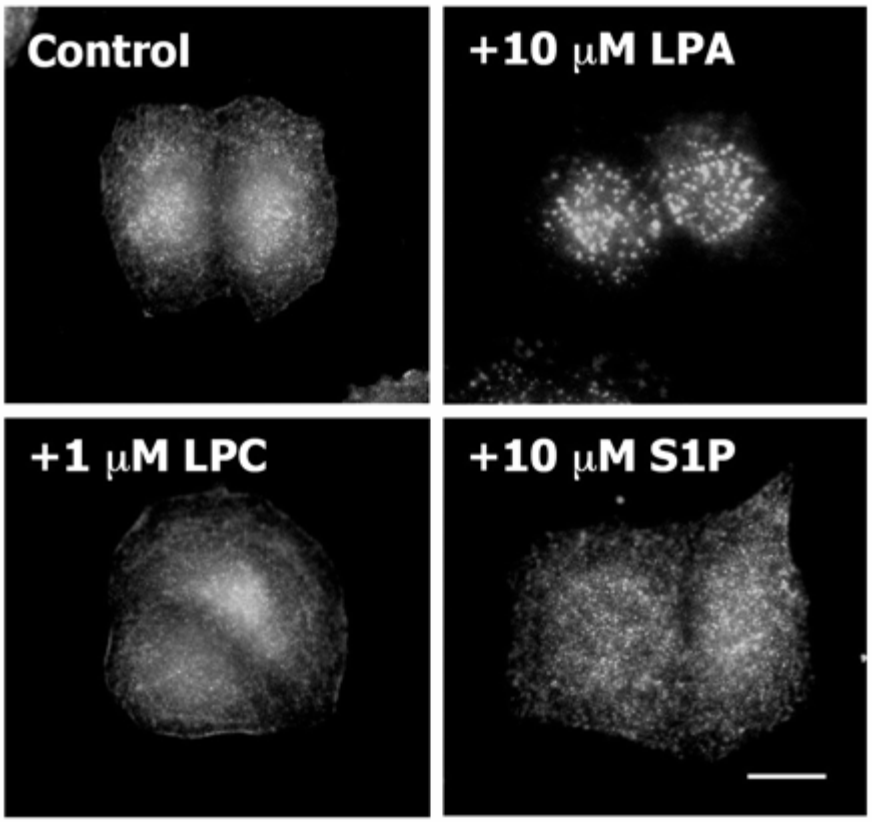

Fig. 20. Lipid specificity of LPA_1 internalization. LPA_1-expressing HeLa cells were incubated in serum-free medium for 16 hours prior to a 30 minutes incubation with no lipid (Control), 10 μM LPA, 1 μM LPC, or 10 μM S1P. Note: compare 1 μM LPC-treated cells with 1 μM LPA-treated cells in Fig. 6. The cells were then fixed and processed for indirect immunofluorescence localization of LPA_1. Bar, 10 μm.

Agonist-induced internalization of LPA_1 is dependent upon functional dynamin2 and Rab5 proteins

Since internalized LPA_1 co-localized with endosomal markers of the clathrin-mediated endocytic pathway, we investigated whether LPA_1 was perhaps internalized by clathrin-dependent mechanisms. To address this question, we examined the effects of either WT or dominant-inhibitory mutants of dynamin2 and Rab5, which are known regulators of clathrin-dependent endocytosis (24, 26, 39). Stably transfected HeLa cells expressing LPA_1 were transiently transfected with GFP-tagged mutants of dynamin2, K44A (Dyn2-GFP K44A) (Fig. 21), or Rab5a, S34N (GFPRab5a S34N) (Fig. 22), as well as GFP-tagged WT forms of these GTPases, and assessed for agonist-induced endocytosis. The 100 kDa GTPase dynamin2 is ubiquitously expressed and is involved in the severing of deeply invaginated clathrincoated pits to form clathrin-coated vesicles (39). In cells expressing Dyn2-GFP K44A, agonist stimulated internalization of LPA_1 was completely inhibited and LPA1 remained at the cell surface (Fig. 21B). In contrast to Dyn2-GFP K44A, cells transfected with WT Dyn2-GFP displayed agonist-induced internalization of LPA_1 that was indistinguishable from cells expressing LPA_1 alone. Both WT and mutant Dyn2 localized in a diffuse cytoplasmic pattern in the transfected cells. This suggested that LPA_1 internalization followed a dynamin-dependent pathway.

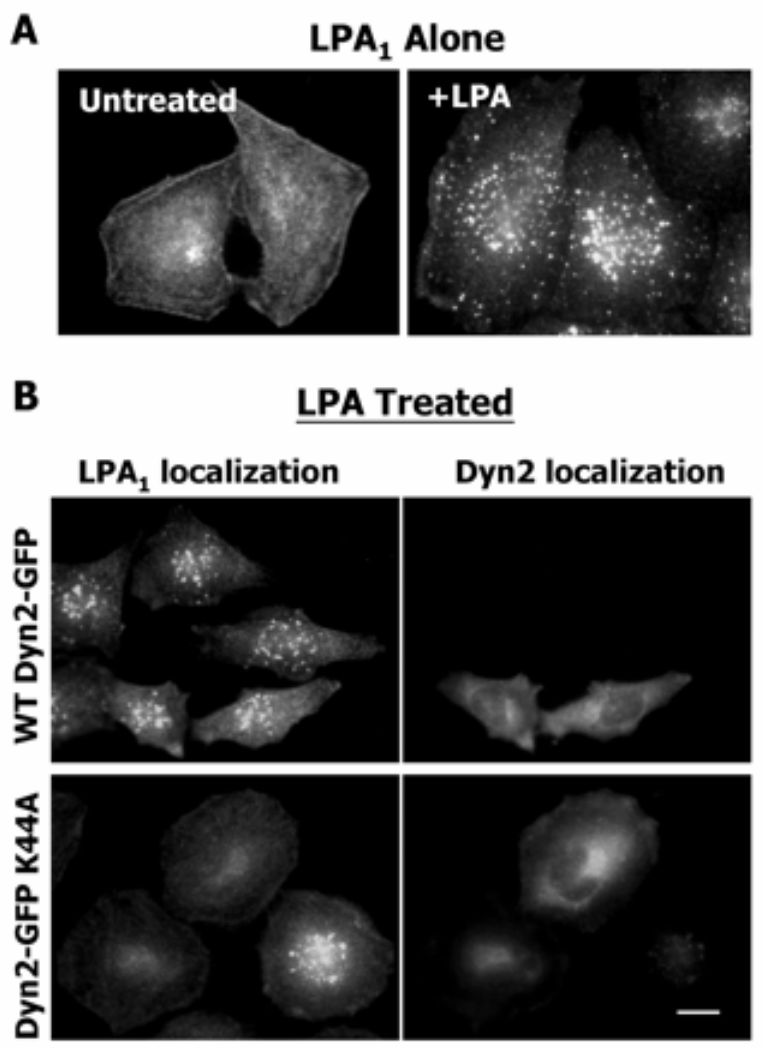

Fig. 21. Dominant-inhibitory dynamin2 K44A inhibits LPA_1 internalization. (A) LPA_1-expressing HeLa cells were incubated for 30 minutes in the absence (Untreated) or presence of 10 μM LPA prior to indirect immunofluorescence localization of LPA_1. (B) Stable LPA_1 transfectants were transiently transfected with plasmids encoding either WT Dyn2-GFP or dominant-inhibitory Dyn2-GFP K44A. The cells were then incubated with 10 μM LPA for 30 minutes, fixed and processed for indirect immunofluorescence localization of LPA_1 using mouse anti-FLAG antibodies followed by Alexa594-labeled goat anti-mouse IgG. Dynamin localization was determined by direct visualization of GFP fluorescence. Bar, 10 μm.

The Ras-related Rab5 GTPase is another regulator of early endocytic traffic between the PM and early endosomes (24). Rab5 is known to stimulate homotypic endosomal fusion following endocytosis. A recent study by Seachrist et al. (180) has shown the dominant-inhibitory GFPtagged Rab5a S34N mutant potently inhibits agonist-induced internalization of β2-adrenergic receptors. Similarly, expression of GFP-Rab5a S34N in LPA_1-expressing HeLa cells strongly inhibited agonist-induced internalization (Fig. 22B). In these cells, Rab5a S34N showed a diffuse cytosolic distribution throughout the cell. In these same cells, LPA_1 was localized at the cell surface and showed no vesicular labeling as observed in cells that were not transfected with GFP-Rab5a S34N. Transfection with WT GFP-Rab5a did not alter agonist-induced internalization of LPA_1, which localized to punctate internal structures as observed in cells expressing LPA_1 alone. To quantify the phenotypic effects of Dyn2-GFP K44A and GFP-Rab5a S34N on LPA1 internalization, we scored the percentage of cells expressing these mutants for the presence of LPA_1+ endocytic structures (Fig. 22C). In the absence of these mutant proteins, 71 ± 4% of the cells contained LPA_1+ endocytic structures following treatment with 10 μM LPA for 30 minutes. However, the results from three independent experiments indicated that expression of either Dyn2-GFP K44A (7 ± 4%) or GFP-Rab5a S34N (2 ± 1%) almost completely inhibited the appearance of LPA_1+ endocytic structures following LPA treatment. Taken together, these results indicated that LPA stimulated endocytosis of LPA_1 is strongly dependent upon both dynamin2 and Rab5a.

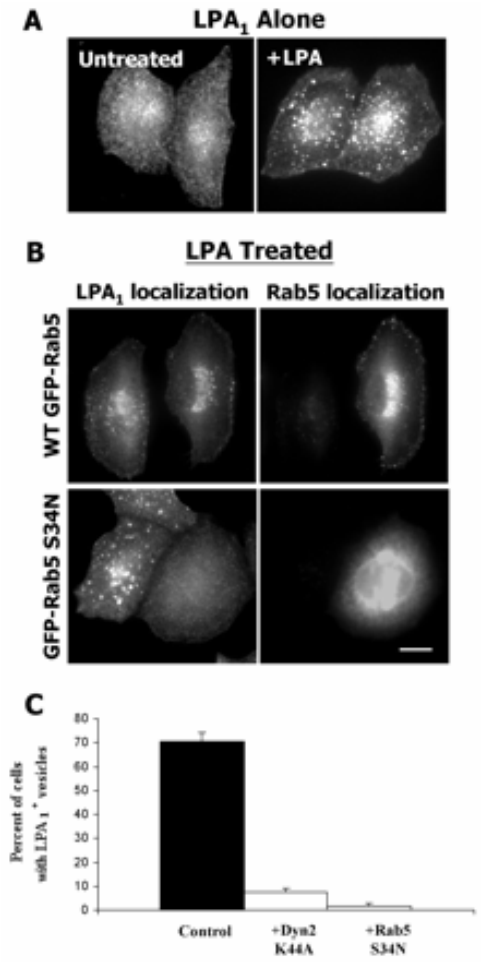

Fig. 22. Dominant-inhibitory GFP-Rab5a S34N inhibits LPA_1 internalization. (A) LPA_1-expressing HeLa cells were incubated for 30 minutes in the absence (Untreated) or presence of 10 μM LPA prior to indirect immunofluorescence localization of LPA_1. (B) Stable LPA_1 transfectants were transiently transfected with plasmids encoding either WT GFP-Rab5a or dominant-inhibitory GFP-Rab5a S34N. The cells were then incubated with 10 μM LPA for 30 minutes, fixed and processed for indirect immunofluorescence localization of LPA_1 using mouse anti-FLAG antibodies. Bar, 10 μm. (C) Quantitation of inhibitory phenotype of dominant-negative dynamin2 and Rab5 mutants on LPA_1 internalization. Stable LPA_1 transfectants that were transiently transfected with no plasmid, Dyn2-GFP K44A, or GFP-Rab5a S34N were then incubated with 10 μM LPA for 30 minutes. The cells were fixed and processed for indirect immunofluorescence localization of LPA_1. Two hundred cells per sample were scored for the presence of endocytic vesicles that contained LPA_1 in an experiment. The data from three independent experiments were expressed as the mean ± s.d. of the percentage of cells that contained LPA_1^+ endosomal structures under each transfection condition (n=3).

To test if either Rab5 S34N or Dyn2 K44A affected LPA_1-mediated signaling, we examined the effects of these mutants on LPA_1-mediated stimulation of transcription via SRF activation (3). These experiments were performed in HepG2 human hepatoma cells since these cells are nonresponsive to LPA (Fig. 23A) and do not express any known LPA receptors (61). SRF activity was monitored using a firefly luciferase reporter gene plasmid that contains three tandem copies of the serum response element upstream of a basal promoter (see Materials and Methods). HepG2 cells were transiently transfected in serum-free medium with plasmids encoding the firefly luciferase reporter plasmid, the *Renilla* luciferase reference plasmid (to normalize for transfection efficiency), and the FLAG-tagged LPA_1 expression plasmid. In addition, the cells were also transfected with either WT or mutant Rab5 or Dyn2 expression plasmids. At 24 hours following transfection, the cells were incubated either in the presence or absence of 1 μM LPA for 16 hours prior to determination of luciferase activity. In cells expressing the SRE-luciferase plasmid alone, LPA treatment did not induce luciferase expression, which is consistent with the absence of LPA receptors in these cells (Fig. 23A, SRE-Luc Alone). By contrast, cells that co-expressed LPA_1 and the SRE-luciferase construct exhibited a 1.5- to 2-fold increase in firefly luciferase activity when treated with 1 μM LPA (Fig. 23A, SRE-Luc + LPA_1). The data in Fig. 23B and 23C show that neither expression of WT Rab5 nor WT Dyn2 significantly affected the LPA_1-mediated induction of firefly luciferase activity in response to agonist treatment. Induction of SRF activity was mildly inhibited in cells expressing dominant-inhibitory Rab5 S34N. Co-expression of dominant-inhibitory Dyn2 K44A greatly elevated SRF activity in both untreated and

LPA-treated cells; however, this increase was observed in cells expressing Dyn2 K44A alone and thus was independent of LPA_1 expression (data not shown). Analysis of the LPA-dependent increase in SRF activity (Fig. 23C) showed that both Rab5 S34N (28% inhibition) and Dyn2 K44A (26% inhibition) slightly diminished LPA_1-dependent SRF activation ($P<0.05$). The fold increase in LPA-stimulated SRF activity was 72% (cells co-expressing LPA_1 and Rab5 S34N) and 74% (cells co-expressing LPA_1 and Dyn2 K44A) of that observed in cells expressing LPA_1 alone. These data indicate that Rab5 and Dyn2 are critical for the agonist-induced internalization of LPA_1 and can also influence LPA_1-dependent SRF activation.

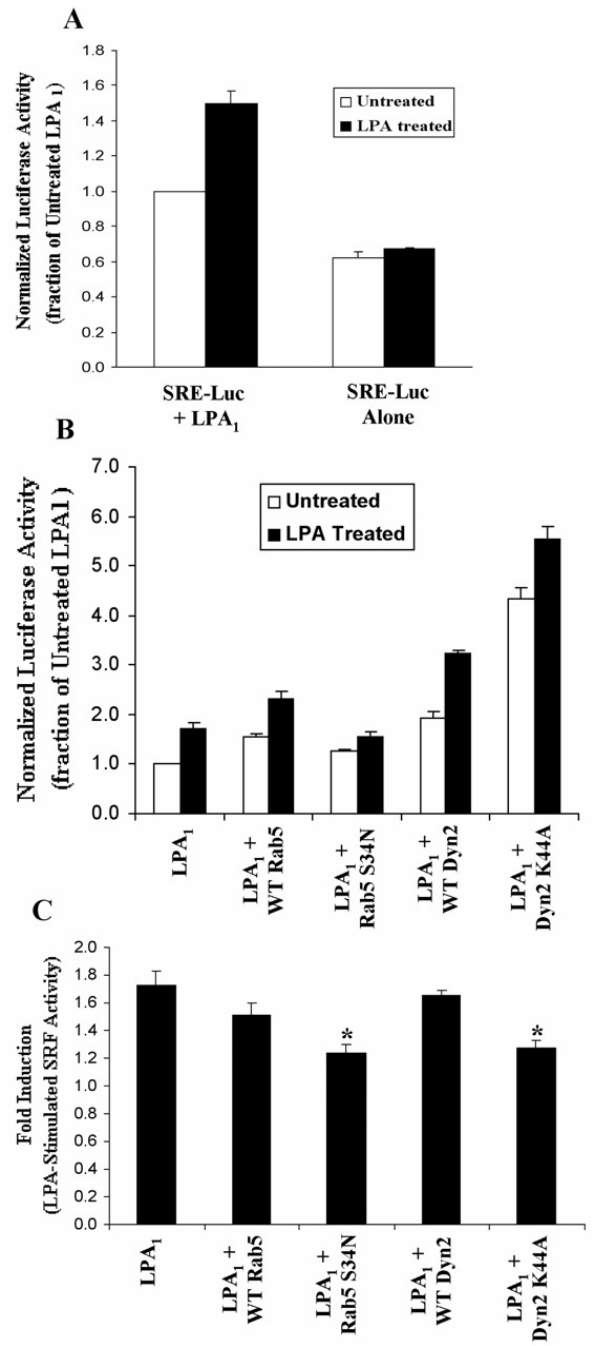

Fig. 23. Effects of WT and mutant Rab5 and dynamin2 on LPA_1 stimulation of SRF-mediated transcription. (A) HepG2 cells were transiently transfected with plasmids encoding SRE-luciferase, pRL-TK alone or with an expression vector for FLAG-tagged LPA_1. Cells were incubated in the absence or presence of 1 μM LPA for 16 hours prior to determination of luciferase. The data are expressed as the mean ± s.e.m. from independent experiments that were performed in triplicate. (B) HepG2 cells were transiently transfected with the indicated plasmids along with SRE-luciferase and pRL-TK. (C) The data shown in B above was re-analyzed to determine the fold induction of luciferase activity by LPA. Fold induction was calculated by dividing the normalized luciferase from each LPA-treated sample by the luciferase data of the corresponding untreated samples and then averaging these ratios. The data shown is the average fold induction ratios ± s.e.m. *P<0.05 compared with LPA_1.

Basal internalization and recycling of LPA1 in serum containing medium

Given that cells in culture are constantly bathed in serum containing medium, we examined whether the LPA present in medium containing 10% FBS was sufficient to trigger LPA_1 internalization. It has been estimated that normal serum levels of LPA range from 0.1 to 10 μM (227). Immunofluorescence localization of LPA_1 in cells grown in 10% serum showed that it was primarily localized to the PM with little vesicular labeling (Fig. 24A, No treatment). To investigate whether LPA_1 was internalized at a low level, we determined the localization of LPA_1 in the presence of 10% serum in the presence of the proton ionophore monensin**.** Monensin has been shown to disrupt the low pH environment of endosomal compartments and, as a consequence, disrupt receptor recycling to the PM (14). Incubation of the LPA_1 stable HeLa transfectants with 25 μM monensin resulted in a time dependent accumulation of LPA_1 in endosomal structures (Fig. 24A, +25 μM monensin, 15 min and 30 min). Labeling of these structures was first observed after 5 minutes of treatment and then steadily increased such that, after 30 minutes of treatment, the pattern of LPA_1 labeling was similar to that of cells treated with 10 μM LPA in serum-free medium for 30 minutes (Fig. 15, 30 min). Monensin treatment itself did not induce LPA_1 internalization since monensin treatment in serum-free medium did not stimulate LPA_1 internalization; internalization in serumfree medium required the addition of LPA (Fig. 24B). Furthermore, monensin treatment inhibited LPA_1 recycling in serum-free medium upon removal of LPA (data not shown). These results suggest that LPA_1 undergoes a low basal internalization and most probably recycles back to the cell surface when cells are cultured in serum-containing medium.

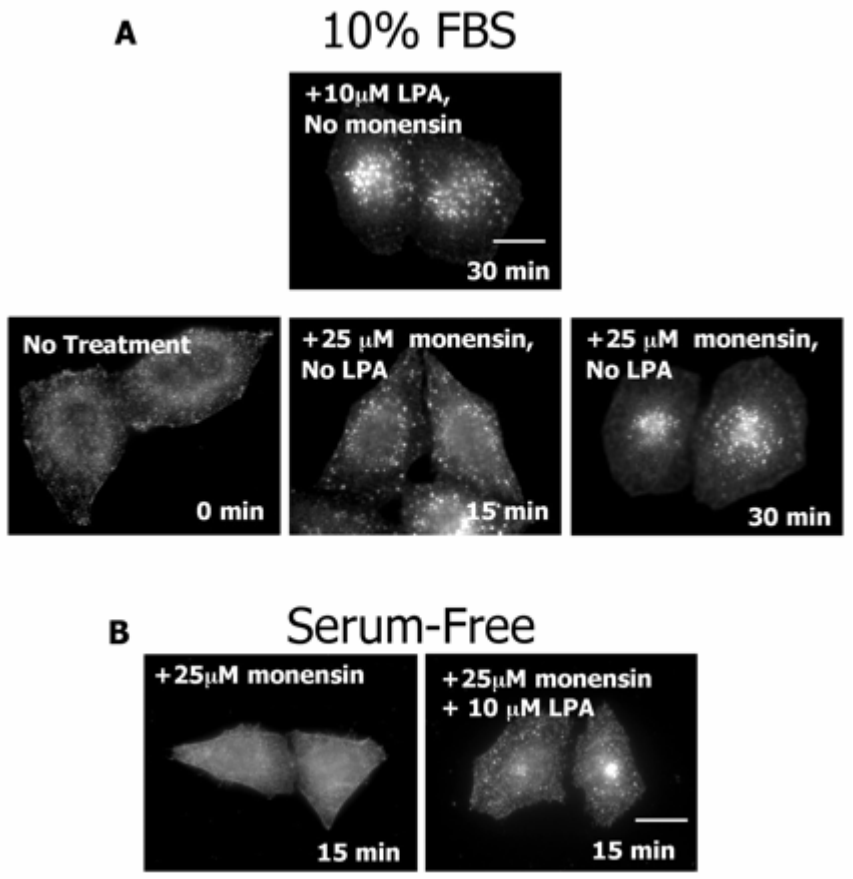

Fig. 24. LPA_1 is constitutively internalized and recycled in serum-containing medium in the absence of added LPA. (A) Stable LPA_1-transfected HeLa cells were incubated in serum-containing medium with 10 μM LPA for 30 minutes prior to fixation and indirect immunofluorescence. Alternatively, cells were incubated in medium containing 10% FBS alone (No Treatment) or incubated in this same medium with 25 μM monensin for the indicated times prior to fixation and indirect immunofluorescence localization of LPA_1. Bar, 10 μm. (B) LPA_1-expressing cells were incubated in serum-free medium for 16 hours and then incubated with either 25 μM monensin alone or 25 μM monensin and 10 μM LPA for 15 minutes prior to fixation and indirect immunofluorescence. Note that there was no vesicular labeling by LPA_1 in the absence of LPA. Bar, 10 μm.

CHAPTER 9

DISCUSSION

In this study, we investigated the agonist-induced trafficking of HeLa cells expressing FLAG-tagged human LPA_1. LPA_1 was rapidly internalized from the PM in response to LPA stimulation in both a time-dependent and dose-dependent manner (Figs 15, 16 and 19). LPA_1 internalization was specific for LPA, since neither S1P nor LPC, which are structurally similar to LPA, stimulated internalization (Fig. 20). Removal of agonist stimulates recycling of LPA_1 back to the PM (Fig. 18). Internalized LPA_1 co-localized with the endosomal markers EEA1 and TfR (Fig. 17), which label early endosomal compartments of the clathrin-dependent endocytic pathway. Dominant-inhibitory mutants of dynamin2 and Rab5a potently inhibited LPA_1 internalization and also slightly diminished LPA_1-dependent stimulation of SRF (Figs 21-23). These results are consistent with the agonist-induced internalization of LPA_1 following a clathrin- or caveolae-dependent process. Finally, our results indicate that LPA_1 cycles between the PM and endosomes at a low basal level in cells that are cultured in serum-containing medium.

LPA_1 internalization is a consequence of receptor activation

Several lines of evidence indicate that LPA_1 internalization is a consequence of agonist-induced receptor activation. First, LPA_1 internalization was dependent upon LPA concentration. We observed that concentrations as low as 10 nM LPA could induce modest LPA_1 internalization (Fig. 19). Internalization continued to increase as the LPA

concentration was increased up to 100 μM LPA. This is consistent with published reports that have shown LPA concentrations in this range (i.e. 0.1-20 μM) potently induce intracellular signaling pathways such as stress fiber formation, inhibition of forskolin-stimulated adenylate cyclase activity and growth stimulation (65, 96, 210).

Second, comparison of the time course of LPA_1 internalization with that of LPA-induced MAPK activation showed that LPA_1 internalization coincides with signal desensitization. Analysis of the time course of LPA stimulation of MAPK activity (Fig. 14B) showed that maximal MAPK activation occurred after approximately 5 minutes of LPA treatment and MAPK activity then decreased between 10 to 30 minutes of LPA treatment. By contrast, LPA_1 was primarily localized to the PM after 5 minutes of LPA treatment (Fig. 15). LPA_1 was first observed in endosomal structures after 10 minutes of LPA stimulation and this endosomal labeling steadily increased thereafter. This is consistent with the internalization of LPA_1 occurring after signal desensitization. Finally, LPA_1 internalization was specific for LPA treatment. Neither S1P (10 μM) nor LPC (0.1 μM) stimulated the internalization of LPA_1. Thus, these observations suggest that LPA_1 internalization is a consequence of receptor activation, similar to other GPCRs that undergo agonist-induced internalization.

LPA_1 is likely to be internalized via clathrin-dependent endocytosis

Several observations from this study are consistent with LPA_1 internalization occurring via clathrin-dependent endocytosis. First, we observed that internalized LPA_1 showed extensive colocalization with the clathrin-dependent endosomal markers EEA1 and TfR

(Fig. 17). TfRs are internalized via clathrin dependent endocytosis and EEA1 is a Rab5 effector that is recruited to early endosomal membranes by activated Rab5 (24).

Second, our findings that LPA_1 internalization is dependent upon the function of dynamin2 and Rab5a suggest that LPA_1 might be internalized via clathrin-dependent endocytosis. Both dynamin2 and Rab5 GTPases are known regulators of clathrin-dependent endocytosis (24, 39). Dynamin2 is ubiquitously expressed and has been shown to be required for the severing of deeply invaginated clathrin-coated pits to form coated vesicles and also for the severing of invaginated caveolae (39, 85). Following coated vesicle formation, the clathrin coats rapidly dissociate from coated vesicles in an ATP-dependent fashion. The Rab5a GTPase then stimulates the homotypic fusion of these uncoated vesicles by regulating the formation of the proper v-SNARE/t-SNARE associations and by recruiting the components of the vesicle fusion machinery (126).

Dominant-inhibitory mutants of both dynamin2 (Dyn2 K44A) and Rab5a (Rab5 S34N) both strongly inhibited the LPA-induced internalization of LPA_1 (Figs 21 and 22). In cells expressing these GTPase mutants, LPA_1 was confined to the cell surface. Given that Rab5a and dynamin2 are known regulators of clathrin-dependent endocytosis, these results suggest that LPA_1 is likely to be internalized via clathrin-dependent endocytosis. However, since Dyn2 K44A inhibits both clathrin-coated vesicle formation as well as formation of caveolae-dependent transport structures; it remains possible that LPA_1 is internalized by either clathrin- or caveolae-dependent mechanisms.

Interestingly, we observed that LPA_1 was confined to the cell surface in cells expressing GFP-Rab5a S34N. The best described role for Rab5 is in mediating the homotypic fusion of early endosomes (126). However, several recent studies have also

shown a role for Rab5 in the sequestration of receptor–ligand complexes into clathrin coated pits (123, 180). A complex of Rab5 and Rab guanine nucleotide dissociation inhibitor (Rab-GDI) has been shown to be a necessary cytosolic component for the sequestration of TfRs into coated pits (123). Thus, failure to internalize LPA_1 in cells expressing GFP-Rab5a S34N may be a consequence of a defect in receptor localization to coated pits.

Liu et al. (115), have previously shown that the S1P-coupled receptor, S1P1/EDG-1, also undergoes agonist stimulated internalization and extensively co-localizes with internalized transferrin and also partially co-localizes with lysosomal markers suggesting that S1P1/EDG-1 is internalized via clathrin-dependent endocytosis. Together with our results on LPA_1 trafficking, these observations suggest that perhaps other lysophospholipid receptors may also undergo agonist induced internalization. Whether or not internalization of these other family members occurs via clathrin-mediated mechanisms or perhaps non-clathrin-dependent pathways remains to be determined.

Role of endocytosis in regulation of LPA_1 function

GPCR endocytosis in many instances occurs subsequently to ligand-induced G-protein activation and involves receptor phosphorylation and the binding of arrestin proteins (57). Internalization is thought to contribute to either signal desensitization and/or resensitization once the internalized GPCR is dephosphorylated in an endosomal compartment. Thus, one role for LPA_1 internalization might be to facilitate its dephosphorylation and subsequent resensitization.

In addition to receptor resensitization, several observations suggest a broader role for GPCR endocytosis in receptor mediated signaling events. Several recent studies suggest that activated GPCRs can assemble multi-protein signaling complexes to initiate secondary signaling events from endosomal compartments within cells. Studies of the thrombin receptor, PAR1, the neurokinin-1 receptor, and the angiotensin 1a receptor have shown that following agonist treatment, these internalized GPCRs form complexes, via β-arrestin, with downstream components of the MAPK signaling pathway including Raf1, MEK1 and ERK2 (41, 118). Interestingly, these MAPK components colocalize with the internalized GPCRs on endosomal structures. It has been suggested that this may provide a G-protein independent mechanism to target activated ERKs to specific intracellular compartments to phosphorylate cytoplasmic targets selectively.

The data in Fig. 23 indicate that inhibition of LPA_1 internalization slightly decreased LPA-dependent induction of SRF-mediated transcription; dominant-inhibitory Rab5a S34N and Dyn2 K44A reduced LPA_1-dependent activation of SRF by 28% and 26%, respectively. However, these mutants strongly inhibited LPA_1 internalization (Fig. 22), suggesting that the primary effect of these mutants was to impede LPA_1 endocytosis. LPA-dependent activation of SRF is mediated through the stimulation of Ras- and Rho-dependent signaling (86, 210) through $G\beta\gamma$ and $G_{12/13}$ signaling pathways. Others have shown that dynamin mutants can inhibit LPA-induced ERK activation via the Ras pathway (38, 105). Thus, one possible explanation for the slight reduction in LPA_1-dependent SRF activation is that dyn2 K44A and Rab5a S34N might inhibit the Ras/ERK-dependent component of SRF activation.

It is also possible that LPA_1 internalization may be important for other LPA-dependent signaling processes. The data in Fig. 24 suggests that LPA_1 is internalized and most probably recycled at a low basal level in cells cultured in serum containing medium. Given that serum contains LPA, this basal internalization is likely to represent agonist-induced uptake. If so, then this raises the question of what the long-term signaling consequence of such basal uptake is on cells. Further studies of the role of LPA_1 localization in the regulation of LPA-stimulated signaling, as well as other LPA-coupled receptors, is likely to provide important information about the role of endocytosis in regulating LPA-induced cellular responses.

Finally, an important implication of our finding that LPA_1 is internalized in serum-containing medium is that LPA_1 internalization may be a useful diagnostic measure of the relative levels of LPA present in clinical serum samples. Recent observations indicate that serum LPA levels are increased in patients with ovarian cancer even at early stages (227). Measurement of LPA_1 internalization could be adapted into a simple bioassay for screening patient serum and/or ascites samples for LPA.

CHAPTER 10

PERSPECTIVE AND FUTURE DIRECTIONS

Discussion of LPA results

Evidence is presented in the first study of this thesis that suggests LPA signaling inhibits p53-mediated transcription and promotes a decrease in total and phosphorylated p53 [S15] protein levels (Fig. 7, 9). In addition, both LPA receptor activation and the presence of the C-terminal PDZ domain appear necessary for mediating the inhibition since LPP-1, PLB, LPA_1-R124A and LPA_1-361 have stabilizing affects on p53 transcription (Fig. 10, 13). Using chemical inhibitors and dominant-negative plasmids expressing G proteins, we were unable to link the LPA affects on p53 to any of the G_i, G_q or $G_{12/13}$ pathways directly (Fig. 12 and data not shown), suggesting that a multi-protein assemblage may be responsible which includes the PDZ binding domain.

In the second study of this thesis, analysis of the LPA-stimulated time course of MAPK activity in HeLa cells stably expressing LPA_1 showed that maximal MAPK activation occurred after approximately 5 minutes of LPA treatment (Fig. 14B top). The response time was twice as fast as that in HeLa cells which were not stably transfected (Fig. 14B bottom), indicating that LPA-activation of the LPA_1 receptor can induce the MAPK pathway rapidly, leading to an increase in cell proliferation and survival. Since the time of MAPK phosphorylation occurs within 5 minutes and the time needed for internalization is at least 15 – 30 minutes (Fig. 15, 16), it is possible that ERK is recruited to the receptor.

GPCR internalization is thought to contribute to either signal desensitization and/or resensitization once the internalized GPCR is dephosphorylated in an endosomal compartment. Thus, one role for LPA_1 internalization might be to facilitate its subsequent resensitization. We analyzed the time needed for LPA_1 receptor recycling (Fig. 18) and found that within 60 minutes after internalization, the receptor is back at the cell surface ready to receive new agonist. Also, the data in Fig. 24 suggests that LPA_1 is internalized and recycled at a low basal level in cells cultured in serum-containing medium. Our data also show that within 1 hour of LPA addition to the cells, total and activated p53 is diminished by 50% (Fig. 7) and this response was sustainable through 6 hours.

The two stories presented in this thesis converge with the consequences of LPA receptor-mediated signaling. Putting together both sets of data, LPA receptor trafficking and p53 signaling, a picture of the time course of LPA receptor-mediated signaling effects begins to emerge. Future directions could include research to further integrate these two separate, but interesting accounts of LPA's affects.

Since normal human serum contains LPA, basal receptor internalization probably represents agonist-induced uptake and that raises the question of what the long-term signaling consequence of LPA is on cells, especially damaged and cancer cells. *In vivo* it is likely that LPA receptors are constantly cycling and a fresh pool of LPA is being manufactured, allowing prolonged cell proliferation (via MAPK) and survival (via p53). Both are unappreciated effects of LPA stimulation.

Future Directions

Two lingering questions exist: first, the LPA signaling pathway initiating the inhibition and second, the mechanism of p53 inhibition by LPA receptors. To address the former question, recent studies suggest that activated GPCRs can assemble multi-protein signaling complexes to initiate secondary signaling events from endosomal compartments within cells. Several GPCRs like the thrombin receptor, PAR1, the neurokinin-1 receptor, and the angiotensin 1a are capable of forming complexes with components of the MAPK signaling pathway following agonist treatment and internalization (41, 118). Interestingly, these MAPK components, Raf1, MEK1 and ERK2, colocalize with the internalized GPCRs on endosomal structures. It has been suggested this may provide a G-protein independent mechanism to target activated ERKs to intracellular compartments to selectively phosphorylate cytoplasmic targets. Perhaps the LPA receptors are capable of forming complexes and through these associations they are able to regulate p53.

Future research on the signaling aspect should include screening LPA_1 receptor tails for protein interactions to determine the nature of the signaling pathway affecting p53. This is especially important because no one has yet been able to discover any interactions with the PDZ-binding domain of LPA_1, although the LPA_2 receptor appears to have several interactions. In this thesis, much emphasis has been placed on the PDZ-binding domain of the LPA receptor tails as the causative factor; however, it could also be the phosphorylation sites within these terminal residues which are responsible for mediating the inhibition on p53. This would better explain the quandary that LPA_3 can also mediate the inhibition, yet it lacks a PDZ-binding domain. To investigate whether these terminal phosphorylation sites are responsible, LPA_3 receptor point mutations can be designed.

Although constitutively-active G proteins did not inhibit p53, a comprehensive analysis of the pathway affecting p53 should also use drug inhibitors to pinpoint and confirm the pathway required for inhibition. For example, we feel confident from the studies using pertussis toxin (Fig. 12) that inhibiting G_i signaling does not alter the inhibitory affects; however drugs to inhibit G_q should be employed to exhaust the G protein signaling. In addition, chemical inhibitors for each component in the MAP kinase pathway are commercially available and could also be used.

Uncovering the location and mechanism of p53 degradation is also needed to fully understand how the inhibition occurs. This might become a massive project as there are so many features and components involved in the regulation of p53, yet it is one of the fundamental questions with this project and will need to be addressed in the future years. From our studies (Fig. 7), we see a large reduction of p53 within 1 h after LPA treatment, but because p53 has such a rapid turn-over rate (30 min), it is possible that the diminution could be a product of reduced p53 transcription. Otherwise, the protein is being degraded in either the nuclear or cytoplasmic proteasomes of the cell.

If the mechanism of inhibition is proteasomic degradation, further questions will need to be addressed. Importantly, what is the affect on the p53-regulator, Mdm2, and is the LPA-mediated inhibition affecting Mdm2 to then increase p53 degradation? In other words, is the decrease in p53 the result of an LPA-mediated stabilizing effect of Mdm2? Mdm2 ubiquitinates p53 and the amount of ubiquitin attached to p53 can determine when it is degraded (either immediately or much later) and where it is degraded (after polyubiquitination degradation occurs in the nucleus while after monoubiquitination degradation occurs primarily in the cytoplasm).

Finally, another important question to answer surrounding the LPA-mediated inhibition is: what exactly are the quantitative consequences of diminished p53 to the cell and which processes, if any, are affected: proliferation, motility, growth, etc.? In other words, what might be some broad beneficial or detrimental outcomes of this effect? To speculate on one possibility, in a developing embryo when you need cells to divide, having LPA and the LPA_1 receptor available is helpful to stimulate growth and proliferation. To aid these processes, limiting the amount of p53 and other proteins which can counteract the cell cycle would also be advantageous to continue unfettered cell division. The inhibition of p53 by LPA is probably just another small part of a larger goal by LPA and its receptors to stimulate the cell to proliferate and divide without regulations in specific situations.

The other project presented in this thesis, the characterization of LPA_1 trafficking, also has several interesting future directions. First, whether LPA_1 requires clathrin-mediated endocytosis, utilizes lipid rafts or is internalized via caveolae is still uncertain. Studies show that dependence on dynamin2 and Rab5 (Fig. 21, 22) for internalization and subsequent sorting to the early endosome does not rule out the aforementioned possibilities of endocytosis requirements.

Similarly, the long-term LPA_1 receptor recycling and receptor down-regulation would be exciting to follow-up because it affects other signaling properties of LPA_1. It is also interesting to speculate the rationale behind receptor cycling. Perhaps the LPA receptors are cycling because they are continually sampling their extracellular environment for the growth factor, LPA. Alternatively, the LPA receptors could be cycling for reasons similar to receptors involved in nutrient uptake if you consider LPA as a precursor for

manufacturing other phospholipids necessary to the cell. More research into the function of the LPA receptors will elucidate the reasons for the trafficking pathway and vice versa.

Putting these two stories together, future research could investigate the LPA-mediated inhibition on p53 and LPA receptor trafficking simultaneously. For example, using the mutants dynamin2 K44A and Rab5 S34N, it would be interesting to see whether transient transfection of these plasmids affected p53 inhibition. Also, it is unclear from our observations where the LPA receptors are localized when the LPA-mediated effects on p53 occur. Since the inhibition happens between 1 to 6 hours after LPA addition, perhaps long-term trafficking studies with the LPA receptor would be beneficial to understanding this process.

Broad implications of the research

LPA and the LPA receptors are critical to the body for important processes like embryonic development and wound healing. For these and other processes, LPA is capable of signaling through its receptors: cell growth, cell proliferation, motility, protection from apoptosis and cell survival. All of these processes mandate a high-level of regulation to maintain homeostasis. More than 100 distinct types of cancer exist and the majority of these have radical transformations in common: self-sufficient cell growth, unlimited cell proliferation, metastasis, sustained angiogenesis, protection from apoptosis and cell survival (82). Looking back over that list, the similarities between LPA-stimulated LPA receptor signaling and the hallmarks of cancer cells are striking. The lipid, LPA, is almost a perfect component to propagate tumorigenesis.

With every new study on LPA, the implications between LPA receptor signaling and negative consequences in cancer and other malefactions continue. Some recent examples of studies include that LPA upregulates FasL which provides immune defense because constitutive FasL expression in normal cells causes apoptosis, yet in malignant cells it allows a retaliation on natural killer cells and cytotoxic T lymphocytes (125). Other recent research has shown that tumor cells stimulate activated platelets to begin producing LPA, overexpression of LPA_1 induces tumor growth and metastasis (20) and that LPA is a survival factor in cell lines, but not normal cells (99).

Although there are beneficial effects that arise from normal functioning of LPA receptors, it would be helpful to have one antagonist that bound to all the LPA receptors for treatment of certain cancers, atherosclerosis and patients with ruptured plaques. Targeting the pool of LPA would also be another method for remediation; however, due to dimerization and transactivation of the LPA receptors from other GPCRs, this approach might be less practical. In this respect, directly targeting the source of the problem would probably be more useful. A small company in Utah, Echelon Biosciences Incorporated, has had success creating antagonists for LPA_3, but there has been limited success with LPA_1 and even less with LPA_2. More research on LPA signaling pathways and *in vivo* consequences of blocking LPA receptors is needed before LPA antagonists are considered therapeutic.

PART III:

TRANSFER OF M2 MUSCARINIC ACETYLCHOLINE RECEPTORS TO CLATHRIN-DERVICED EARLY ENDOSOMES FOLLOWING CLATHRIN-INDEPENDENT ENDOCYTOSIS

CHAPTER 11

OVERVIEW

Upon agonist stimulation, many G protein-coupled receptors such as β_2-adrenergic receptors are internalized via β-arrestin- and clathrin-dependent mechanisms, whereas others, like M_2 muscarinic acetylcholine receptors (mAChRs), are internalized by clathrin- and arrestin-independent mechanisms. To gain further insight into the mechanisms that regulate M_2 mAChR endocytosis, we investigated the post-endocytic trafficking of M_2 mAChRs in HeLa cells and the role of the ADP-ribosylation factor 6 (Arf6) GTPase in regulating M_2 mAChR internalization. Here, we report that M_2 mAChRs are rapidly internalized by a clathrin-independent pathway that is inhibited up to 50% by expression of either GTPase-defective Arf6 Q67L or an upstream Arf6 activator, $G\alpha_q$ Q209L. In contrast, M_2 mAChR internalization was not affected by expression of dominant-negative dynamin 2 K44A, which is a known inhibitor of clathrin-dependent endocytosis. Nevertheless, M_2 mAChRs, which are initially internalized in structures that lack clathrin-dependent endosomal markers, quickly localize to endosomes that contain the clathrin-dependent, early endosomal markers early endosome autoantigen-1, transferrin receptor, and GTPase-defective Rab5 Q79L, which is known to swell early endosomal compartments. These results suggest that M_2 mAChRs initially internalize via an Arf6-associated, clathrin-independent pathway but then quickly merge with the clathrin endocytic pathway at the level of early endosomes.

CHAPTER 12

INTRODUCTION

Endocytosis is an important mechanism that is used to regulate the activity of a variety of cell surface receptors, including G protein-coupled receptors (GPCRs) (33, 57). Defining the cellular mechanisms by which GPCR endocytosis is regulated is important for understanding how cells attenuate GPCR signaling as well as understanding the role of receptor endocytosis in cell signaling. Over the past several years, it has become clear that different GPCRs utilize multiple, distinct pathways of internalization that display differential sensitivities to either pharmacological inhibitors or dominant-inhibitory mutants that are pathway-selective. The mechanisms that regulate the internalization of some receptors, such as β_2-adrenergic receptors (β_2ARs), have been well characterized. However, the mechanisms that regulate both internalization and sorting of other receptors, such as the M_2 muscarinic acetylcholine receptor (mAChR), are not as well understood (211).

The sequence of events leading to GPCR endocytosis is shared by many receptors. Upon agonist binding, these heptahelical GPCRs activate heterotrimeric G protein signaling pathways, which in turn regulate a variety of intracellular processes (17). Many GPCRs then become rapidly phosphorylated either by second messenger kinases such as protein kinase A or by specific G protein receptor kinases on serine/threonine residues present in cytoplasmically exposed domains (149). In the case of β_2ARs, the critical serine/threonine residues reside in the cytoplasmic tail, whereas in mAChRs, the relevant

residues reside in the third intracellular loop (145). Phosphorylation facilitates the binding of a β-arrestin family member, which inhibits further receptor-G protein coupling and thus attenuates receptor signaling. In many instances, the binding of β-arrestin targets the GPCR to clathrin-coated pits for rapid endocytosis (58, 76, 108). Dominant-inhibitory mutants of either β-arrestins, the 100-kDa GTPase dynamin, or clathrin heavy chain (Hub mutants) inhibit the internalization of GPCRs such as β_2ARs, which use clathrin-dependent mechanisms (57, 213).

In contrast to the β_2AR, several observations indicate that the G_i-linked, M_2 mAChR is internalized via a poorly characterized clathrin-independent endocytic pathway (25, 144, 165, 177, 204, 211, 214). First, although β-arrestin binding to this receptor is essential for signal attenuation, it is not required for M_2 mAChR endocytosis in HEK 293 cells (144, 214). Second, dominant-negative clathrin Hub mutants do not inhibit the agonist-induced M_2 mAChR internalization (214). Finally, M_2 mAChR internalization shows a differential sensitivity to mutants of dynamin, which is required for clathrin- and caveolae-mediated internalization (39, 85, 219). Mutant dynamin K44A potently inhibits the clathrin-dependent internalization of GPCRs but has little effect on M_2 mAChR internalization. However, recent studies have shown that M_2 mAChR internalization is strongly inhibited by mutants of dynamin that lack the N-terminal GTP-binding domain (Δ1-272 dynamin) or the K535M dynamin mutant, which cannot be stimulated by phosphatidylinositol 4,5-bisphosphate (219). This suggests that although M_2 mAChR internalization is clathrin- and β-arrestin-independent, dynamin is still required. These findings raise the question: what is the endocytic pathway by which M_2 mAChRs are internalized? One possible regulator of M_2 mAChR trafficking might be the ADP-ribosylation factor 6 (Arf6)

GTPase, which has been shown to influence both clathrin-independent and clathrin-dependent endocytic trafficking.

The Arf family of Ras-related GTPases is known to regulate intracellular trafficking processes in both the endocytic and secretory pathways (46, 160). The Arf6 GTPase, which is located at the plasma membrane (PM) and on endosomal structures, has been shown to influence the actin cytoskeleton (19, 62, 156) as well as clathrin-independent and clathrin-dependent endocytic processes (155). Activation of Arf6 can initiate cortical actin rearrangements to form either protrusive structures or lamellar structures in cells(19, 156). It has recently been shown that the effects of Arf6 on membrane traffic and actin rearrangements in cells involves the localized elevation of cellular phosphatidylinositol 4,5-bisphosphate levels through the stimulation of phosphatidylinositol 4-phosphate 5-kinase α (23, 89).

Arf6 is also involved in the regulation of membrane trafficking in the endocytic pathway and has been shown to influence endosomal membrane recycling via clathrin-independent mechanisms (155), clathrin-dependent trafficking of transferrin receptors (36), Fc γ receptor-mediated phagocytosis in macrophages (238), apical endocytosis of polymeric IgA receptors in Madin-Darby canine kidney cells (2), and exocytosis of chromaffin granules (27). More recently, Arf6 has been implicated in the β-arrestin- and clathrin-dependent endocytic trafficking of β_2ARs (32, 151). It was shown that agonist-bound β_2ARs stimulated the β-arrestin-mediated activation of Arf6, which was required for the efficient internalization of these receptors (32). In addition, it has been shown that overexpression of the ARF6 exchange factor ARNO stimulates the release of β-arrestin

from membrane-docking sites, which then binds to the luteinizing hormone/choriogonadotropin receptor to mediate desensitization (136).

In this study, we investigated the intracellular trafficking of the M_2 mAChR in HeLa cells. Our studies suggest that M_2 mAChRs are rapidly internalized by a clathrin-independent pathway, which is sensitive to mutants of Arf6. After internalization, M_2 mAChRs, which are initially observed in structures that lack clathrin-dependent endosomal markers, localize to early endosomes of the clathrin pathway that contain the early endosome autoantigen 1 (EEA-1) and internalized transferrin receptors. Thus, the M_2 mAChR appears to utilize a novel endosomal trafficking pathway whereby it is transferred from a clathrin-independent endocytic pathway to endosomal compartments of the clathrin-dependent pathway.

CHAPTER 13

MATERIALS AND METHODS

Reagents and Antibodies

Rat monoclonal antibodies against human M_2 mAChRs were purchased from Chemicon International (Temecula, CA), and mouse antibodies against the early endosomal marker, EEA-1, were obtained from Transduction Laboratories (Burlingame, CA). Mouse antibodies against the human transferrin receptor (clone B3/25) were purchased from Roche Biochemicals. Alexa 594- and Alexa 488-conjugated goat anti-mouse, goat anti-rat, and goat anti-rabbit IgG and Alexa 594-labeled transferrin were purchased from Molecular Probes, Inc. (Eugene, OR). ^{3}H-Labeled *N*-methylscopolamine ([^{3}H]NMS) was purchased from PerkinElmer Life Sciences. All other reagents were obtained from Sigma.

Cell Culture and DNA Transfections

HeLa cells were maintained in Dulbecco's modified Eagle's medium supplemented with 10% fetal bovine serum, 100 IU/ml penicillin, and 100 µg/ml streptomycin (complete medium) at 37 °C with 5% CO_2. The HeLa cells were either grown on glass coverslips (for immunolocalization) and transfected in 6-well dishes or grown in 12-well dishes (for [^{3}H]NMS binding) using FuGENE 6 (Roche Biochemicals) according to the manufacturer's directions. Plasmids encoding M_2 mAChRs were transiently transfected into HeLa cells at 1 µg/well (6-well dish). Wild type and mutant Arf6 plasmids were transiently transfected at 0.5 µg of plasmid DNA/well (6-well dish), whereas $G\alpha_q$

plasmids and GFP-Rab5 plasmids were transiently transfected into 6-well dishes using 2.5 μg of DNA; wild type and mutant dynamin plasmids were transfected using 10 μg of plasmid/well.

To generate stable HeLa cell transfectants, wild type M_2 mAChR plasmid was transfected into HeLa cells using the calcium phosphate co-precipitation method (155). Thirty-six hours after transfection, the cells were detached and replated at a 1:25 dilution into complete medium containing 600 μg/ml G418 (Invitrogen). Approximately 2 weeks later, G418-resistant clones were amplified and tested for M_2 mAChR expression by indirect immunofluorescence microscopy. The positive clones were expanded, and one of these (clone 17) was found to express moderate levels of M_2 mAChRs, as judged by relative fluorescence intensity, and was chosen for further studies.

Indirect Immunofluorescence

The cells were treated as described in the figure legends at 30-36 h following transfection, fixed in 2% formaldehyde in phosphate-buffered saline (PBS) for 10 min, and rinsed with 10% fetal bovine serum and 0.02% azide in PBS (PBS-serum). Fixed cells were incubated with primary antibodies diluted in PBS- serum containing 0.2% saponin for 45 min and then washed (three times, 5 min each) with PBS-serum. The cells were then incubated in fluorescently labeled secondary antibodies diluted in PBS-serum plus 0.2% saponin for 45 min, washed with PBS-serum (three times, 5 min each) and once with PBS, and mounted on glass slides.

For Alexa 594-transferrin internalization, transfected cells expressing M_2 mAChRs were briefly rinsed three times with 0.5% bovine serum albumin in Dulbecco's modified

Eagle's medium and incubated in the same medium for 30 min at 37 °C. The cells were then incubated with both 1 mM carbamoylcholine chloride (carbachol) and Alexa 594-transferrin (50 μg/ml) for various times, briefly rinsed with an acid wash (0.5% acetic acid, 0.5 M NaCl, pH 3.0) and complete medium, and then fixed and processed for immunofluorescence localization of M_2 mAChRs. The samples were observed using an Olympus BX40 epifluorescence microscope equipped with a 60× Plan pro lens, and photomicrographs were prepared using a Spot RT monochrome C digital camera (Diagnostic Instruments, Inc., Sterling Heights, MI) or were observed and photographed with a Zeiss LSM 510 laser scanning confocal microscope.

Loss of Cell Surface Receptor Assay

1.5×10^5 transfected HeLa cells were grown in 4- or 12-well dishes for 24 h in complete Dulbecco's modified Eagle's medium and treated with or without 1 mM carbachol as described in the figure legends and then rinsed three times with ice-cold PBS, pH 7.4, on ice. Surface M_2 mAChRs were detected as described (166, 214) by incubating cells with the cell-impermeant muscarinic ligand, [^{3}H]NMS (2 nM), for 2 h at 4 °C. The cells were washed three times (5 min each) with ice-cold PBS and solubilized with 1% Triton X-100 in PBS for 10 min. The cell extracts were transferred to microcentrifuge tubes, and the insoluble material was pelleted by microcentrifugation at 14,000 rpm for 15 min at 4 °C. The supernatant was collected, and the protein concentration was determined from an aliquot using a micro-BCA protein assay (Pierce). The radioactivity present in the remaining sample was determined by scintillation counting. Nonspecific binding of [^{3}H]NMS to untransfected HeLa cells was subtracted from the transfected samples. The mass of [^{3}H]NMS bound to cells (in fmol) was calculated using the bound radioactive

counts/min and the specific activity of the [^{3}H]NMS (70 Ci/mmol); this was normalized to the protein content of the samples. Receptor internalization is defined as the percentage of surface M_2 receptors not accessible to [^{3}H]NMS at each time relative to non-carbachol-treated cells.

Statistical Analysis

The data are expressed as the means ± S.E. from the indicated number of independent experiments performed in either triplicate or quadruplicate. Statistical analysis was performed using a single-factor analysis of variance followed by a Tukey's statistical test.

CHAPTER 14

RESULTS

Agonist-induced Internalization and Recycling of M_2 mAChRs in HeLa Cells

To investigate the intracellular trafficking of the M_2 mAChR, HeLa cells were transiently transfected with a plasmid encoding the wild type human M_2 mAChR. Using a rat monoclonal antibody against M_2 mAChRs and confocal microscopy, we examined the effects of agonist stimulation on the cellular distribution of M_2 mAChRs (Fig. 25*a*). In untreated cells, M_2 mAChRs were distributed in a diffuse pattern along the PM. The addition of 1 mM carbachol induced a rapid redistribution of surface M_2 mAChRs into numerous punctate endosomal structures within 15 min at 37 °C. These endosomal structures were initially dispersed near the cell periphery but became clustered in the juxtanuclear region of cells within 20-30 min. This distribution did not noticeably change even up to 60 min of incubation with carbachol.

Next, we quantified the kinetics of M_2 mAChR internalization in stably transfected HeLa cells for comparison with the behavior of M_2 mAChRs in stably transfected HEK 293 cells (166). M_2 mAChRs exhibit rapid internalization kinetics in response to agonist stimulation but slow and incomplete recycling behavior in HEK 293 cells. Stably transfected HeLa cells expressing M_2 mAChRs were incubated with 1 mM carbachol for various times at 37 °C and then chilled to 4 °C, and the loss of surface receptor-binding sites for the cell-impermeant mAChR ligand [^{3}H]NMS was determined (Fig. *25b*). Within 10 min after the addition of carbachol, ~80% of the initial surface [^{3}H]NMS-binding sites is lost. This coincides with the time of appearance of M_2 mAChRs within

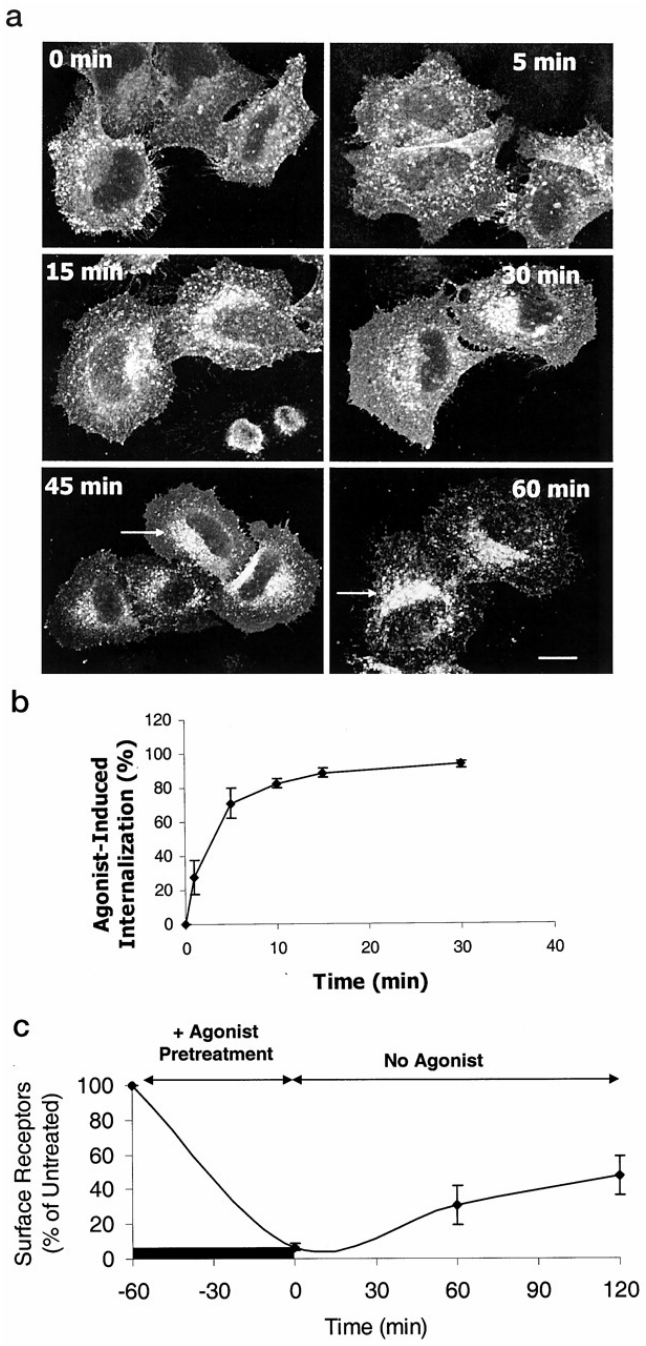

Fig. 25. Agonist-induced internalization and recycling of M_2 mAChRs in HeLa cells. *a*, HeLa cells were transiently transfected with a plasmid that encodes wild type human M_2 mAChR and then treated with 1 mM carbachol for various times and processed for confocal microscopy using a monoclonal rat anti-M_2 mAChR antibody. *Bar*, 10 μm. *b*, Stably transfected HeLa cells expressing M_2 mAChRs were incubated for various times with 1 mM carbachol prior to determination of surface M_2 mAChRs using [^{3}H]NMS binding. M_2 mAChR internalization is expressed as the percentage of surface M_2 receptors that became inaccessible to [^{3}H]NMS at each time, relative to non-carbachol-treated cells (mean ± S.E.; $n = 3$ independent experiments, in triplicate). *c*, Time course of recycling. Stable M_2 mAChR transfectants were incubated with 1 mM carbachol for 60 min, washed, and incubated for various times in carbachol-free medium prior to the determination of surface M_2 mAChRs. The data are expressed as the percentages of surface M_2 receptors present at each time, after agonist removal, relative to non-carbachol-treated cells (mean ± S.E.; $n = 5$ independent experiments, in triplicate).

punctate endosomal structures (Fig. *25a*). The kinetics of M_2 internalization was also determined in transiently transfected cells (see Fig. 29, *diamonds*), where we observed that ~50% of surface M_2 mAChRs were internalized after 15 min of agonist treatment. This is consistent with the immunofluorescence observations in Fig. 25*a* showing both PM and endosomal staining in transiently transfected cells after 15 min of agonist treatment. Thus, M_2 mAChRs are rapidly internalized in HeLa cells, which is similar to what has been reported for M_2 mAChR internalization in HEK 293 cells (166).

Next, we examined whether internalized M_2 mAChRs recycled back to the cell surface upon agonist removal (Fig. 25*c*). Stably transfected cells were treated with 1 mM carbachol for 60 min at 37 °C, washed, and warmed for various times in growth medium that did not contain carbachol, prior to quantifying the reappearance of surface [^{3}H]NMS-binding sites. After 2 h of agonist removal, we observed a recovery of surface M_2 mAChRs to ~50% of the level observed in unstimulated cells. This was not due to new synthesis of M_2 mAChRs, because the observed increase in [^{3}H]NMS-binding sites after 2 h of agonist removal was the same when measured in the presence or absence of 20 μg/ml cycloheximide (data not shown). These results indicated that M_2 mAChRs were rapidly internalized in HeLa cells in response to agonist stimulation, whereas M_2 mAChR recycling was a relatively slow and incomplete process. The kinetics of internalization and recycling were similar to those described for M_2 mAChRs expressed in HEK 293 cells (166).

In the studies below, we used a transient co-transfection approach to investigate the effects of different mutant proteins, known to affect endocytosis, on M_2 mAChR

internalization. Although the overall transfection efficiency in our experiments ranged from 30 to 50%, the co-transfection efficiency in these experiments was ~95-100% (as judged by indirect immunofluorescence staining for both M_2 mAChRs and a given mutant protein) (data not shown). This permitted us to quantify the effects of endocytic mutants on M_2 mAChR internalization without background from cells that expressed M_2 mAChRs but not an endocytic mutant.

Previous studies have shown that agonist-induced internalization of M_2 mAChRs in HEK 293 cells occurs via clathrin-independent endocytosis (214). M_2 mAChR internalization is insensitive to inhibition by the K44A mutant of the 100-kDa GTPase, dynamin (dyn) (213), which mediates the scission of clathrin-coated pits at the PM and Golgi complex and also the scission of caveolae (26, 39, 85). To investigate whether M_2 mAChR internalization involved clathrin-independent mechanisms in HeLa cells, we transiently co-transfected HeLa cells with plasmids encoding green fluorescent protein (GFP)-tagged dynamin 2 K44A (dyn2-GFP K44A) and M_2 mAChR or M_2 mAChR plasmid alone and determined the effects of agonist stimulation on M_2 receptor internalization (Fig. 26). In cells expressing M_2 mAChR alone or M_2 mAChR and dyn2-GFP K44A, treatment with 1 mM carbachol for 30 min induced M_2 mAChR internalization into numerous punctate endosomal structures (Fig. 26, *A* and *B*). In contrast, expression of dyn2-GFP K44A in HeLa cells completely blocked the clathrin-dependent internalization of Alexa 594-labeled transferrin (Fig. 26*C*). Thus, agonist-induced internalization of M_2 mAChRs in HeLa cells appears to be mediated by clathrin-independent mechanisms.

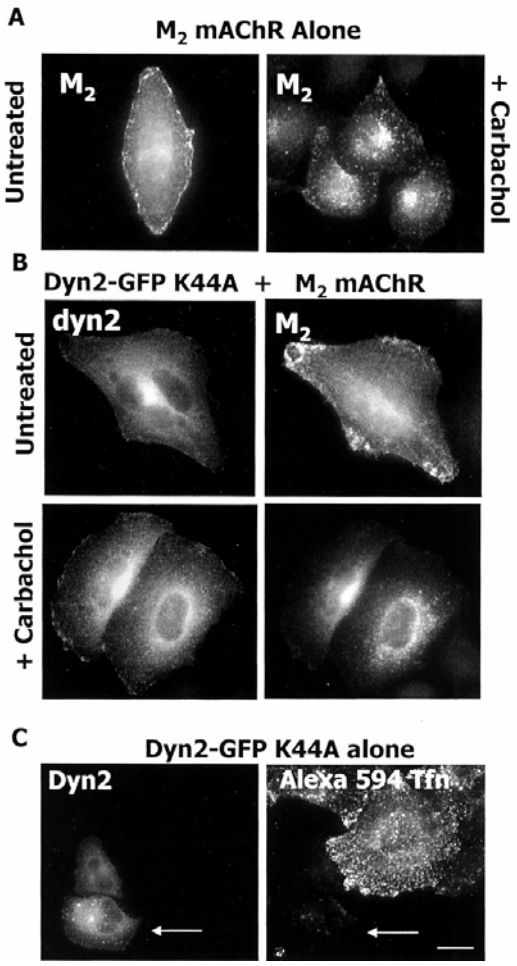

Fig. 26. Dominant-inhibitory dynamin 2-GFP K44A does not block internalization of M_2 mAChRs in HeLa cells. HeLa cells transfected with plasmids encoding M_2 mAChR alone (*A*) or M_2 mAChR and dyn2-GFP K44A (*B*) were incubated in the presence or absence of 1 mM carbachol for 30 min and then fixed and processed for indirect immunofluorescence localization of M_2 mAChRs and direct epifluorescence visualization of dyn2-GFP. *C*, HeLa cells expressing dyn2-GFP K44A (*arrows*) were incubated with Alexa 594-labeled transferrin for 15 min, fixed, and processed for epifluorescence microscopy as described under "Experimental Procedures." *Bar*, 10 μm.

Internalized M_2 mAChRs Merge with Early Endosomes of the Clathrin-dependent Endocytic Pathway

Given the findings above, we sought to determine the identity of the endosomal structures to which internalized M_2 mAChRs localized following agonist treatment. We performed double labeling immunofluorescence experiments using antibodies against known markers of endosomal compartments along with antibodies against M_2 mAChRs. We compared the distribution of internalized M_2 with that of the early endosome marker EEA-1, with transferrin receptors, and with the lysosomal marker, LAMP2.

We observed that the M_2 mAChR$^+$ endosomal structures extensively co-localized with the early endosomal marker, EEA-1, and to a lesser extent with transferrin receptors (Fig. 27). This suggested that once M_2 mAChRs are internalized via a clathrin-independent pathway, they are transferred to early endosomes of the clathrin endocytic pathway. We also examined the localization of internalized M_2 mAChRs in cells expressing GTPase-defective Rab5 Q79L, which is known to stimulate homotypic early endosomal fusion and results in the swelling of early endosomes (24). Treatment of cells co-expressing M_2 and GFP-Rab5 Q79L with 1 mM carbachol resulted in the localization of M_2 mAChRs to very large swollen endosomal structures that extensively co-localized with GFP-Rab5 Q79L. This indicated that M_2 mAChRs, once internalized by clathrin-independent mechanisms, indeed become localized to early endosomes of the clathrin-mediated endocytic pathway. In contrast to early endosomal markers, internalized M_2 mAChRs did not significantly co-localize with the lysosomal marker, LAMP2 (data not shown).

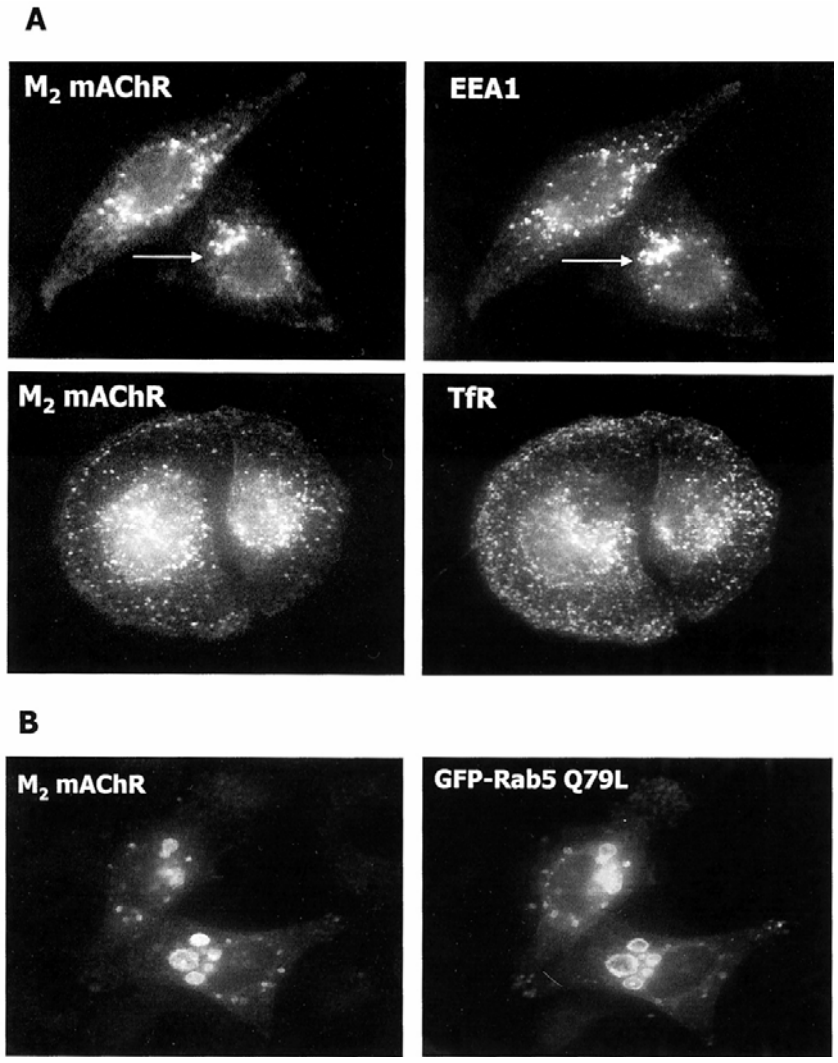

Fig. 27. Internalized M_2 mAChRs co-localize with clathrin-dependent early endosomal markers. *A*, transiently transfected HeLa cells expressing M_2 mAChRs were treated with 1 mM carbachol at 37 °C for 30 min, fixed, and processed for immunofluorescence co-localization of M_2 mAChRs, using rat anti-M_2 mAChR monoclonal antibodies and using mouse monoclonal Abs against EEA-1 or transferrin receptors. Primary antibodies were visualized using fluorescently labeled, non-cross-reactive secondary antibodies. The *arrows* indicate endosomal profiles that co-label with antibodies against both M_2 mAChRs and EEA-1. *B*, transiently transfected HeLa cells expressing M_2 mAChRs and GFP-Rab5 Q79L were treated with 1 mM carbachol for 30 min prior to fixation and indirect immunofluorescence. *Bar*, 10 μM.

To further explore this apparent transfer of M_2 mAChRs between the clathrin-independent and clathrin-dependent pathways, we compared the intracellular localization of M_2 mAChRs and Alexa 594-labeled transferrin over time in co-internalization experiments (Fig. 28). Transiently transfected HeLa cells expressing M_2 mAChRs were simultaneously incubated with 1 mM carbachol and with 50 μg/ml Alexa 594-labeled transferrin for various times at 37 °C, and the distributions of the two proteins were determined. After 5 min of internalization, M_2 mAChRs localized to large endosomal structures, whereas Alexa 594-transferrin localized to distinct endosomal structures that lacked M_2 mAChRs. After 15-30 min of internalization, both M_2 mAChRs and Alexa 594-transferrin extensively co-localized to large endosomal structures in the juxtanuclear region of cells. These results indicated that M_2 mAChR and transferrin are initially internalized in discrete endosomal carriers but then converge in common endosomal structures.

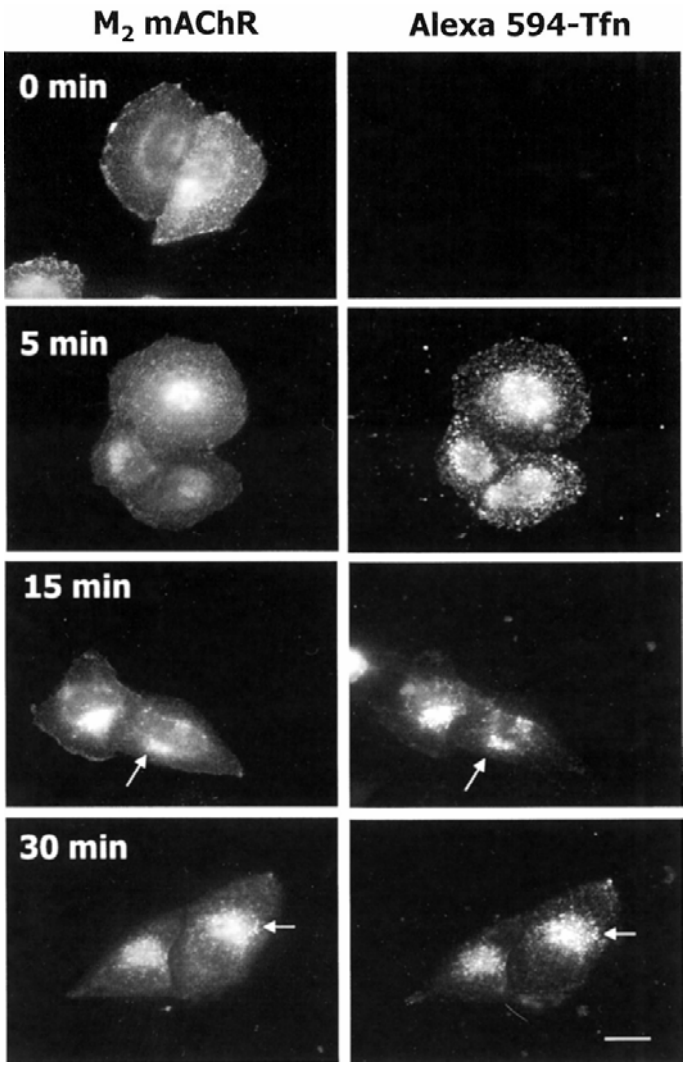

Fig. 28. M_2 mAChRs and Alexa 594-transferrin are initially internalized in distinct punctate structures but later merge into common endosomal compartments. Transiently transfected HeLa cells expressing M_2 mAChRs were simultaneously incubated with both 1 mM carbachol and 50 μg/ml Alexa 594-transferrin for various times prior to fixation and indirect immunofluorescence localization of M_2 mAChRs. *Bar*, 10 μM.

Arf6 Involvement in M_2 mAChR Internalization

To date, very little is known about the regulation of the endocytic pathway followed by the M_2 mAChR. We have previously shown that the Arf6 GTPase regulates endocytic trafficking along a clathrin-independent pathway and delivers cargo to tubular endosomal structures that emanate from the centrosomal region of cells (155). Using the interleukin-2 receptor α subunit Tac as an endocytic marker of this pathway, we observed that expression of the GTPase-deficient Arf6 mutant, Q67L, inhibits internalization of Tac into cells when assessed after 40 h of transfection. In contrast, expression of the GTP binding-defective Arf6 mutant T27N inhibits the recycling of internalized Tac back to the cell surface. Recent studies have also shown that both Arf6 Q67L and Arf6 T27N inhibit the clathrin-mediated internalization of β_2ARs (32, 151). However, nothing is known about the effects of these Arf6 mutants on clathrin-independent GPCR internalization.

We first investigated the effects of wild type (WT) Arf6 and GTP binding-defective Arf6 T27N on M_2 mAChR internalization in transiently transfected HeLa cells by measuring the agonist-induced loss of surface M_2 mAChRs with the [^{3}H]NMS binding assay (Fig. 29). We observed that neither co-transfection with WT Arf6 nor Arf6 T27N significantly affected M_2 mAChR internalization after either 15 or 30 min of agonist treatment. After 30 min of carbachol treatment, ~60% of surface M_2 receptors were internalized in cells expressing either M_2 mAChR alone or M_2 mAChR co-transfected with either WT Arf6 or Arf6 T27N.

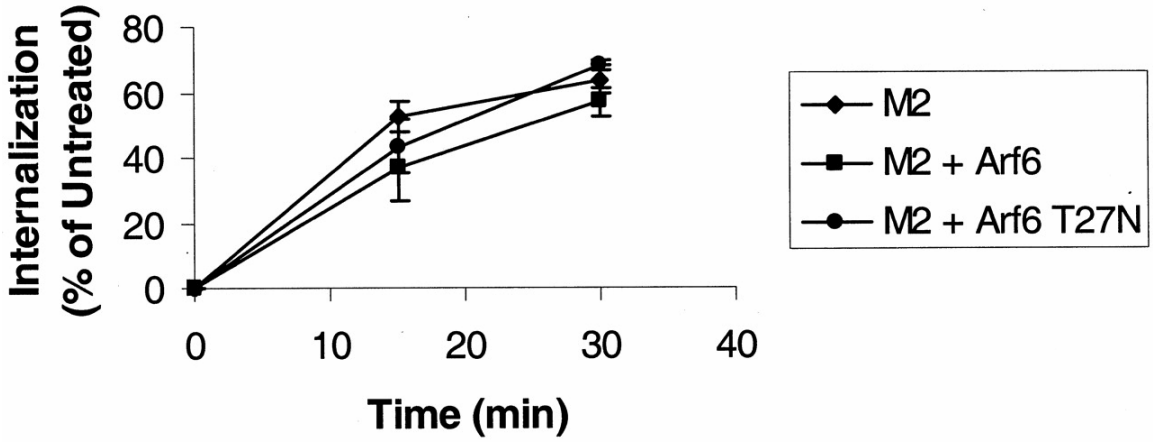

Fig. 29. Neither wild type Arf6 nor GTP binding-defective Arf6 T27N inhibit M_2 mAChR internalization. Transiently transfected HeLa cells expressing M_2 mAChR alone or M_2 mAChR plus either wild type Arf6 or Arf6 T27N were incubated in the presence or absence of 1 mM carbachol for 0, 15, and 30 min prior to determination of surface M_2 mAChRs using [^{3}H]NMS. Internalization of M_2 mAChRs is expressed as the percentage of surface M_2 mAChRs that became inaccessible to [^{3}H]NMS following carbachol treatment. The data represent the means ± S.E. of four measurements from a representative experiment that was repeated three times.

We next examined the effects of persistent activation of Arf6 in cells by expressing the GTPase defective mutant of either Arf6 itself (Arf6 Q67L) or of an upstream activator of Arf6, HA-tagged $G\alpha_q$ Q209L (HA-$G\alpha_q$ Q209L), by measuring the loss of surface M_2 mAChRs with the [^{3}H]NMS binding assay. A recent study by Boshans *et al.* (19) showed that co-expression of wild type Arf6 and a constitutively activated mutant of $G\alpha_q$ could mimic bombesin-induced activation of Arf6 in Chinese hamster ovary cells. We have previously observed that co-transfection of WT Arf6 and HA-$G\alpha_q$ Q209L together induces cell surface protrusions, a phenotype that is indicative of Arf6 activation (156). Fig. 30 shows that in cells expressing M_2 mAChR alone, treatment with 1 mM carbachol for 30 min induced the internalization of ~78% of surface M_2 mAChRs. In contrast, only 36 and 39% of surface M_2 mAChRs were internalized in cells co-expressing either Arf6

Q67L or $G\alpha_q$ Q209L, respectively. This suggested that persistent activation of Arf6 inhibited M_2 mAChR internalization. In these experiments, we also observed that cells co-transfected with Arf6 Q67L expressed significantly fewer surface M_2 mAChRs (116 ± 57 fmol [^{3}H]NMS bound/mg protein or $7 \pm 2\%$) when compared with cells expressing M_2 mAChRs alone (1977 ± 979 fmol [^{3}H]NMS bound/mg protein). This suggested that M_2 receptors may be sequestered within intracellular compartments even in unstimulated Arf6 Q67L-transfected cells.

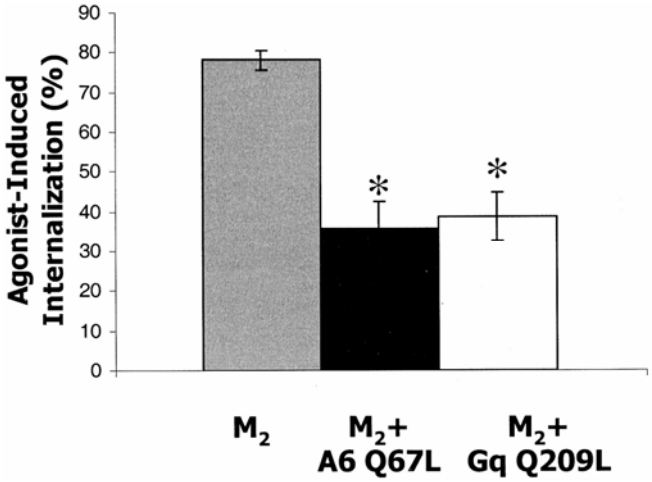

Fig. 30. GTPase-defective Arf6 Q67L and $G\alpha_q$ Q209L mutants inhibit M_2 mAChR internalization. Transiently transfected HeLa cells expressing M_2 mAChR alone or M_2 mAChR plus either Arf6-HA Q67L or HA-$G\alpha_q$ Q209L were incubated in the presence or absence of 1 mM carbachol for 30 min prior to determination of surface M_2 mAChRs using [^{3}H]NMS binding. Internalization of M_2 mAChRs is expressed as the percentage of surface M_2 mAChRs that became inaccessible to [^{3}H]NMS following carbachol treatment. The data represent the means ± S.E. of eight measurements from two independent experiments. *, $p < 0.001$ compared with M_2 mAChR alone values.

To further investigate these effects of Arf6 Q67L and $G\alpha_q$ Q209L on M_2 internalization, we examined the effects of these mutants on the intracellular localization of M_2 mAChR using indirect immunofluorescence microscopy (Figs. 31 and 32). In untreated cells, which co-expressed M_2 mAChR and Arf6 Q67L, M_2 mAChRs were localized both at the cell surface and also to large endosomal clusters where M_2 mAChRs co-localized with Arf6 Q67L (Fig. 31*B*). These results indicated that there indeed was significant intracellular accumulation of M_2 mAChRs in unstimulated Arf6 Q67L-transfected cells, which is consistent with the reduced levels of surface M_2 mAChRs

observed in these cells. Recent studies (23) showed that these large Arf6 Q67L$^+$ endosomal clusters are enriched in phosphatidylinositol 4,5-bisphosphate and F-actin.

These cells also exhibited an altered morphology with many protrusive structures, which we have previously shown to be a phenotype of cells expressing Arf6 Q67L (23, 156). Following carbachol treatment, the M_2 receptors remained in a localization pattern that was indistinguishable from untreated Arf6 Q67L-transfected cells (Fig. 31*B*) and did not show the punctate vesicular structures observed in cells expressing M_2 mAChR alone (Fig. 31*A*). The results of the [^{3}H]NMS binding experiments above (Fig. 30) further indicate that Arf6 Q67L inhibits the internalization of the M_2 mAChRs that are present at the cell surface in these cells. Expression of Arf6 Q67L did not affect the clathrin-mediated endocytosis of Alexa 594-Tfn, which is consistent with our previous studies showing that Arf6 Q67L does not inhibit transferrin internalization in HeLa cells (155).

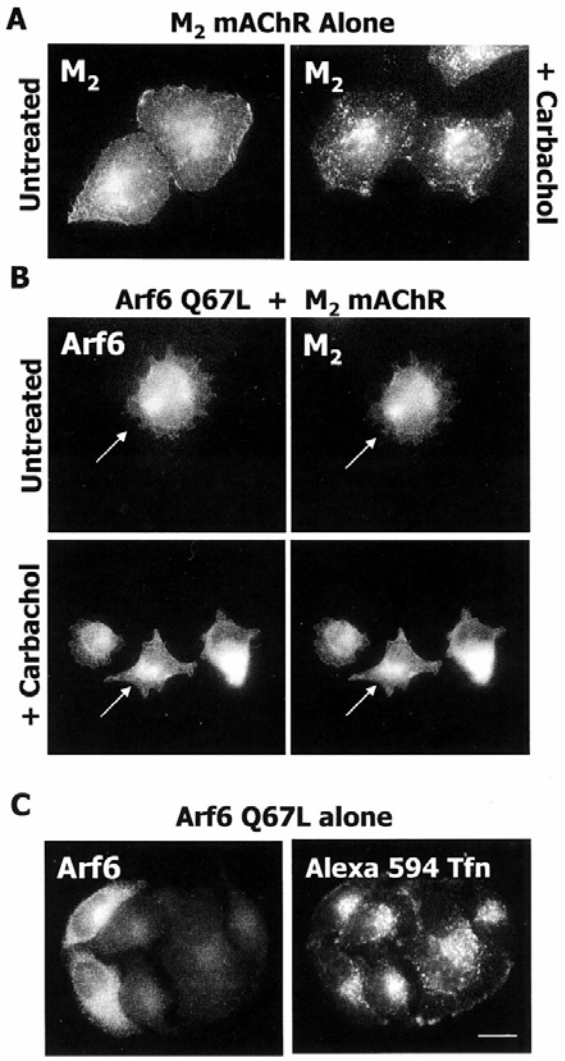

Fig. 31. M_2 mAChRs are sequestered in large endosomal clusters in HeLa cells expressing constitutively active Arf6 Q67L. HeLa cells were transiently transfected with plasmids encoding M_2 mAChR alone (*A*) or M_2 mAChR and Arf6-HA Q67L (*B*) and then treated for 30 min with or without 1 mM carbachol, fixed, and processed for indirect immunofluorescence localization of M_2 mAChRs and Arf6. The *arrows* indicate fluorescent clusters that label with antibodies against both M_2 mAChRs and Arf6 Q67L. *Bar*, 10 μm. *C*, HeLa cells were transiently transfected with a plasmid encoding Arf6 Q67L and incubated with Alexa 594-labeled transferrin for 15 min prior to processing for indirect immunofluorescence (see "Experimental Procedures"). *Bar*, 10 μm.

In cells co-expressing M_2 mAChR and HA-Gα_q Q209L, the M_2 receptors were primarily localized at the cell surface (Fig. 32*B*). Following carbachol treatment, cells expressing HA-Gα_q Q209L contained far fewer M_2 mAChR-labeled endosomal structures than cells expressing M_2 mAChR alone. As observed with Arf6 Q67L, expression of HA-Gα_q Q209L did not affect the clathrin-mediated internalization of transferrin. Taken together, these results indicated that persistent activation of Arf6 via expression of constitutively activated Arf6 Q67L or the upstream activator, Gα_q Q209L, inhibited M_2 mAChR internalization but that co-expression of WT Arf6 and GTP binding-defective Arf6 T27N did not.

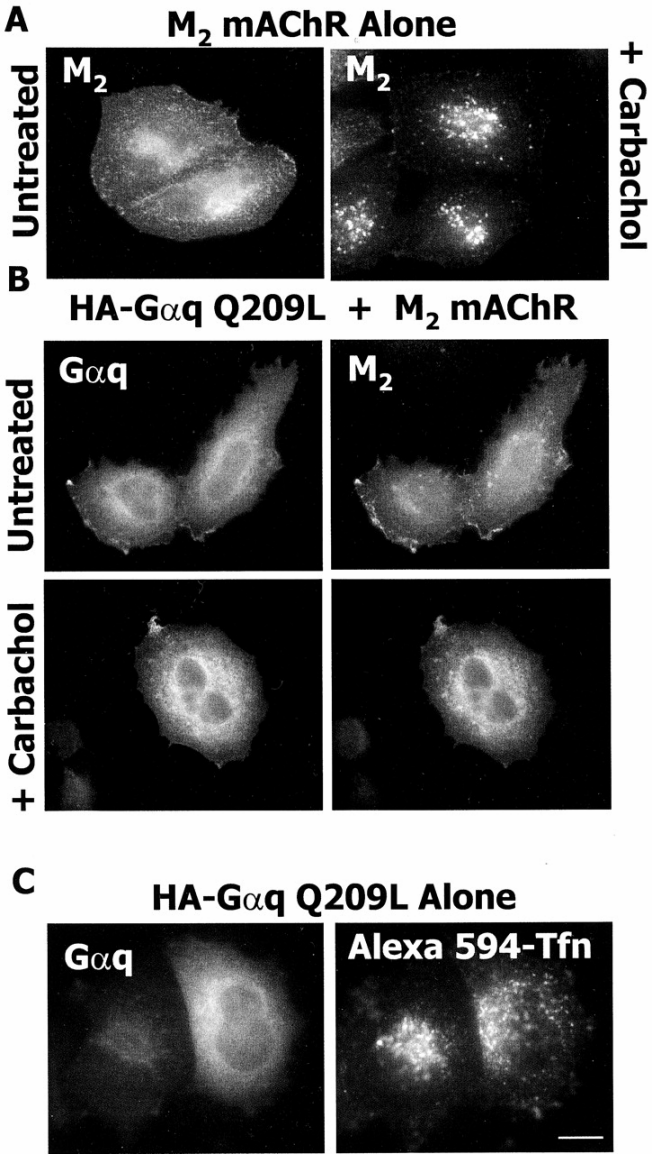

Fig. 32. Constitutively active $G\alpha_q$ Q209L inhibits M_2mAChR but not transferrin internalization. HeLa cells were transiently transfected with plasmids encoding M_2 mAChR alone (*A*) or M_2 mAChR and HA-$G\alpha_q$ Q209L (*B*) and then treated for 30 min with or without 1 mM carbachol, fixed, and processed for indirect immunofluorescence localization of M_2 mAChRs and $G\alpha_q$. *Bar*, 10 μm. *C*, HeLa cells were transiently transfected with a plasmid encoding HA-$G\alpha_q$ Q209L and incubated with Alexa 594-labeled transferrin for 15 min prior to processing for indirect immunofluorescence (see "Experimental Procedures"). *Bar*, 10 μm.

CHAPTER 15

DISCUSSION

In this study, we investigated the intracellular trafficking of the M_2 mAChR via a clathrin-independent endocytic pathway in HeLa cells. The M_2 receptor has been shown to be internalized in HEK293 cells by a poorly characterized, clathrin- and arrestin-independent mechanism (145, 165, 177, 204, 213, 214). Our present results indicate that persistent activation of the small GTPase Arf6 inhibits M_2 mAChR internalization but does not affect the clathrin-mediated internalization of transferrin receptors. Interestingly, following internalization in structures that initially lack clathrin endocytic markers, M_2 mAChRs rapidly localize to early endosomes of the clathrin endocytic pathway where they co-localize with the endosomal marker EEA-1 and with internalized Alexa 594-transferrin. This raises the intriguing possibility that although the M_2 mAChR is initially internalized via an Arf6-associated pathway, it is quickly transferred to endosomes of the clathrin-dependent pathway.

We observed that dominant-inhibitory dynamin 2 K44A did not interfere with the internalization of M_2 receptors in HeLa cells but completely blocked the clathrin-dependent internalization of transferrin. This suggested that M_2 internalization was clathrin-independent in HeLa cells and is consistent with published reports that the K44A mutant of dynamin does not inhibit M_2 mAChR internalization in HEK293 cells (213). Recent reports also indicate that M_2 mAChRs and angiotensin AT_{1A} receptors exhibit a differential sensitivity to mutants of dynamin (219) and suggest that although M_2 mAChR internalization is clathrin-independent, it still requires dynamin.

To gain some insight into the nature of the endocytic pathway followed by M_2 mAChR, we investigated the identity of the endosomal structures to which internalized M_2 receptors localized. To our surprise, there was extensive overlap in staining between internalized M_2 mAChR and the early endosomal marker EEA-1. EEA-1 is a Rab5 effector that is recruited to the cytosolic leaflet of early endosomes in a phosphatidylinositol 3-phosphate-dependent manner (121). It is involved in both the tethering of vesicles and their subsequent fusion through the assembly of oligomeric complexes that mediate vesicle fusion. Our observations that internalized M_2 mAChRs also co-localize to the swollen early endosomal structures induced by expression of constitutively activated Rab5 Q79L lend further support to the early endosomal localization of internalized M_2 receptors. A recent study has shown that internalized M_4 mAChRs also localize to EEA-1^+ endosomes and with internalized transferrin receptors in PC12 cells (215). Furthermore, M_4 mAChRs were shown to localize to swollen multivesicular endosomes formed in cells expressing constitutively activated Rab5 Q79L. In other studies, M_4 mAChRs have been shown to internalize via arrestin- and clathrin-dependent mechanisms (214). This suggests that different mAChRs that are internalized by distinct mechanisms can meet up in and transit through common endosomal compartments. In support of this hypothesis, we also observed that M_2 mAChRs and fluorescently labeled transferrin are initially internalized in distinct endosomal structures but converge into common endosomal structures within 15 min after internalization.

But what is the clathrin-independent pathway by which the M_2 receptor is initially internalized from the PM? Our results implicate a pathway that is regulated by the Arf6 GTPase. We have previously shown that the Arf6 GTPase regulates a clathrin-

independent endocytic pathway between the PM and tubulovesicular endosomes in HeLa cells (155). Arf6 itself cycles between these two cellular locations according to its GTP cycle (146). We and others have shown that GTP-bound Arf6 preferentially localizes to the PM, whereas GDP-bound Arf6 localizes to a juxtanuclear tubular endosomal compartment (37, 146, 155). Constitutively activated Arf6 Q67L inhibits the internalization of proteins that transit the Arf6-regulated pathway, such as the major histocompatability complex I, whereas GTP binding-defective Arf6 T27N inhibits recycling of such proteins from tubulovesicular endosomes back to the PM (23, 155).

Two observations suggest that the M_2 mAChR is also internalized via an Arf6-associated endocytic pathway. First, Arf6 Q67L strongly inhibited the agonist-induced internalization of M_2 receptors (Fig. 30) but did not perturb the clathrin-mediated internalization of fluorescently labeled transferrin (Fig. 31). We also observed that M_2 mAChRs were sequestered into large endosomal clusters even in the absence of agonist stimulation, where they co-localized with Arf6 Q67L (Fig. 31), suggesting that M_2 mAChRs were internalized earlier in the transfection. Brown *et al.* (23) recently reported that major histocompatability complex I co-localizes with Arf6 Q67L after 20 h of transfection in tightly clustered endosomal structures, which accumulate in cells with time after transfection and are highly enriched in phosphatidylinositol 4,5-bisphosphate and F-actin. In contrast, after 40 h of transfection, major histocompatability complex I internalization was strongly inhibited by Arf6 Q67L. One explanation for the different temporal effects of Arf6 Q67L on M_2 mAChR internalization, which we have observed, is that as endosomal membranes accumulate in cells, further internalization is inhibited

because of a depletion of either membrane and/or critical components necessary for vesicle formation.

To independently test the effects of persistent Arf6 activation on M_2 mAChR endocytosis, we examined the effects of GTPase-defective $G\alpha_q$ Q209L on M_2 internalization. We observed that co-transfection of M_2 mAChRs with constitutively activated $G\alpha_q$ Q209L greatly inhibited M_2 mAChR internalization and to the same extent as Arf6 Q67L (~50% inhibition). Constitutively activated $G\alpha_q$ mutants have been shown to enhance Arf6 activation and to mimic, in part, the phenotypic effects of Arf6 Q67L in cells (19). We have observed that co-expression of wild type Arf6 and $G\alpha_q$ Q209L recreates the surface protrusions observed following aluminum fluoride stimulation of HeLa cells expressing WT Arf6 alone. A recent study showed that stimulation of the $G\alpha_q$-coupled bombesin receptor increased the proportion of GTP-bound Arf6 in Chinese hamster ovary cells. The precise mechanism by which $G\alpha_q$ Q209L enhances Arf6 activation remains to be determined. The observation that persistent activation of $G\alpha_q$ can inhibit M_2 mAChR internalization raises the intriguing possibility that $G\alpha_q$-coupled receptors may influence the behavior of M_2 receptor trafficking.

We also observed that neither WT Arf6 nor the GTP binding-defective Arf6 T27N mutant affected M_2 mAChR internalization (Fig. 29). These observations contrast with those of Claing *et al.* (32), who recently showed that both Arf6 Q67L and Arf6 T27N inhibit the clathrin- and arrestin-mediated internalization of β_2ARs. These authors also showed that isoproteronol stimulation of β_2ARs results in the β-arrestin-dependent stimulation of GTP exchange onto Arf6. Previous work has shown that overexpression of

the Arf6-specific GTPase-activating protein GIT1 also inhibits β_2AR internalization but not M_2 receptor internalization (34, 151). One major difference between β_2ARs and the M_2 mAChR is that the former requires β-arrestins for internalization and the latter does not (145, 214). One possible explanation for the differential sensitivities of these two receptors to Arf6 mutants is that β-arrestin stimulation of Arf6 activation is not critical for M_2 mAChR internalization but is important for β_2AR internalization. These results raise the exciting possibility that Arf6 can differentially affect GPCR internalization via both clathrin-dependent and clathrin-independent mechanisms. The significance of such a dual role for Arf6 in endocytic trafficking along distinct pathways is unknown.

Taken together, our results indicate that the clathrin-independent internalization of the M_2 mAChR initially follows an Arf6-associated endocytic pathway but then quickly merges with early endosomes of the clathrin-dependent pathway. From these EEA-1^+ endosomes, M_2 mAChRs either can recycle back to the PM, can remain sequestered in endosomes by unknown mechanisms, or eventually could be sorted to lysosomes for degradation. Given the differential effects of Arf6 on the clathrin-dependent and clathrin-independent internalization of GPCRs, determining the mechanisms by which Arf6 exerts its effects on these two endocytic pathways will be an important goal for future studies.

APPENDIX A

PROTOCOLS

Splitting Mammalian Cells

1. Rinse cells with 1 mL versene.
2. Add 2 mL trypsin and incubate for 1-2 minutes to loosen cells.
3. Add 4 mL complete media to cells and pipet cells 10 times to get uniform suspension.
4. Place 10 mL fresh, warm media into a new 10 cm dish.
5. Add 0.4-0.6 mL suspended cells to new flask to get a 1:10 split.
6. Label top of dish with date and split number, cell line, dilution, and initials.
7. If plating cells for experiment, place a few drops of suspended cells to petri dish with coverslips before bleaching old flask of cells.

Plating Mammalian Cells

1. Place several acid washed coverslips into a 10 cm petri dish.
2. Pour 70% EtOH over the coverslips.
3. Flame 4-5 slips at a time very quickly and then let air dry for a few seconds. (Make sure that all EtOH is evaporated or cells will not grow on the slip.)
4. Place ~20 slips in a sterile tissue petri dish for plating.
5. Place 10 mL of complete media into the petri dish.
6. Add a few drops of suspended cells (from flask spilt) to the dish.
7. Add appropriate drug/inhibitor and place in CO2 incubator overnight to do transfection next afternoon. If cells are plated early in morning, then they can be transfected that same evening.

Lipofectamine Transfection

For a transfection in a 24- well dish:
1. Plate 70,000 HepG2 cells in complete media into each well for ~24 h.
2. The following day, change the media to serum-free in each well.
3. For each transfected row (6 wells total/row) dilute a total of 0.5 μg/well of DNA into 300μl serum-free media into one labeled tube. Repeat for each row.
4. Incubate the mixture for 15 min.
5. Dilute lipofectamine into another labeled tube at the ratio (0.4μg DNA: 1μl lipofectamine) with 300 μl serum-free media.
6. Immediately combine the tube with DNA and the tube with lipofectamine and incubate the mixture for 15-45 min.
7. Add 100 μl of the mixture into each well of the 24-well plate.

Lipofectin Transfection

Notes for consideration:
1. This works better in media without serum or in less than 5% serum solution.

2. Do not add any antibiotics to the media.
3. Cell density must be optimized and kept consistent for reproducible results.

For a Transfection in a 6 Well Dish:

1. Plate cells to get recommended cell density of 40-60% confluent on day of transfection.
2. For each transfection:
   a. dilute 1 μg of DNA into 100 μl SFM media into 1 labeled tube
   b. dilute 1.5 μl (per 1 μg plasmid) Lipofectin into 100 μl of SFM media into 1 labeled tube
3. Let stand at room temperature for 30 – 45 min (45 min is optimal).
4. Combine the two solutions and let stand for 10 min at room temperature.
5. Wash cells in 6 well once with 2 mL SFM and replace with 1.8 mL SFM.
6. Add DNA/Lipofectin mix to the well and place in 37°C incubator for 4-6 h.
7. Replace the DNA containing media with complete media and return to incubator for 48-72 h when you can perform the experiment.

ExGen 500 *in vitro* Transfection

Considerations:

1. High quality DNA of 1.8 OD ratio or higher is recommended.
2. Recommended cell density is around 50% at time of transfection.
3. Optimal detection of transfection determined by a reporter gene.
4. Transfection efficiency is higher in the presence of serum w/o antibiotics.

Day 1: Seed 0.45x 10^6 HeLa cells (density depends on cell type) in a 10 cm dish containing complete DMEM (-antibiotics).
Day 2: Transfect in the morning. Prior to transfection, transfer coverslips to a 6-well plate containing 2 mL of complete DMEM (-antibiotics).
Day 3: Change the media.
Day 4: Perform the assay.

Day 2: Procedure for 6-well plate: Use 1 μg :3.3 μl ratio of DNA to Ex-Gen.

1. Dilute recommended amount of DNA (Total 2.0 μg/6-well) into 200 μl of 150 mM NaCl.
2. Vortex briefly and spin down.
3. Add 7.0 μl of ExGen500 to DNA solution and immediately vortex for 10 sec.
4. Incubate at room temperature for 10 min.
5. Add the ExGen500/DNA mixture to one well of 6-well plate and place on shaker for 5 min.
6. Incubate for 24 h and change media following day.
7. Assay 48 h after transfection.

Indirect Immunofluorescence

1. Day 1: Grow cells on 12 mm acid-washed No. 1 circle glass coverslips in a 10 cm dish. Coveslips should sit in 70% ETOH. Flame coverslips prior to use and transfer

to 10cm dish. Density of cells depends on cell type. (HeLa – $0.45x10^6$; MEFs – $1.0x10^6$)

2. Day 2: Transfer individual coverslips to the wells of a 24, 12, or 6-well dish that contains the appropriate amount of media. Begin transfection protocol.
3. Day 3: Remove media and replace with serum free or complete media.
4. Day 4: Treat as required for experimental protocol.
5. Transfer coverlslip to one well in a 12-well dish containing 1 mL of 2% formaldehyde in PBS pH 7.4.
   a. 2% formaldehyde in PBS
      i. Add 27 mL of 37% formaldehyde stock into a graduated cylinder.
      ii. Fill to 500 mL with PBS pH 7.4
6. Incubate for 10 min at room temperature (RT).
7. Remove fixative and add 1 mL of 10% Adult calf serum in PBS (PBS/serum/azide) and incubate for 5 min at room temperature. This can be stored overnight at 4°C.
   PBS/serum
   i. Add 50 mL of calf serum to 500 mL graduated cylinder.
   ii. Add 0.5 mL of 20% sodium azide stock soln.
   iii. Fill to 500 mL with PBS pH 7.4
8. Dilute primary antibodies into PBS/serum containing 0.2% saponin and spin for 5 min at 14,000 rpm.
   PBS/serum + 0.2% saponin
   i. Add 20 µl of 10% saponin stock (made in dH_2O) to microfuge tube
   ii. Add 980 µl of PBS/serum for a total of 1 mL.
9. Place a piece of parafilm in the bottom of a 150 mm petri dish and label with numbers corresponding to 12-well dish.
10. Add 25 µl of the appropriate diluted antibody solution to each spot on the parafilm.
11. Pick up individual coverslips with tweezers and wick excess fluid on paper towel.
12. Invert coverslip onto antibody drop (i.e. cell side down), cover dish and incubate in a bench drawer for 1 h.
13. Carefully transfer coverslip, cell-side up, back into 12-well dish.
14. Wash coverslips with 1 ml PBS/serum (3 x for 5 min).
15. Dilute fluorescently-labeled secondary antibodies in PBS/serum + 0.2% saponin and spin for 5 min at 14,000 rpm.
16. Invert coverslips onto 25 µl drops of antibody on parafilm as described above and incubate for 1 h.
17. Wash coverslips 3 x 5 min with PBS/serum.
18. Rinse coverslips with PBS alone and mount onto glass slides with fluoromount G and seal with nail polish.

Metamorph Co-localization

1. Open and load image of interest
   Deconvolute images prior to quantitation
2. Process Menu
   Select "2D deconvolution"
   Click nearest neighbor and Apply (adjust if needed)

Display color combine

3. Display Menu
   Select "Color Separate"
   Click red, green or blue ---"new"
4. Select rectangle box in Regions tools and place in Blank region of image
5. Regions Menu
   Select "Transfer Region" to place blank in all colors of image
6. Measure Menu
   Select "Show Region Statistics"
   *the "Use Threshold" box should NOT be checked
   *region around box should be blinking (active)
   *Add the sum of average and standard deviation computed for each color image. Record measurements for each color.
7. Measure Menu
   Select "Threshold Image"
   *Make sure State is Off
   Insert the values derived from previous step into the "Low Intensity" box
8. Region Tools
   Select line or box tool to mark the areas of image to analyze. Double click to activate.
9. Regions Menu
   With image outline blinking, select Transfer Region
   Transfer outline of interest to all the color images separated earlier
10. Measure Menu
    Select "Show Region Statistics"
    *Check the "inclusive" box for each color of the image
    * Add the sum of the average and standard deviation computed
11. Measure Menu
    Select "Threshold Image"
    *input the sum calculated above into the "Low intensity" box
12. Applications Menu
    Select "Measure colocalization"
    *set image to "A" or "B" as appropriate
    *check the "show percentage box"
    *log into Excel spreadsheet

LOSR Quantitation Assay

1. Grow cells directly on bottom of wells that contain 1 mL media. (this works best at 150,000 cells per well).
2. Treat as required for experimental protocol.
3. Remove medium and fix cells with 1 mL of 2% formaldehyde in PBS pH 7.4.
   2% formaldehyde in PBS
   i. Add 27 mL of 37% formaldehyde stock into a graduated cylinder.
   ii. Fill to 500 mL with PBS pH 7.4
4. Incubate for 10 min at room temperature (RT).

5. Remove fix and add 1 ml of 10% Adult calf serum in PBS (PBS/serum) and incubate for 5 min at room temperature. This can be stored overnight at 4°C.

PBS/serum

i. Add 50 mL of calf serum to 500 mL graduated cylinder.
ii. Fill to 500 mL with PBS pH 7.4

6. Dilute primary antibodies into PBS/serum without saponin and spin for 4 min at 14,000 rpm.

b. Mouse anti Flag use at 1:750. (stock = 2-5 mg/ mL)
c. ConA Biotin use at 1:750. (stock = 5 mg/ mL) (used at 5 µg/ mL) (Vector Laboratories, B-1005)

7. Remove the PBS serum from the wells.
8. Add 250 µl of primary antibody to each well.
9. Cover dish and incubate in drawer for 45 min.
10. Wash cells with 1 ml PBS/Serum (3 x 3 min).
11. Dilute fluorescently-labeled secondary antibodies in PBS/serum without saponin and spin for 4 min at 14,000 rpm.

d. Goat anti Mouse HRP Conjugate use at 1:1000. (stock = 0.8 mg/mL) (used at 0.3 µg/mL) (Promega, W4021)
e. AP Streptavidin use at 1:1000. (stock = 1 mg/mL) (used at 5 µg/mL) (Alkaline Phosphatase Streptavidin, SA-5100, Vector Laboratories)

12. Remove the PBS Serum and add 250 µl secondary antibody to each well.
13. Cover and incubate in bench drawer for 45 min.
14. Wash cells with 1 mL PBS/Serum (3 x 3 min).
15. Aliquot out approximate amount of 1 Step ABTS necessary and warm it up in dH_2O bath, keeping stock bottle in fridge. (Pierce, 37615)
16. Rinse cells with 1 mL 1 X PBS alone for 5 min.
17. Aliquot out approximate amount of pNPP/Sodium Bicarbonate

pNitroPhenylPhoshate (pNPP) (vector Laboratories, SK5900)
add 5 drops per 2 mL of 100 mM Sodium Bicarbonate

100 mM Sodium Bicarbonate
75 ml dH_2O
0.84 g Sodium Bicarbonate
pH to 10.0 with NaOH
fill to 100 mL with dH_2O

18. Remove PBS.

f. Add 150 µl pre-warmed ABTS to wells stained with Donkey anti Mouse HRP and to first column of a 96 well dish to be used as a standard.
g. Add 150 µl pNPP solution to wells stained with AP Streptavidin and to first column of a second 96 well dish to be used as a standard.
h. Incubate on benchtop for 15 min.

19. After the 15 min, add 150 µl 1% SDS to all wells containing ABTS, including those of the 96 well dish.

20. a. Mix thoroughly by pipetting up and down and quickly add all 300 µl of ABTS/SDS wells to corresponding well of 96 well dish .
b. Mix thoroughly by pipetting up and down and quickly add all 150 µl of pNPP wells to corresponding well of 96 well dish.

c. ABTS/SDS wells should turn green
d. pNPP wells should turn yellow

21. Read absorbances on plate reader at 405 nm in SoftMax Pro Program.
e. Assay for ABTS/SDS: Endpoint ELISA: HRP and ABTS w SDS stop
f. Assay for pNPP: Endpoint ELISA: AP and pNPP

Cloning of FLAG-LPA_3

Forward LPA_3 primer: 5'-GCC ACC ATG AAT GAG TGT CA-3'
Backward LPA_3 primer: 5'-CGA TTT AGG AAG TGC TTT TA-3'

HAss FLAG-LPA_3 forward primer: 5'-GATC ATG AAG ACC ATC ATC GCC CTG AGC TAC ATC TTC TGC CTG GTG TTC GCC GAC TAC AAG GAC GAT GAT GAC AAG ATG AAT GAG TGT CAC -3'

Protocol adapted from Invitrogen Cloning Kit (Carlsbad, CA)

1. Isolated the mRNA (GenElute Direct mRNA Miniprep kit - Sigma) from OVCAR3 which highly express LPA_3.
2. Performed RT-PCR to obtain cDNA. The reaction used:
10 ng RNA
10 µM sense and anti-sense primers
1 µl deoxynucleotides
1 µl reaction buffer
0.5 U of Taq DNA polymerase
H_20 for a final volume of 50 µl

3. The PCR cycle was:

50°C	94°C	(94°C	55°C	72°C)	72°C	4°C
30 min	2 min	15 s	30 s	2 min	10 min	X h
		---------- 40 times ----------				

4. After the PCR cycle, the product was run on a 1% agarose gel for 1 h:
0.5 g agarose
50 mL 1X TAE
2.5 µl ethidium bromide
5. Roughly 15 µl of product was mixed with loading dye for the unknown sample. About 4 µl of the lambda marker was mixed with 2 µl of 6X loading dye and 6 µl H_2O for the standard ladder.
6. A single 1062 bp band was observed, which was purified and subcloned into pcDNA3.1 V5/His mammalian expression vector (Invitrogen).

Luciferase Assay of Transiently Transfected HepG2 Cells

Day 1:
1. Split cells as usual except get a count of the cells in the trypsin/media solution using a hemocytometer
2. Plate cells in a 12-well dish, 70,000 cells/well
3. Incubate at 37°C

Day 2:
1. Change media on cells from complete to serum free right before transfection
2. Transfect cells using Lipofectamine from Invitrogen or some other lipid-based reagent, 0.5 μg/total plasmid/well
3. Incubate 37°C

Day 3:
1. Treat the cells with agonist such that the treatment lasts for approximately 16 h

Day 4:
1. Follow protocol for Dual Luciferase Assay:
2. Lyse cells with 0.25 mL 1X Passive lysis buffer, 15-20 min.
3. Thaw LARII at room temperature water bath and add 50 μL to each tube
4. Mix 1X Stop and Glo reagent.
5. Add 20 μL lysate to LARII, pipet 2-3 times, read in luminometer.
6. Add 50 μL Stop and Glo, flick tube to mix, read in luminometer.
7. Divide first reading by second to get normalized RLUs

BCA Protein Concentration Assay

1. Make BSA standard (1 mg/mL) solutions by adding the appropriate amount of BSA to microfuge tubes (0 μl, 5, 10, 15, 20, 25).
2. Add 5 μl of protein sample to a new microfuge tube.
3. Add 0.5 ml of BCA mixture to each microfuge tube:
   1 part Soln. B to 50 parts Soln. A
4. Incubate for 30 min at 37° C.
5. Read at 562 nm on plate reader.

SDS-PAGE Gel Recipes

MINIGEL: SEPARATING GEL (10ml)

Reagent	**8%**	**10%**	**13%**	**15%**
40% Acrylamide	2ml	2.5ml	3.25ml	3.75ml
1.5M Tris, 0.4% SDS ph 8.8	2.5ml	2.5ml	2.5ml	2.5ml
ddH_20	5.5ml	5ml	4.25ml	3.75ml
10% APS	50μl	50μl	50μl	50μl
TEMED	10μl	10μl	10μl	10μl

MINIGEL: STACKING GEL (10ml)

40% Acrylamide	.75ml
0.5M Tris, 0.4% SDS pH 6.8	2.5ml

ddH_20	6.75ml
10% APS	100µl
TEMED	12µl

SDS-PAGE Set Up

1. Insert comb into rig and mark a line about 1 cm below the bottom of comb.
2. Add appropriate percentage separating gel first using a Pasteur pipet. This can store at 4°C overnight. Leave pipet in gel mixture and wait to harden (about 10-15 min).
3. Add a layer of 0.1% SDS.
4. Pour stacking gel using a Pasteur pipet taking care to get rid of bubbles. Insert comb into rig, making sure no bubbles form and allow this to dry like the separating gel.
5. Load gels into running rig, short plate towards the inside.
6. Add 1X SDS running buffer in between 2 gel rigs, check for leaks.
7. Load bench mark standard and samples with 2X or 4X sample buffer.
8. Fill 1X SDS running buffer on out side of gel rig till it covers the wire running across the inside of gel rig.
9. Run gel at ~150V until the dye runs out into the running buffer, usually 1 h.

Cell Lysis prior to Western Blotting

1. Rinse culture dishes of cells twice with ice-cold 1X PBS
2. Scrape cells into a pool at the bottom of the dish using 1X PBS with protease and phosphatase inhibitors added fresh each time
3. Transfer pool of cells into an ice-cold microfuge tube and spin in a cold centrifuge at 500-1200 rpm for about 5-15 min.
4. Add 50 µl (A549) or 200-500 µl (HeLa, HepG2) of lysis buffer to the cell pellet after removing the supernatant.

Lysis Buffer:

1% NP-40 (IPEGAL)	1mL
1% deoxycholate salt	1g
0.15M NaCl (from 5M stock)	3mL
0.1% SDS (from 20% stock)	0.5mL
0.01M sodium phosphate 7.2	10mL
2mM EDTA (from 0.5M stock)	400µl
50mM NaF (from 1M stock-poison)	5mL
0.2M orthovanadate (from 0.1M stock)	2mL
H_20 (to 100mL total volume)	78mL

*Fresh protease inhibitors each time

5. Allow the cells to lyse on ice for 30 min with vortexing every 10 min.
6. Spin in the cold centrifuge for 15 min, remove supernatant for BCA Assay.

Western Blotting (ECL Detection)

1. After electrophoresis, soak gel in transfer buffer (chilled) for 5-10 min.

2. Assemble sandwich in the order indicated on the black side of cassette:
    a. Scotch-brite pad
    b. Whatman filter paper (cut slightly larger than the gel)
    c. SDS-PAGE Gel
    d. Nitrocellulose paper (roll out bubbles with pipet)
    e. Whatman filter paper (roll out bubbles with pipet)
    f. Scotch-brite pad
3. Seal cassette, place in apparatus, fill with transfer buffer, add a stir bar, and place the ice pack in the back.
4. Place on stir plate and stir, hook up leads (- to – and + to +)
5. Transfer at 100V for 1 h.
6. Break down apparatus, store nitrocellulose in a dry petri dish until blotting.
7. Block nitrocellulose filter with 5% milk/0.1% Tx-100/PBS for 1 h on shaker.
8. Remove blocking solution.
9. Incubate with 1° Ab diluted in milk solution for 1 h on shaker.
10. Wash with Triton/PBS (1x 15 min, 3x 5 min).
11. Incubate with 2° Ab for 1 h on shaker (HRP conjugated Donkey 1:5000).
12. Wash with Triton/PBS (1x 15 min, 4x 5 min).
13. Treat on saran wrap with ECL soln (1:1 mixture of Soln A and Soln B; make up just before use) 1 min, and expose the film (start with 1 min exposure).

MAP Kinase Antibody Western Blot

1. Block nitrocellulose with TBS/5% milk for 1 h at 37°C or overnight at 4°C.
2. Dump off the milk wash.
3. Cover with TBST/0.1% BSA containing anti-active MAPK antibody (1:5000) for 2 h at room temperature with agitation.
4. Dump off antibody wash.
5. Wash 3 times with 75 ml of TBS-Tween for 15 min each.
6. Apply TBS-Tween/0.1% BSA containing Donkey anit-Rabbit HRP (1:1000) for 1 h at room temperature with agitation.
7. Wash 3 times with 75 ml TBS-Tween for 15 min each.
8. Wash 2 times with TBS only.
9. Soak for 1 min in ECL Reagent.
10. Expose to blot film in dark room.

Immunoprecipitation and Kinase Assay

1. Transfect HeLa cells in 35 mm dishes (1 well of 6 well dish)
2. Rinse cells twice with ice-cold PBS, add 0.5 mL of lysis buffer and incubate on ice 10 min.
3. Scrape cells and collect lysate in microfuge tubes, vortex to break up clumps.
4. Spin in the chilled centrifuge at 14,000 rpm (or top speed), at 4°C for 15 min.
5. Transfer lysate to fresh tube, assay 10 μl for protein concentration with BCA mix.
    (BSA stds: 0, 2, 4, 6, 8, 10, 15, and 20 μg)
6. Wash 30 μl protein A-sepharose beads with PBS.

7. Transfer equal amount of lysate (equal protein ~ 600-800 μg) to tube with protein A-sepharose beads and add 1 μl of mouse anti-HA antibody (BABCO clone 16B12). Tumble 1 h at 4°C.
8. Pellet beads and wash 3x with IP wash buffer, and once with kinase buffer.
9. Resuspend beads in 30 μl kinase rxn mixture (specific for each kinase) and incubate in a 30°C water bath for 30 min.
10. Add 10μl of 4X reducing sample buffer, boil 3 min.
11. Pellet beads and load 35 μl of supe onto a large 13% SDS gel (load around 5:00 pm). Run at 50V overnight (usually done around 7:30-8:00 am).
12. Dry gel at 80°C for 1.5 h.
13. Expose to phosporimager screen about 2-3 h.
14. Expose to film about 6h- 12h at RT using an intensifying screen. Sometimes 24 h is okay.

Human total and [pS15] p53 ELISA (Biosource Kits)

Lysing the Cells
1. Plate A549 cells into 10 cm dishes and grow ~24 h before 16 h serum starvation followed by treatment with appropriate drug or lipid.
2. Rinse the cells with cold PBS immediately before scraping.
3. Collect the cells in PBS (with phosphatase and protease inhibitors) by scraping adherent cells from the culture flasks.
4. Centrifuge (500-1200 rpm) the cells in the small, cold centrifuge.
5. Remove and discard the supernatant carefully to collect the cell pellet (at this point the cell pellet can be frozen at -80°C and lysed later).
6. Lyse the cell pellet in 50-200 μL Cell Extraction Buffer (purchase from Biosource because this one is compatible and low cost) for 30 min on ice with vortexing every 10 min.
7. Centrifuge the extract at 13,000 rpm for 10 min at 4°C. Lysate can be stored at -80°C until you are ready to perform the ELISA but avoid freeze/thaw cycles.

ELISA Procedure
1. Add 100 μL of the Biosource *Standard Diluent Buffer* to zero the wells.
2. Add 100 μL of standards, samples or controls to the wells. (Samples prepared in Cell Extraction Buffer must be diluted at least 1:10 in the *Standard Diluent Buffer*.)
3. Cover wells and incubate for 2 h at room temperature. (Can also do overnight at 4°C.)
4. Aspirate the solution from the wells and discard liquid. Wash the wells 4 times.
5. Pipette 100 μL of the *Detection Antibody* solution into each well.
6. Cover wells and incubate for 1 h at room temperature.
7. Aspirate the solution from the wells and discard liquid. Wash the wells 4 times.
8. Add 100 μL of the *anti-rabbit IgG-HRP* working solution to each well and incubate at room temperature for 30 min.
9. Aspirate the solution from the wells and discard liquid. Wash the wells 4 times.
10. Add 100 μL of *Stabilized chromogen* to each well (including doing a blank well at this point). The wells will turn blue. Incubate for 30 min at room temperature in the dark.

11. Add 100 µL *Stop Solution* to each well. The solution will turn yellow.
12. Read the absorbance at 450 nm having blanked using the well: chromogen +stops olution as the blank.
13. Plot the standards against the standard concentration. Do not extrapolate unknowns!

Making Stable Cell Lines

1. Transfect cells with appropriate DNA.
2. On day supposed to do experiment, change media and let cells grow another day.
3. Next day trypsinize cells and split 1:25 into 5, 10 cm dishes. Cover with 10 mL complete media containing 0.05 mg/mL G418.
4. On Monday, Wed, and Friday of next week, feed and treat cells with G418 (100 µl of the solution per dish).
5. When colonies are large enough to see, pick them very sterilely.
    -place 1 mL of complete media into 12 well dishes with 0.05 mg/mL G418
    -add 25 µl trypsin to lid of each well.
    -mark 5 well isolated colonies on each dish
    -remove media from cells
    -pick colony with P100 tip and transfer onto drop of trypsin with ~5 µl of trypsin in tip
    -Let sit for 2-5 minutes
6. Add cell/trypsin mixture to corresponding well of 12 well dish.
7. Place into CO2 incubator.
8. Feed cells every 3 – 4 days.
9. When see definite colonies in 12 wells split into 10 cm dish and plate onto coverslips. Keep feeding/splitting 10 cm dishes while test by Immunofluorescence for stable transfection.
10. When have identified stably transfected line, freeze it down and bleach the rest.
**Take notes every time you feed the cells (~ every 3 days)

LITERATURE CITED

1. 2004. Screening for ovarian cancer: recommendation statement. Ann Fam Med **2:**260-2.

2. **Altschuler, Y., S. Liu, L. Katz, K. Tang, S. Hardy, F. Brodsky, G. Apodaca, and K. Mostov.** 1999. ADP-ribosylation factor 6 and endocytosis at the apical surface of Madin-Darby canine kidney cells. J Cell Biol **147:**7-12.

3. **An, S.** 2000. Molecular identification and characterization of G protein-coupled receptors for lysophosphatidic acid and sphingosine 1-phosphate. Ann N Y Acad Sci **905:**25-33.

4. **An, S., T. Bleu, O. G. Hallmark, and E. J. Goetzl.** 1998. Characterization of a novel subtype of human G protein-coupled receptor for lysophosphatidic acid. J Biol Chem **273:**7906-10.

5. **An, S., T. Bleu, W. Huang, O. G. Hallmark, S. R. Coughlin, and E. J. Goetzl.** 1997. Identification of cDNAs encoding two G protein-coupled receptors for lysosphingolipids. FEBS Lett **417:**279-82.

6. **An, S., T. Bleu, Y. Zheng, and E. J. Goetzl.** 1998. Recombinant human G protein-coupled lysophosphatidic acid receptors mediate intracellular calcium mobilization. Mol Pharmacol **54:**881-8.

7. **An, S., M. A. Dickens, T. Bleu, O. G. Hallmark, and E. J. Goetzl.** 1997. Molecular cloning of the human Edg2 protein and its identification as a functional cellular receptor for lysophosphatidic acid. Biochem Biophys Res Commun **231:**619-22.

8. **Arias, E., R. N. Anderson, H. C. Kung, S. L. Murphy, and K. D. Kochanek.** 2003. Deaths: final data for 2001. Natl Vital Stat Rep **52:**1-115.

9. **Auwerx, J.** 1999. PPARgamma, the ultimate thrifty gene. Diabetologia **42:**1033-49.

10. **Baker, D. L., D. M. Desiderio, D. D. Miller, B. Tolley, and G. J. Tigyi.** 2001. Direct quantitative analysis of lysophosphatidic acid molecular species by stable isotope dilution electrospray ionization liquid chromatography-mass spectrometry. Anal Biochem **292:**287-95.

11. **Bandoh, K., J. Aoki, H. Hosono, S. Kobayashi, T. Kobayashi, K. Murakami-Murofushi, M. Tsujimoto, H. Arai, and K. Inoue.** 1999. Molecular cloning and characterization of a novel human G-protein-coupled receptor, EDG7, for lysophosphatidic acid. J Biol Chem **274:**27776-85.

12. **Banin, S., L. Moyal, S. Shieh, Y. Taya, C. W. Anderson, L. Chessa, N. I. Smorodinsky, C. Prives, Y. Reiss, Y. Shiloh, and Y. Ziv.** 1998. Enhanced phosphorylation of p53 by ATM in response to DNA damage. Science **281:**1674-7.

13. **Bartek, J., R. Iggo, J. Gannon, and D. P. Lane.** 1990. Genetic and immunochemical analysis of mutant p53 in human breast cancer cell lines. Oncogene **5:**893-9.

14. **Basu, S. K., J. L. Goldstein, R. G. Anderson, and M. S. Brown.** 1981. Monensin interrupts the recycling of low density lipoprotein receptors in human fibroblasts. Cell **24:**493-502.

15. **Behan, D. P., and D. T. Chalmers.** 2001. The use of constitutively active receptors for drug discovery at the G protein-coupled receptor gene pool. Curr Opin Drug Discov Devel **4:**548-60.

16. **Berek, J. S., C. Chung, K. Kaldi, J. M. Watson, R. M. Knox, and O. Martinez-Maza.** 1991. Serum interleukin-6 levels correlate with disease status in patients with epithelial ovarian cancer. Am J Obstet Gynecol **164:**1038-42; discussion 1042-3.

17. **Bockaert, J., and J. P. Pin.** 1999. Molecular tinkering of G protein-coupled receptors: an evolutionary success. Embo J **18:**1723-9.

18. **Bodmer, W. F., S. Cottrell, A. M. Frischauf, I. B. Kerr, V. A. Murday, A. J. Rowan, M. F. Smith, E. Solomon, H. Thomas, and L. Varesco.** 1989. Genetic analysis of colorectal cancer. Princess Takamatsu Symp **20:**49-59.

19. **Boshans, R. L., S. Szanto, L. van Aelst, and C. D'Souza-Schorey.** 2000. ADP-ribosylation factor 6 regulates actin cytoskeleton remodeling in coordination with Rac1 and RhoA. Mol Cell Biol **20:**3685-94.

20. **Boucharaba, A., C. M. Serre, S. Gres, J. S. Saulnier-Blache, J. C. Bordet, J. Guglielmi, P. Clezardin, and O. Peyruchaud.** 2004. Platelet-derived lysophosphatidic acid supports the progression of osteolytic bone metastases in breast cancer. J Clin Invest **114:**1714-25.

21. **Boyd, S. D., K. Y. Tsai, and T. Jacks.** 2000. An intact HDM2 RING-finger domain is required for nuclear exclusion of p53. Nat Cell Biol **2:**563-8.

22. **Brindley, D. N.** 2004. Lipid phosphate phosphatases and related proteins: signaling functions in development, cell division, and cancer. J Cell Biochem **92:**900-12.

23. **Brown, F. D., A. L. Rozelle, H. L. Yin, T. Balla, and J. G. Donaldson.** 2001. Phosphatidylinositol 4,5-bisphosphate and Arf6-regulated membrane traffic. J Cell Biol **154:**1007-17.

24. **Bucci, C., A. Lutcke, O. Steele-Mortimer, V. M. Olkkonen, P. Dupree, M. Chiariello, C. B. Bruni, K. Simons, and M. Zerial.** 1995. Co-operative regulation of endocytosis by three Rab5 isoforms. FEBS Lett **366:**65-71.

25. **Bunemann, M., K. B. Lee, R. Pals-Rylaarsdam, A. G. Roseberry, and M. M. Hosey.** 1999. Desensitization of G-protein-coupled receptors in the cardiovascular system. Annu Rev Physiol **61:**169-92.

26. **Cao, H., F. Garcia, and M. A. McNiven.** 1998. Differential distribution of dynamin isoforms in mammalian cells. Mol Biol Cell **9:**2595-609.

27. **Caumont, A. S., M. C. Galas, N. Vitale, D. Aunis, and M. F. Bader.** 1998. Regulated exocytosis in chromaffin cells. Translocation of ARF6 stimulates a plasma membrane-associated phospholipase D. J Biol Chem **273:**1373-9.

28. **Cavalieri, L. F., and R. G. Nemchin.** 1968. The binding of actinomycin D and F to bacterial DNA. Biochim Biophys Acta **166:**722-5.

29. **Chou, C. H., L. H. Wei, M. L. Kuo, Y. J. Huang, K. P. Lai, C. A. Chen, and C. Y. Hsieh.** 2004. Up-regulation of interleukin-6 in human ovarian cancer cell via a Gi/PI3K-Akt/NF-{kappa}B pathway by lysophosphatidic acid, an ovarian cancer activating factor. Carcinogenesis.

30. **Chun, J.** 1999. Lysophospholipid receptors: implications for neural signaling. Crit Rev Neurobiol **13:**151-68.

31. **Chun, J., T. Kwon, E. Lee, P. G. Suh, E. J. Choi, and S. Sun Kang.** 2002. The Na(+)/H(+) exchanger regulatory factor 2 mediates phosphorylation of serum- and glucocorticoid-induced protein kinase 1 by 3-phosphoinositide-dependent protein kinase 1. Biochem Biophys Res Commun **298:**207-15.

32. **Claing, A., W. Chen, W. E. Miller, N. Vitale, J. Moss, R. T. Premont, and R. J. Lefkowitz.** 2001. beta-Arrestin-mediated ADP-ribosylation factor 6 activation and beta 2-adrenergic receptor endocytosis. J Biol Chem **276:**42509-13.

33. **Claing, A., S. A. Laporte, M. G. Caron, and R. J. Lefkowitz.** 2002. Endocytosis of G protein-coupled receptors: roles of G protein-coupled receptor kinases and beta-arrestin proteins. Prog Neurobiol **66:**61-79.

34. **Claing, A., S. J. Perry, M. Achiriloaie, J. K. Walker, J. P. Albanesi, R. J. Lefkowitz, and R. T. Premont.** 2000. Multiple endocytic pathways of G protein-

coupled receptors delineated by GIT1 sensitivity. Proc Natl Acad Sci U S A **97:**1119-24.

35. **Contos, J. J., and J. Chun.** 2001. The mouse lp(A3)/Edg7 lysophosphatidic acid receptor gene: genomic structure, chromosomal localization, and expression pattern. Gene **267:**243-53.

36. **D'Souza-Schorey, C., G. Li, M. I. Colombo, and P. D. Stahl.** 1995. A regulatory role for ARF6 in receptor-mediated endocytosis. Science **267:**1175-8.

37. **D'Souza-Schorey, C., E. van Donselaar, V. W. Hsu, C. Yang, P. D. Stahl, and P. J. Peters.** 1998. ARF6 targets recycling vesicles to the plasma membrane: insights from an ultrastructural investigation. J Cell Biol **140:**603-16.

38. **Daaka, Y., L. M. Luttrell, S. Ahn, G. J. Della Rocca, S. S. Ferguson, M. G. Caron, and R. J. Lefkowitz.** 1998. Essential role for G protein-coupled receptor endocytosis in the activation of mitogen-activated protein kinase. J Biol Chem **273:**685-8.

39. **Damke, H., T. Baba, D. E. Warnock, and S. L. Schmid.** 1994. Induction of mutant dynamin specifically blocks endocytic coated vesicle formation. J Cell Biol **127:**915-34.

40. **Das, A. K., and A. K. Hajra.** 1989. Quantification, characterization and fatty acid composition of lysophosphatidic acid in different rat tissues. Lipids **24:**329-33.

41. **DeFea, K. A., J. Zalevsky, M. S. Thoma, O. Dery, R. D. Mullins, and N. W. Bunnett.** 2000. beta-arrestin-dependent endocytosis of proteinase-activated receptor 2 is required for intracellular targeting of activated ERK1/2. J Cell Biol **148:**1267-81.

42. **Demoulin, J. B., J. K. Seo, S. Ekman, E. Grapengiesser, U. Hellman, L. Ronnstrand, and C. H. Heldin.** 2003. Ligand-induced recruitment of Na+/H+-exchanger regulatory factor to the PDGF (platelet-derived growth factor) receptor regulates actin cytoskeleton reorganization by PDGF. Biochem J **376:**505-10.

43. **Deng, W., L. Balazs, D. A. Wang, L. Van Middlesworth, G. Tigyi, and L. R. Johnson.** 2002. Lysophosphatidic acid protects and rescues intestinal epithelial cells from radiation- and chemotherapy-induced apoptosis. Gastroenterology **123:**206-16.

44. **Deng, W., H. Poppleton, S. Yasuda, N. Makarova, Y. Shinozuka, D. A. Wang, L. R. Johnson, T. B. Patel, and G. Tigyi.** 2004. Optimal lysophosphatidic acid-induced DNA synthesis and cell migration but not survival

require intact autophosphorylation sites of the epidermal growth factor receptor. J Biol Chem **279:**47871-80.

45. **Deng, W., D. A. Wang, E. Gosmanova, L. R. Johnson, and G. Tigyi.** 2003. LPA protects intestinal epithelial cells from apoptosis by inhibiting the mitochondrial pathway. Am J Physiol Gastrointest Liver Physiol **284:**G821-9.

46. **Donaldson, J. G., and C. L. Jackson.** 2000. Regulators and effectors of the ARF GTPases. Curr Opin Cell Biol **12:**475-82.

47. **Downward, J.** 2004. PI 3-kinase, Akt and cell survival. Semin Cell Dev Biol **15:**177-82.

48. **Eder, A. M., T. Sasagawa, M. Mao, J. Aoki, and G. B. Mills.** 2000. Constitutive and lysophosphatidic acid (LPA)-induced LPA production: role of phospholipase D and phospholipase A2. Clin Cancer Res **6:**2482-91.

49. **Eichholtz, T., K. Jalink, I. Fahrenfort, and W. H. Moolenaar.** 1993. The bioactive phospholipid lysophosphatidic acid is released from activated platelets. Biochem J **291 (Pt 3):**677-80.

50. **el-Deiry, W. S., T. Tokino, V. E. Velculescu, D. B. Levy, R. Parsons, J. M. Trent, D. Lin, W. E. Mercer, K. W. Kinzler, and B. Vogelstein.** 1993. WAF1, a potential mediator of p53 tumor suppression. Cell **75:**817-25.

51. **English, D., Y. Cui, R. Siddiqui, C. Patterson, V. Natarajan, D. N. Brindley, and J. G. Garcia.** 1999. Induction of endothelial monolayer permeability by phosphatidate. J Cell Biochem **75:**105-17.

52. **Essler, M., M. Retzer, M. Bauer, J. W. Heemskerk, M. Aepfelbacher, and W. Siess.** 1999. Mildly oxidized low density lipoprotein induces contraction of human endothelial cells through activation of Rho/Rho kinase and inhibition of myosin light chain phosphatase. J Biol Chem **274:**30361-4.

53. **Fang, X., D. Gaudette, T. Furui, M. Mao, V. Estrella, A. Eder, T. Pustilnik, T. Sasagawa, R. Lapushin, S. Yu, R. B. Jaffe, J. R. Wiener, J. R. Erickson, and G. B. Mills.** 2000. Lysophospholipid growth factors in the initiation, progression, metastases, and management of ovarian cancer. Ann N Y Acad Sci **905:**188-208.

54. **Fang, X., M. Schummer, M. Mao, S. Yu, F. H. Tabassam, R. Swaby, Y. Hasegawa, J. L. Tanyi, R. LaPushin, A. Eder, R. Jaffe, J. Erickson, and G. B. Mills.** 2002. Lysophosphatidic acid is a bioactive mediator in ovarian cancer. Biochim Biophys Acta **1582:**257-64.

55. **Fang, X., S. Yu, R. C. Bast, S. Liu, H. J. Xu, S. X. Hu, R. LaPushin, F. X. Claret, B. B. Aggarwal, Y. Lu, and G. B. Mills.** 2004. Mechanisms for lysophosphatidic acid-induced cytokine production in ovarian cancer cells. J Biol Chem **279:**9653-61.

56. **Fang, X., S. Yu, R. LaPushin, Y. Lu, T. Furui, L. Z. Penn, D. Stokoe, J. R. Erickson, R. C. Bast, Jr., and G. B. Mills.** 2000. Lysophosphatidic acid prevents apoptosis in fibroblasts via G(i)-protein-mediated activation of mitogen-activated protein kinase. Biochem J **352 Pt 1:**135-43.

57. **Ferguson, S. S.** 2001. Evolving concepts in G protein-coupled receptor endocytosis: the role in receptor desensitization and signaling. Pharmacol Rev **53:**1-24.

58. **Ferguson, S. S., W. E. Downey, 3rd, A. M. Colapietro, L. S. Barak, L. Menard, and M. G. Caron.** 1996. Role of beta-arrestin in mediating agonist-promoted G protein-coupled receptor internalization. Science **271:**363-6.

59. **Ferry, G., E. Tellier, A. Try, S. Gres, I. Naime, M. F. Simon, M. Rodriguez, J. Boucher, I. Tack, S. Gesta, P. Chomarat, M. Dieu, M. Raes, J. P. Galizzi, P. Valet, J. A. Boutin, and J. S. Saulnier-Blache.** 2003. Autotaxin is released from adipocytes, catalyzes lysophosphatidic acid synthesis, and activates preadipocyte proliferation. Up-regulated expression with adipocyte differentiation and obesity. J Biol Chem **278:**18162-9.

60. **Filmore, D.** 2004. It's a GPCR World. Modern Drug Discovery from Concept to Development**:**24-28.

61. **Fischer, D. J., K. Liliom, Z. Guo, N. Nusser, T. Virag, K. Murakami-Murofushi, S. Kobayashi, J. R. Erickson, G. Sun, D. D. Miller, and G. Tigyi.** 1998. Naturally occurring analogs of lysophosphatidic acid elicit different cellular responses through selective activation of multiple receptor subtypes. Mol Pharmacol **54:**979-88.

62. **Franco, M., P. J. Peters, J. Boretto, E. van Donselaar, A. Neri, C. D'Souza-Schorey, and P. Chavrier.** 1999. EFA6, a sec7 domain-containing exchange factor for ARF6, coordinates membrane recycling and actin cytoskeleton organization. Embo J **18:**1480-91.

63. **Frankel, A., and G. B. Mills.** 1996. Peptide and lipid growth factors decrease cis-diamminedichloroplatinum-induced cell death in human ovarian cancer cells. Clin Cancer Res **2:**1307-13.

64. **Freund, A., C. Chauveau, J. P. Brouillet, A. Lucas, M. Lacroix, A. Licznar, F. Vignon, and G. Lazennec.** 2003. IL-8 expression and its possible relationship

with estrogen-receptor-negative status of breast cancer cells. Oncogene **22:**256-65.

65. **Fukushima, N., Y. Kimura, and J. Chun.** 1998. A single receptor encoded by vzg-1/lpA1/edg-2 couples to G proteins and mediates multiple cellular responses to lysophosphatidic acid. Proc Natl Acad Sci U S A **95:**6151-6.

66. **Fukushima, N., J. A. Weiner, and J. Chun.** 2000. Lysophosphatidic acid (LPA) is a novel extracellular regulator of cortical neuroblast morphology. Dev Biol **228:**6-18.

67. **Furui, T., R. LaPushin, M. Mao, H. Khan, S. R. Watt, M. A. Watt, Y. Lu, X. Fang, S. Tsutsui, Z. H. Siddik, R. C. Bast, and G. B. Mills.** 1999. Overexpression of edg-2/vzg-1 induces apoptosis and anoikis in ovarian cancer cells in a lysophosphatidic acid-independent manner. Clin Cancer Res **5:**4308-18.

68. **G.B. Mills, C. M.** 1989. Regulatory mechanisms in ascitic fluid. Chapman & Hall Medical, London.

69. **Garcia, J. F., R. Villuendas, M. Sanchez-Beato, A. Sanchez-Aguilera, L. Sanchez, I. Prieto, and M. A. Piris.** 2002. Nucleolar p14(ARF) overexpression in Reed-Sternberg cells in Hodgkin's lymphoma: absence of p14(ARF)/Hdm2 complexes is associated with expression of alternatively spliced Hdm2 transcripts. Am J Pathol **160:**569-78.

70. **Geyer, R. K., Z. K. Yu, and C. G. Maki.** 2000. The MDM2 RING-finger domain is required to promote p53 nuclear export. Nat Cell Biol **2:**569-73.

71. **Gobeil, F., Jr., S. G. Bernier, A. Vazquez-Tello, S. Brault, M. H. Beauchamp, C. Quiniou, A. M. Marrache, D. Checchin, F. Sennlaub, X. Hou, M. Nader, G. Bkaily, A. Ribeiro-da-Silva, E. J. Goetzl, and S. Chemtob.** 2003. Modulation of pro-inflammatory gene expression by nuclear lysophosphatidic acid receptor type-1. J Biol Chem **278:**38875-83.

72. **Goetzl, E. J., H. Dolezalova, Y. Kong, Y. L. Hu, R. B. Jaffe, K. R. Kalli, and C. A. Conover.** 1999. Distinctive expression and functions of the type 4 endothelial differentiation gene-encoded G protein-coupled receptor for lysophosphatidic acid in ovarian cancer. Cancer Res **59:**5370-5.

73. **Goetzl, E. J., H. Dolezalova, Y. Kong, and L. Zeng.** 1999. Dual mechanisms for lysophospholipid induction of proliferation of human breast carcinoma cells. Cancer Res **59:**4732-7.

74. **Goetzl, E. J., Y. Kong, and B. Mei.** 1999. Lysophosphatidic acid and sphingosine 1-phosphate protection of T cells from apoptosis in association with suppression of Bax. J Immunol **162:**2049-56.

75. **Goetzl, E. J., and G. Tigyi.** 2004. Lysophospholipids and their G protein-coupled receptors in biology and diseases. J Cell Biochem **92:**867-8.

76. **Goodman, O. B., Jr., J. G. Krupnick, F. Santini, V. V. Gurevich, R. B. Penn, A. W. Gagnon, J. H. Keen, and J. L. Benovic.** 1996. Beta-arrestin acts as a clathrin adaptor in endocytosis of the beta2-adrenergic receptor. Nature **383:**447-50.

77. **Hainaut, P., T. Soussi, B. Shomer, M. Hollstein, M. Greenblatt, E. Hovig, C. C. Harris, and R. Montesano.** 1997. Database of p53 gene somatic mutations in human tumors and cell lines: updated compilation and future prospects. Nucleic Acids Res **25:**151-7.

78. **Hall, R. A., L. S. Ostedgaard, R. T. Premont, J. T. Blitzer, N. Rahman, M. J. Welsh, and R. J. Lefkowitz.** 1998. A C-terminal motif found in the beta2-adrenergic receptor, P2Y1 receptor and cystic fibrosis transmembrane conductance regulator determines binding to the Na+/H+ exchanger regulatory factor family of PDZ proteins. Proc Natl Acad Sci U S A **95:**8496-501.

79. **Hall, R. A., R. T. Premont, C. W. Chow, J. T. Blitzer, J. A. Pitcher, A. Claing, R. H. Stoffel, L. S. Barak, S. Shenolikar, E. J. Weinman, S. Grinstein, and R. J. Lefkowitz.** 1998. The beta2-adrenergic receptor interacts with the Na+/H+-exchanger regulatory factor to control Na+/H+ exchange. Nature **392:**626-30.

80. **Hall, R. A., R. T. Premont, and R. J. Lefkowitz.** 1999. Heptahelical receptor signaling: beyond the G protein paradigm. J Cell Biol **145:**927-32.

81. **Hama, K., J. Aoki, M. Fukaya, Y. Kishi, T. Sakai, R. Suzuki, H. Ohta, T. Yamori, M. Watanabe, J. Chun, and H. Arai.** 2004. Lysophosphatidic acid and autotaxin stimulate cell motility of neoplastic and non-neoplastic cells through LPA1. J Biol Chem **279:**17634-9.

82. **Hanahan, D., and R. A. Weinberg.** 2000. The hallmarks of cancer. Cell **100:**57-70.

83. **Haupt, Y., R. Maya, A. Kazaz, and M. Oren.** 1997. Mdm2 promotes the rapid degradation of p53. Nature **387:**296-9.

84. **Hecht, J. H., J. A. Weiner, S. R. Post, and J. Chun.** 1996. Ventricular zone gene-1 (vzg-1) encodes a lysophosphatidic acid receptor expressed in neurogenic regions of the developing cerebral cortex. J Cell Biol **135:**1071-83.

85. **Henley, J. R., E. W. Krueger, B. J. Oswald, and M. A. McNiven.** 1998. Dynamin-mediated internalization of caveolae. J Cell Biol **141:**85-99.

86. **Hill, C. S., J. Wynne, and R. Treisman.** 1995. The Rho family GTPases RhoA, Rac1, and CDC42Hs regulate transcriptional activation by SRF. Cell **81:**1159-70.

87. **Hla, T., M. J. Lee, N. Ancellin, J. H. Paik, and M. J. Kluk.** 2001. Lysophospholipids--receptor revelations. Science **294:**1875-8.

88. **Hofseth, L. J., S. P. Hussain, and C. C. Harris.** 2004. p53: 25 years after its discovery. Trends Pharmacol Sci **25:**177-81.

89. **Honda, A., M. Nogami, T. Yokozeki, M. Yamazaki, H. Nakamura, H. Watanabe, K. Kawamoto, K. Nakayama, A. J. Morris, M. A. Frohman, and Y. Kanaho.** 1999. Phosphatidylinositol 4-phosphate 5-kinase alpha is a downstream effector of the small G protein ARF6 in membrane ruffle formation. Cell **99:**521-32.

90. **Honda, R., H. Tanaka, and H. Yasuda.** 1997. Oncoprotein MDM2 is a ubiquitin ligase E3 for tumor suppressor p53. FEBS Lett **420:**25-7.

91. **Hsu, I. C., T. Tokiwa, W. Bennett, R. A. Metcalf, J. A. Welsh, T. Sun, and C. C. Harris.** 1993. p53 gene mutation and integrated hepatitis B viral DNA sequences in human liver cancer cell lines. Carcinogenesis **14:**987-92.

92. **Hu, L. A., Y. Tang, W. E. Miller, M. Cong, A. G. Lau, R. J. Lefkowitz, and R. A. Hall.** 2000. beta 1-adrenergic receptor association with PSD-95. Inhibition of receptor internalization and facilitation of beta 1-adrenergic receptor interaction with N-methyl-D-aspartate receptors. J Biol Chem **275:**38659-66.

93. **Hu, Y. L., M. K. Tee, E. J. Goetzl, N. Auersperg, G. B. Mills, N. Ferrara, and R. B. Jaffe.** 2001. Lysophosphatidic acid induction of vascular endothelial growth factor expression in human ovarian cancer cells. J Natl Cancer Inst **93:**762-8.

94. **Imai, A., T. Furui, T. Tamaya, and G. B. Mills.** 2000. A gonadotropin-releasing hormone-responsive phosphatase hydrolyses lysophosphatidic acid within the plasma membrane of ovarian cancer cells. J Clin Endocrinol Metab **85:**3370-5.

95. **Inoue, C. N., I. Nagano, R. Ichinohasama, N. Asato, Y. Kondo, and K. Iinuma.** 2001. Bimodal effects of platelet-derived growth factor on rat mesangial cell proliferation and death, and the role of lysophosphatidic acid in cell survival. Clin Sci (Lond) **101:**11-9.

96. **Ishii, I., J. J. Contos, N. Fukushima, and J. Chun.** 2000. Functional comparisons of the lysophosphatidic acid receptors, LP(A1)/VZG-1/EDG-2, LP(A2)/EDG-4, and LP(A3)/EDG-7 in neuronal cell lines using a retrovirus expression system. Mol Pharmacol **58:**895-902.

97. **Jalink, K., E. J. van Corven, T. Hengeveld, N. Morii, S. Narumiya, and W. H. Moolenaar.** 1994. Inhibition of lysophosphatidate- and thrombin-induced neurite retraction and neuronal cell rounding by ADP ribosylation of the small GTP-binding protein Rho. J Cell Biol **126:**801-10.

98. **Jasinska, R., Q. X. Zhang, C. Pilquil, I. Singh, J. Xu, J. Dewald, D. A. Dillon, L. G. Berthiaume, G. M. Carman, D. W. Waggoner, and D. N. Brindley.** 1999. Lipid phosphate phosphohydrolase-1 degrades exogenous glycerolipid and sphingolipid phosphate esters. Biochem J **340 (Pt 3):**677-86.

99. **Johnston, J. B., J. T. Paul, N. J. Neufeld, N. Haney, D. M. Kropp, X. Hu, M. Cheang, and S. B. Gibson.** 2004. Role of myeloid cell factor-1 (Mcl-1) in chronic lymphocytic leukemia. Leuk Lymphoma **45:**2017-27.

100. **Kelley, L. L., W. F. Green, G. G. Hicks, M. C. Bondurant, M. J. Koury, and H. E. Ruley.** 1994. Apoptosis in erythroid progenitors deprived of erythropoietin occurs during the G1 and S phases of the cell cycle without growth arrest or stabilization of wild-type p53. Mol Cell Biol **14:**4183-92.

101. **Kirk, J. M.** 1960. The mode of action of actinomycin D. Biochim Biophys Acta **42:**167-9.

102. **Kolch, W.** 2000. Meaningful relationships: the regulation of the Ras/Raf/MEK/ERK pathway by protein interactions. Biochem J **351 Pt 2:**289-305.

103. **Komarov, P. G., E. A. Komarova, R. V. Kondratov, K. Christov-Tselkov, J. S. Coon, M. V. Chernov, and A. V. Gudkov.** 1999. A chemical inhibitor of p53 that protects mice from the side effects of cancer therapy. Science **285:**1733-7.

104. **Kooijman, E. E., V. Chupin, B. de Kruijff, and K. N. Burger.** 2003. Modulation of membrane curvature by phosphatidic acid and lysophosphatidic acid. Traffic **4:**162-74.

105. **Kranenburg, O., I. Verlaan, and W. H. Moolenaar.** 1999. Dynamin is required for the activation of mitogen-activated protein (MAP) kinase by MAP kinase kinase. J Biol Chem **274:**35301-4.

106. **Kubbutat, M. H., S. N. Jones, and K. H. Vousden.** 1997. Regulation of p53 stability by Mdm2. Nature **387:**299-303.

107. **Kuliopulos, A., and L. Covic.** 2003. Blocking receptors on the inside: pepducin-based intervention of PAR signaling and thrombosis. Life Sci **74:**255-62.

108. **Laporte, S. A., R. H. Oakley, J. A. Holt, L. S. Barak, and M. G. Caron.** 2000. The interaction of beta-arrestin with the AP-2 adaptor is required for the

clustering of beta 2-adrenergic receptor into clathrin-coated pits. J Biol Chem **275:**23120-6.

109. **Lee, H., E. J. Goetzl, and S. An.** 2000. Lysophosphatidic acid and sphingosine 1-phosphate stimulate endothelial cell wound healing. Am J Physiol Cell Physiol **278:**C612-8.

110. **Lee, H. Y., G. U. Bae, I. D. Jung, J. S. Lee, Y. K. Kim, S. H. Noh, M. L. Stracke, C. G. Park, H. W. Lee, and J. W. Han.** 2002. Autotaxin promotes motility via G protein-coupled phosphoinositide 3-kinase gamma in human melanoma cells. FEBS Lett **515:**137-40.

111. **Lee, M. J., J. R. Van Brocklyn, S. Thangada, C. H. Liu, A. R. Hand, R. Menzeleev, S. Spiegel, and T. Hla.** 1998. Sphingosine-1-phosphate as a ligand for the G protein-coupled receptor EDG-1. Science **279:**1552-5.

112. **Leung, D. W., C. K. Tompkins, and T. White.** 1998. Molecular cloning of two alternatively spliced forms of human phosphatidic acid phosphatase cDNAs that are differentially expressed in normal and tumor cells. DNA Cell Biol **17:**377-85.

113. **Levine, J. S., J. S. Koh, V. Triaca, and W. Lieberthal.** 1997. Lysophosphatidic acid: a novel growth and survival factor for renal proximal tubular cells. Am J Physiol **273:**F575-85.

114. **Linzer, D. I., and A. J. Levine.** 1979. Characterization of a 54K dalton cellular SV40 tumor antigen present in SV40-transformed cells and uninfected embryonal carcinoma cells. Cell **17:**43-52.

115. **Liu, C. H., S. Thangada, M. J. Lee, J. R. Van Brocklyn, S. Spiegel, and T. Hla.** 1999. Ligand-induced trafficking of the sphingosine-1-phosphate receptor EDG-1. Mol Biol Cell **10:**1179-90.

116. **Lowe, S. W., and H. E. Ruley.** 1993. Stabilization of the p53 tumor suppressor is induced by adenovirus 5 E1A and accompanies apoptosis. Genes Dev **7:**535-45.

117. **Lu, W., J. Lin, and J. Chen.** 2002. Expression of p14ARF overcomes tumor resistance to p53. Cancer Res **62:**1305-10.

118. **Luttrell, L. M., F. L. Roudabush, E. W. Choy, W. E. Miller, M. E. Field, K. L. Pierce, and R. J. Lefkowitz.** 2001. Activation and targeting of extracellular signal-regulated kinases by beta-arrestin scaffolds. Proc Natl Acad Sci U S A **98:**2449-54.

119. **Maltzman, W., and L. Czyzyk.** 1984. UV irradiation stimulates levels of p53 cellular tumor antigen in nontransformed mouse cells. Mol Cell Biol **4:**1689-94.

120. **Marchese, A., and J. L. Benovic.** 2001. Agonist-promoted ubiquitination of the G protein-coupled receptor CXCR4 mediates lysosomal sorting. J Biol Chem **276:**45509-12.

121. **McBride, H. M., V. Rybin, C. Murphy, A. Giner, R. Teasdale, and M. Zerial.** 1999. Oligomeric complexes link Rab5 effectors with NSF and drive membrane fusion via interactions between EEA1 and syntaxin 13. Cell **98:**377-86.

122. **McIntyre, T. M., A. V. Pontsler, A. R. Silva, A. St Hilaire, Y. Xu, J. C. Hinshaw, G. A. Zimmerman, K. Hama, J. Aoki, H. Arai, and G. D. Prestwich.** 2003. Identification of an intracellular receptor for lysophosphatidic acid (LPA): LPA is a transcellular PPARgamma agonist. Proc Natl Acad Sci U S A **100:**131-6.

123. **McLauchlan, H., J. Newell, N. Morrice, A. Osborne, M. West, and E. Smythe.** 1998. A novel role for Rab5-GDI in ligand sequestration into clathrin-coated pits. Curr Biol **8:**34-45.

124. **McNiven, M. A.** 1998. Dynamin: a molecular motor with pinchase action. Cell **94:**151-4.

125. **Meng, Y., L. Graves, T. V. Do, J. So, and D. A. Fishman.** 2004. Upregulation of FasL by LPA on ovarian cancer cell surface leads to apoptosis of activated lymphocytes. Gynecol Oncol **95:**488-95.

126. **Miaczynska, M., and M. Zerial.** 2002. Mosaic organization of the endocytic pathway. Exp Cell Res **272:**8-14.

127. **Middeler, G., K. Zerf, S. Jenovai, A. Thulig, M. Tschodrich-Rotter, U. Kubitscheck, and R. Peters.** 1997. The tumor suppressor p53 is subject to both nuclear import and export, and both are fast, energy-dependent and lectin-inhibited. Oncogene **14:**1407-17.

128. **Mihara, M., S. Erster, A. Zaika, O. Petrenko, T. Chittenden, P. Pancoska, and U. M. Moll.** 2003. p53 has a direct apoptogenic role at the mitochondria. Mol Cell **11:**577-90.

129. **Mills, G. B., and W. H. Moolenaar.** 2003. The emerging role of lysophosphatidic acid in cancer. Nat Rev Cancer **3:**582-91.

130. **Momand, J., G. P. Zambetti, D. C. Olson, D. George, and A. J. Levine.** 1992. The mdm-2 oncogene product forms a complex with the p53 protein and inhibits p53-mediated transactivation. Cell **69:**1237-45.

131. **Moolenaar, W. H.** 1999. Bioactive lysophospholipids and their G protein-coupled receptors. Exp Cell Res **253:**230-8.

132. **Moolenaar, W. H., O. Kranenburg, F. R. Postma, and G. C. Zondag.** 1997. Lysophosphatidic acid: G-protein signalling and cellular responses. Curr Opin Cell Biol **9:**168-73.

133. **Mori, M., T. Nishida, T. Sugiyama, K. Komai, M. Yakushiji, K. Fukuda, T. Tanaka, M. Yokoyama, and H. Sugimori.** 1998. Anthropometric and other risk factors for ovarian cancer in a case-control study. Jpn J Cancer Res **89:**246-53.

134. **Moughal, N. A., C. Waters, B. Sambi, S. Pyne, and N. J. Pyne.** 2004. Nerve growth factor signaling involves interaction between the Trk A receptor and lysophosphatidate receptor 1 systems: nuclear translocation of the lysophosphatidate receptor 1 and Trk A receptors in pheochromocytoma 12 cells. Cell Signal **16:**127-36.

135. **Mukai, M., H. Nakamura, M. Tatsuta, T. Iwasaki, A. Togawa, F. Imamura, and H. Akedo.** 2000. Hepatoma cell migration through a mesothelial cell monolayer is inhibited by cyclic AMP-elevating agents via a Rho-dependent pathway. FEBS Lett **484:**69-73.

136. **Mukherjee, S., V. V. Gurevich, J. C. Jones, J. E. Casanova, S. R. Frank, E. T. Maizels, M. F. Bader, R. A. Kahn, K. Palczewski, K. Aktories, and M. Hunzicker-Dunn.** 2000. The ADP ribosylation factor nucleotide exchange factor ARNO promotes beta-arrestin release necessary for luteinizing hormone/choriogonadotropin receptor desensitization. Proc Natl Acad Sci U S A **97:**5901-6.

137. **Nguyen, G. H., R. French, and H. Radhakrishna.** 2004. Protein kinase A inhibits lysophosphatidic acid induction of serum response factor via alterations in the actin cytoskeleton. Cell Signal **16:**1141-51.

138. **Noguchi, K., S. Ishii, and T. Shimizu.** 2003. Identification of p2y9/GPR23 as a novel G protein-coupled receptor for lysophosphatidic acid, structurally distant from the Edg family. J Biol Chem **278:**25600-6.

139. **O'Keefe, K., H. Li, and Y. Zhang.** 2003. Nucleocytoplasmic shuttling of p53 is essential for MDM2-mediated cytoplasmic degradation but not ubiquitination. Mol Cell Biol **23:**6396-405.

140. **Oakley, R. H., S. A. Laporte, J. A. Holt, L. S. Barak, and M. G. Caron.** 1999. Association of beta-arrestin with G protein-coupled receptors during clathrin-mediated endocytosis dictates the profile of receptor resensitization. J Biol Chem **274:**32248-57.

141. **Oh, Y. S., N. W. Jo, J. W. Choi, H. S. Kim, S. W. Seo, K. O. Kang, J. I. Hwang, K. Heo, S. H. Kim, Y. H. Kim, I. H. Kim, J. H. Kim, Y. Banno, S. H.**

Ryu, and P. G. Suh. 2004. NHERF2 specifically interacts with LPA2 receptor and defines the specificity and efficiency of receptor-mediated phospholipase C-beta3 activation. Mol Cell Biol **24:**5069-79.

142. **Okusa, M. D., H. Ye, L. Huang, L. Sigismund, T. Macdonald, and K. R. Lynch.** 2003. Selective blockade of lysophosphatidic acid LPA3 receptors reduces murine renal ischemia-reperfusion injury. Am J Physiol Renal Physiol **285:**F565-74.

143. **Oliner, J. D., J. A. Pietenpol, S. Thiagalingam, J. Gyuris, K. W. Kinzler, and B. Vogelstein.** 1993. Oncoprotein MDM2 conceals the activation domain of tumour suppressor p53. Nature **362:**857-60.

144. **Pals-Rylaarsdam, R., V. V. Gurevich, K. B. Lee, J. A. Ptasienski, J. L. Benovic, and M. M. Hosey.** 1997. Internalization of the m2 muscarinic acetylcholine receptor. Arrestin-independent and -dependent pathways. J Biol Chem **272:**23682-9.

145. **Pals-Rylaarsdam, R., and M. M. Hosey.** 1997. Two homologous phosphorylation domains differentially contribute to desensitization and internalization of the m2 muscarinic acetylcholine receptor. J Biol Chem **272:**14152-8.

146. **Peters, P. J., V. W. Hsu, C. E. Ooi, D. Finazzi, S. B. Teal, V. Oorschot, J. G. Donaldson, and R. D. Klausner.** 1995. Overexpression of wild-type and mutant ARF1 and ARF6: distinct perturbations of nonoverlapping membrane compartments. J Cell Biol **128:**1003-17.

147. **Piazza, G. A., J. L. Ritter, and C. A. Baracka.** 1995. Lysophosphatidic acid induction of transforming growth factors alpha and beta: modulation of proliferation and differentiation in cultured human keratinocytes and mouse skin. Exp Cell Res **216:**51-64.

148. **Pilquil, C., I. Singh, Q. Zhang, Z. Ling, K. Buri, L. M. Stromberg, J. Dewald, and D. N. Brindley.** 2001. Lipid phosphate phosphatase-1 dephosphorylates exogenous lysophosphatidate and thereby attenuates its effects on cell signalling. Prostaglandins **64:**83-92.

149. **Pitcher, J. A., N. J. Freedman, and R. J. Lefkowitz.** 1998. G protein-coupled receptor kinases. Annu Rev Biochem **67:**653-92.

150. **Pitcher, J. A., E. S. Payne, C. Csortos, A. A. DePaoli-Roach, and R. J. Lefkowitz.** 1995. The G-protein-coupled receptor phosphatase: a protein phosphatase type 2A with a distinct subcellular distribution and substrate specificity. Proc Natl Acad Sci U S A **92:**8343-7.

151. **Premont, R. T., A. Claing, N. Vitale, J. L. Freeman, J. A. Pitcher, W. A. Patton, J. Moss, M. Vaughan, and R. J. Lefkowitz.** 1998. beta2-Adrenergic receptor regulation by GIT1, a G protein-coupled receptor kinase-associated ADP ribosylation factor GTPase-activating protein. Proc Natl Acad Sci U S A **95:**14082-7.

152. **Pustilnik, T. B., V. Estrella, J. R. Wiener, M. Mao, A. Eder, M. A. Watt, R. C. Bast, Jr., and G. B. Mills.** 1999. Lysophosphatidic acid induces urokinase secretion by ovarian cancer cells. Clin Cancer Res **5:**3704-10.

153. **Radeff-Huang, J., T. M. Seasholtz, R. G. Matteo, and J. H. Brown.** 2004. G protein mediated signaling pathways in lysophospholipid induced cell proliferation and survival. J Cell Biochem **92:**949-66.

154. **Radhakrishna, H., O. Al-Awar, Z. Khachikian, and J. G. Donaldson.** 1999. ARF6 requirement for Rac ruffling suggests a role for membrane trafficking in cortical actin rearrangements. J Cell Sci **112 (Pt 6):**855-66.

155. **Radhakrishna, H., and J. G. Donaldson.** 1997. ADP-ribosylation factor 6 regulates a novel plasma membrane recycling pathway. J Cell Biol **139:**49-61.

156. **Radhakrishna, H., R. D. Klausner, and J. G. Donaldson.** 1996. Aluminum fluoride stimulates surface protrusions in cells overexpressing the ARF6 GTPase. J Cell Biol **134:**935-47.

157. **Rady, P., F. Scinicariello, R. F. Wagner, Jr., and S. K. Tyring.** 1992. p53 mutations in basal cell carcinomas. Cancer Res **52:**3804-6.

158. **Raj, G. V., J. A. Sekula, R. Guo, J. F. Madden, and Y. Daaka.** 2004. Lysophosphatidic acid promotes survival of androgen-insensitive prostate cancer PC3 cells via activation of NF-kappaB. Prostate **61:**105-13.

159. **Ramet, M., K. Castren, K. Jarvinen, K. Pekkala, T. Turpeenniemi-Hujanen, Y. Soini, P. Paakko, and K. Vahakangas.** 1995. p53 protein expression is correlated with benzo[a]pyrene-DNA adducts in carcinoma cell lines. Carcinogenesis **16:**2117-24.

160. **Randazzo, P. A., Z. Nie, K. Miura, and V. W. Hsu.** 2000. Molecular aspects of the cellular activities of ADP-ribosylation factors. Sci STKE **2000:**RE1.

161. **Raycroft, L., J. R. Schmidt, K. Yoas, M. M. Hao, and G. Lozano.** 1991. Analysis of p53 mutants for transcriptional activity. Mol Cell Biol **11:**6067-74.

162. **Reiss, M., D. E. Brash, T. Munoz-Antonia, J. A. Simon, A. Ziegler, V. F. Vellucci, and Z. L. Zhou.** 1992. Status of the p53 tumor suppressor gene in human squamous carcinoma cell lines. Oncol Res **4:**349-57.

163. **Rodriguez, C., E. E. Calle, D. Fakhrabadi-Shokoohi, E. J. Jacobs, and M. J. Thun.** 2002. Body mass index, height, and the risk of ovarian cancer mortality in a prospective cohort of postmenopausal women. Cancer Epidemiol Biomarkers Prev **11:**822-8.

164. **Rodriguez, C., A. V. Patel, E. E. Calle, E. J. Jacob, and M. J. Thun.** 2001. Estrogen replacement therapy and ovarian cancer mortality in a large prospective study of US women. Jama **285:**1460-5.

165. **Roseberry, A. G., and M. M. Hosey.** 2001. Internalization of the M2 muscarinic acetylcholine receptor proceeds through an atypical pathway in HEK293 cells that is independent of clathrin and caveolae. J Cell Sci **114:**739-46.

166. **Roseberry, A. G., and M. M. Hosey.** 1999. Trafficking of M(2) muscarinic acetylcholine receptors. J Biol Chem **274:**33671-6.

167. **Rother, E., R. Brandl, D. L. Baker, P. Goyal, H. Gebhard, G. Tigyi, and W. Siess.** 2003. Subtype-selective antagonists of lysophosphatidic Acid receptors inhibit platelet activation triggered by the lipid core of atherosclerotic plaques. Circulation **108:**741-7.

168. **Rotter, V., H. Abutbul, and A. Ben-Ze'ev.** 1983. P53 transformation-related protein accumulates in the nucleus of transformed fibroblasts in association with the chromatin and is found in the cytoplasm of non-transformed fibroblasts. Embo J **2:**1041-7.

169. **Runnebaum, I. B., M. Nagarajan, M. Bowman, D. Soto, and S. Sukumar.** 1991. Mutations in p53 as potential molecular markers for human breast cancer. Proc Natl Acad Sci U S A **88:**10657-61.

170. **Sakaguchi, K., H. Sakamoto, M. S. Lewis, C. W. Anderson, J. W. Erickson, E. Appella, and D. Xie.** 1997. Phosphorylation of serine 392 stabilizes the tetramer formation of tumor suppressor protein p53. Biochemistry **36:**10117-24.

171. **Salinsky, E. a. W., Scott.** 2003. Obesity in America: A Growing Threat. National Health Policy Forum. The George Washington University.

172. **Sardar, V. M., D. L. Bautista, D. J. Fischer, K. Yokoyama, N. Nusser, T. Virag, D. A. Wang, D. L. Baker, G. Tigyi, and A. L. Parrill.** 2002. Molecular basis for lysophosphatidic acid receptor antagonist selectivity. Biochim Biophys Acta **1582:**309-17.

173. **Sasagawa, T., M. Okita, J. Murakami, T. Kato, and A. Watanabe.** 1999. Abnormal serum lysophospholipids in multiple myeloma patients. Lipids **34:**17-21.

174. **Sasagawa, T., K. Suzuki, T. Shiota, T. Kondo, and M. Okita.** 1998. The significance of plasma lysophospholipids in patients with renal failure on hemodialysis. J Nutr Sci Vitaminol (Tokyo) **44:**809-18.

175. **Sawabu, N., H. Watanabe, Y. Yamaguchi, K. Ohtsubo, and Y. Motoo.** 2004. Serum tumor markers and molecular biological diagnosis in pancreatic cancer. Pancreas **28:**263-7.

176. **Schindler, A. E.** 1998. [Obesity and risk of cancer in the woman]. Zentralbl Gynakol **120:**235-40.

177. **Schlador, M. L., R. D. Grubbs, and N. M. Nathanson.** 2000. Multiple topological domains mediate subtype-specific internalization of the M2 muscarinic acetylcholine receptor. J Biol Chem **275:**23295-302.

178. **Schmidt, A., M. Wolde, C. Thiele, W. Fest, H. Kratzin, A. V. Podtelejnikov, W. Witke, W. B. Huttner, and H. D. Soling.** 1999. Endophilin I mediates synaptic vesicle formation by transfer of arachidonate to lysophosphatidic acid. Nature **401:**133-41.

179. **Sciorra, V. A., and A. J. Morris.** 2002. Roles for lipid phosphate phosphatases in regulation of cellular signaling. Biochim Biophys Acta **1582:**45-51.

180. **Seachrist, J. L., P. H. Anborgh, and S. S. Ferguson.** 2000. beta 2-adrenergic receptor internalization, endosomal sorting, and plasma membrane recycling are regulated by rab GTPases. J Biol Chem **275:**27221-8.

181. **Selvakumaran, M., H. K. Lin, T. Miyashita, H. G. Wang, S. Krajewski, J. C. Reed, B. Hoffman, and D. Liebermann.** 1994. Immediate early up-regulation of bax expression by p53 but not TGF beta 1: a paradigm for distinct apoptotic pathways. Oncogene **9:**1791-8.

182. **Shaw, P., R. Bovey, S. Tardy, R. Sahli, B. Sordat, and J. Costa.** 1992. Induction of apoptosis by wild-type p53 in a human colon tumor-derived cell line. Proc Natl Acad Sci U S A **89:**4495-9.

183. **She, Q. B., N. Chen, and Z. Dong.** 2000. ERKs and p38 kinase phosphorylate p53 protein at serine 15 in response to UV radiation. J Biol Chem **275:**20444-9.

184. **Shen, D. W., F. X. Real, A. B. DeLeo, L. J. Old, P. A. Marks, and R. A. Rifkind.** 1983. Protein p53 and inducer-mediated erythroleukemia cell commitment to terminal cell division. Proc Natl Acad Sci U S A **80:**5919-22.

185. **Shen, Z., J. Belinson, R. E. Morton, Y. Xu, and Y. Xu.** 1998. Phorbol 12-myristate 13-acetate stimulates lysophosphatidic acid secretion from ovarian and

cervical cancer cells but not from breast or leukemia cells. Gynecol Oncol **71:**364-8.

186. **Shenoy, S. K., P. H. McDonald, T. A. Kohout, and R. J. Lefkowitz.** 2001. Regulation of receptor fate by ubiquitination of activated beta 2-adrenergic receptor and beta-arrestin. Science **294:**1307-13.

187. **Shida, D., J. Kitayama, H. Yamaguchi, Y. Okaji, N. H. Tsuno, T. Watanabe, Y. Takuwa, and H. Nagawa.** 2003. Lysophosphatidic acid (LPA) enhances the metastatic potential of human colon carcinoma DLD1 cells through LPA1. Cancer Res **63:**1706-11.

188. **Shieh, S. Y., M. Ikeda, Y. Taya, and C. Prives.** 1997. DNA damage-induced phosphorylation of p53 alleviates inhibition by MDM2. Cell **91:**325-34.

189. **Shieh, S. Y., Y. Taya, and C. Prives.** 1999. DNA damage-inducible phosphorylation of p53 at N-terminal sites including a novel site, Ser20, requires tetramerization. Embo J **18:**1815-23.

190. **Siess, W., K. J. Zangl, M. Essler, M. Bauer, R. Brandl, C. Corrinth, R. Bittman, G. Tigyi, and M. Aepfelbacher.** 1999. Lysophosphatidic acid mediates the rapid activation of platelets and endothelial cells by mildly oxidized low density lipoprotein and accumulates in human atherosclerotic lesions. Proc Natl Acad Sci U S A **96:**6931-6.

191. **Slee, E. A., D. J. O'Connor, and X. Lu.** 2004. To die or not to die: how does p53 decide? Oncogene **23:**2809-18.

192. **So, J., J. Navari, F. Q. Wang, and D. A. Fishman.** 2004. Lysophosphatidic acid enhances epithelial ovarian carcinoma invasion through the increased expression of interleukin-8. Gynecol Oncol **95:**314-322.

193. **Spector, A. A.** 2003. Plaque rupture, lysophosphatidic acid, and thrombosis. Circulation **108:**641-3.

194. **Stam, J. C., F. Michiels, R. A. van der Kammen, W. H. Moolenaar, and J. G. Collard.** 1998. Invasion of T-lymphoma cells: cooperation between Rho family GTPases and lysophospholipid receptor signaling. Embo J **17:**4066-74.

195. **Stracke, M. L., T. Clair, and L. A. Liotta.** 1997. Autotaxin, tumor motility-stimulating exophosphodiesterase. Adv Enzyme Regul **37:**135-44.

196. **Stracke, M. L., H. C. Krutzsch, E. J. Unsworth, A. Arestad, V. Cioce, E. Schiffmann, and L. A. Liotta.** 1992. Identification, purification, and partial sequence analysis of autotaxin, a novel motility-stimulating protein. J Biol Chem **267:**2524-9.

197. **Sutphen, R., Y. Xu, G. D. Wilbanks, J. Fiorica, E. C. Grendys, Jr., J. P. LaPolla, H. Arango, M. S. Hoffman, M. Martino, K. Wakeley, D. Griffin, R. W. Blanco, A. B. Cantor, Y. J. Xiao, and J. P. Krischer.** 2004. Lysophospholipids are potential biomarkers of ovarian cancer. Cancer Epidemiol Biomarkers Prev **13:**1185-91.

198. **Symonds, H., L. Krall, L. Remington, M. Saenz-Robles, S. Lowe, T. Jacks, and T. Van Dyke.** 1994. p53-dependent apoptosis suppresses tumor growth and progression in vivo. Cell **78:**703-11.

199. **Tanyi, J. L., Y. Hasegawa, R. Lapushin, A. J. Morris, J. K. Wolf, A. Berchuck, K. Lu, D. I. Smith, K. Kalli, L. C. Hartmann, K. McCune, D. Fishman, R. Broaddus, K. W. Cheng, E. N. Atkinson, J. M. Yamal, R. C. Bast, E. A. Felix, R. A. Newman, and G. B. Mills.** 2003. Role of decreased levels of lipid phosphate phosphatase-1 in accumulation of lysophosphatidic acid in ovarian cancer. Clin Cancer Res **9:**3534-45.

200. **Tigyi, G., L. Hong, M. Yakubu, H. Parfenova, M. Shibata, and C. W. Leffler.** 1995. Lysophosphatidic acid alters cerebrovascular reactivity in piglets. Am J Physiol **268:**H2048-55.

201. **Tigyi, G., and R. Miledi.** 1992. Lysophosphatidates bound to serum albumin activate membrane currents in Xenopus oocytes and neurite retraction in PC12 pheochromocytoma cells. J Biol Chem **267:**21360-7.

202. **Tigyi, G., and A. L. Parrill.** 2003. Molecular mechanisms of lysophosphatidic acid action. Prog Lipid Res **42:**498-526.

203. **Tokumura, A., E. Majima, Y. Kariya, K. Tominaga, K. Kogure, K. Yasuda, and K. Fukuzawa.** 2002. Identification of human plasma lysophospholipase D, a lysophosphatidic acid-producing enzyme, as autotaxin, a multifunctional phosphodiesterase. J Biol Chem **277:**39436-42.

204. **Tsuga, H., K. Kameyama, T. Haga, T. Honma, J. Lameh, and W. Sadee.** 1998. Internalization and down-regulation of human muscarinic acetylcholine receptor m2 subtypes. Role of third intracellular m2 loop and G protein-coupled receptor kinase 2. J Biol Chem **273:**5323-30.

205. **Umezu-Goto, M., Y. Kishi, A. Taira, K. Hama, N. Dohmae, K. Takio, T. Yamori, G. B. Mills, K. Inoue, J. Aoki, and H. Arai.** 2002. Autotaxin has lysophospholipase D activity leading to tumor cell growth and motility by lysophosphatidic acid production. J Cell Biol **158:**227-33.

206. **Umezu-Goto, M., J. Tanyi, J. Lahad, S. Liu, S. Yu, R. Lapushin, Y. Hasegawa, Y. Lu, R. Trost, T. Bevers, E. Jonasch, K. Aldape, J. Liu, R. D.**

James, C. G. Ferguson, Y. Xu, G. D. Prestwich, and G. B. Mills. 2004. Lysophosphatidic acid production and action: validated targets in cancer? vol. 92.

207. **Valet, P., C. Pages, O. Jeanneton, D. Daviaud, P. Barbe, M. Record, J. S. Saulnier-Blache, and M. Lafontan.** 1998. Alpha2-adrenergic receptor-mediated release of lysophosphatidic acid by adipocytes. A paracrine signal for preadipocyte growth. J Clin Invest **101:**1431-8.

208. **van Corven, E. J., A. Groenink, K. Jalink, T. Eichholtz, and W. H. Moolenaar.** 1989. Lysophosphatidate-induced cell proliferation: identification and dissection of signaling pathways mediated by G proteins. Cell **59:**45-54.

209. **van Corven, E. J., P. L. Hordijk, R. H. Medema, J. L. Bos, and W. H. Moolenaar.** 1993. Pertussis toxin-sensitive activation of p21ras by G protein-coupled receptor agonists in fibroblasts. Proc Natl Acad Sci U S A **90:**1257-61.

210. **van Corven, E. J., A. van Rijswijk, K. Jalink, R. L. van der Bend, W. J. van Blitterswijk, and W. H. Moolenaar.** 1992. Mitogenic action of lysophosphatidic acid and phosphatidic acid on fibroblasts. Dependence on acyl-chain length and inhibition by suramin. Biochem J **281 (Pt 1):**163-9.

211. **van Koppen, C. J.** 2001. Multiple pathways for the dynamin-regulated internalization of muscarinic acetylcholine receptors. Biochem Soc Trans **29:**505-8.

212. **Vance, J. E., and D. E. Vance.** 1985. The role of phosphatidylcholine biosynthesis in the secretion of lipoproteins from hepatocytes. Can J Biochem Cell Biol **63:**870-81.

213. **Vogler, O., G. S. Bogatkewitsch, C. Wriske, P. Krummenerl, K. H. Jakobs, and C. J. van Koppen.** 1998. Receptor subtype-specific regulation of muscarinic acetylcholine receptor sequestration by dynamin. Distinct sequestration of m2 receptors. J Biol Chem **273:**12155-60.

214. **Vogler, O., B. Nolte, M. Voss, M. Schmidt, K. H. Jakobs, and C. J. van Koppen.** 1999. Regulation of muscarinic acetylcholine receptor sequestration and function by beta-arrestin. J Biol Chem **274:**12333-8.

215. **Volpicelli, L. A., J. J. Lah, and A. I. Levey.** 2001. Rab5-dependent trafficking of the m4 muscarinic acetylcholine receptor to the plasma membrane, early endosomes, and multivesicular bodies. J Biol Chem **276:**47590-8.

216. **Waggoner, D. W., J. Xu, I. Singh, R. Jasinska, Q. X. Zhang, and D. N. Brindley.** 1999. Structural organization of mammalian lipid phosphate phosphatases: implications for signal transduction. Biochim Biophys Acta **1439:**299-316.

217. **Wang, D. A., Z. Lorincz, D. L. Bautista, K. Liliom, G. Tigyi, and A. L. Parrill.** 2001. A single amino acid determines lysophospholipid specificity of the S1P1 (EDG1) and LPA1 (EDG2) phospholipid growth factor receptors. J Biol Chem **276:**49213-20.

218. **Weiner, J. A., and J. Chun.** 1999. Schwann cell survival mediated by the signaling phospholipid lysophosphatidic acid. Proc Natl Acad Sci U S A **96:**5233-8.

219. **Werbonat, Y., N. Kleutges, K. H. Jakobs, and C. J. van Koppen.** 2000. Essential role of dynamin in internalization of M2 muscarinic acetylcholine and angiotensin AT1A receptors. J Biol Chem **275:**21969-74.

220. **Whistler, J. L., J. Enquist, A. Marley, J. Fong, F. Gladher, P. Tsuruda, S. R. Murray, and M. Von Zastrow.** 2002. Modulation of postendocytic sorting of G protein-coupled receptors. Science **297:**615-20.

221. **Wu, X., J. H. Bayle, D. Olson, and A. J. Levine.** 1993. The p53-mdm-2 autoregulatory feedback loop. Genes Dev **7:**1126-32.

222. **Xie, Y., T. C. Gibbs, and K. E. Meier.** 2002. Lysophosphatidic acid as an autocrine and paracrine mediator. Biochim Biophys Acta **1582:**270-81.

223. **Xing, Z., J. Gauldie, G. Cox, H. Baumann, M. Jordana, X. F. Lei, and M. K. Achong.** 1998. IL-6 is an antiinflammatory cytokine required for controlling local or systemic acute inflammatory responses. J Clin Invest **101:**311-20.

224. **Xiong, Y., G. J. Hannon, H. Zhang, D. Casso, R. Kobayashi, and D. Beach.** 1993. p21 is a universal inhibitor of cyclin kinases. Nature **366:**701-4.

225. **Xu, J., Y. J. Lai, W. C. Lin, and F. T. Lin.** 2004. TRIP6 enhances lysophosphatidic acid-induced cell migration by interacting with the lysophosphatidic acid 2 receptor. J Biol Chem **279:**10459-68.

226. **Xu, Y., X. J. Fang, G. Casey, and G. B. Mills.** 1995. Lysophospholipids activate ovarian and breast cancer cells. Biochem J **309 (Pt 3):**933-40.

227. **Xu, Y., Z. Shen, D. W. Wiper, M. Wu, R. E. Morton, P. Elson, A. W. Kennedy, J. Belinson, M. Markman, and G. Casey.** 1998. Lysophosphatidic acid as a potential biomarker for ovarian and other gynecologic cancers. Jama **280:**719-23.

228. **Xu, Y., Y. J. Xiao, K. Zhu, L. M. Baudhuin, J. Lu, G. Hong, K. S. Kim, K. L. Cristina, L. Song, S. W. F, P. Elson, M. Markman, and J. Belinson.** 2003.

Unfolding the pathophysiological role of bioactive lysophospholipids. Curr Drug Targets Immune Endocr Metabol Disord **3:**23-32.

229. **Xu, Y. J., O. A. Aziz, P. Bhugra, A. S. Arneja, M. R. Mendis, and N. S. Dhalla.** 2003. Potential role of lysophosphatidic acid in hypertension and atherosclerosis. Can J Cardiol **19:**1525-36.

230. **Xu, Y. J., S. S. Rathi, D. C. Chapman, A. S. Arneja, and N. S. Dhalla.** 2003. Mechanisms of lysophosphatidic acid-induced DNA synthesis in vascular smooth muscle cells. J Cardiovasc Pharmacol **41:**381-7.

231. **Yaginuma, Y., and H. Westphal.** 1992. Abnormal structure and expression of the p53 gene in human ovarian carcinoma cell lines. Cancer Res **52:**4196-9.

232. **Yamada, T., K. Sato, M. Komachi, E. Malchinkhuu, M. Tobo, T. Kimura, A. Kuwabara, Y. Yanagita, T. Ikeya, Y. Tanahashi, T. Ogawa, S. Ohwada, Y. Morishita, H. Ohta, D. S. Im, K. Tamoto, H. Tomura, and F. Okajima.** 2004. Lysophosphatidic acid (LPA) in malignant ascites stimulates motility of human pancreatic cancer cells through LPA1. J Biol Chem **279:**6595-605.

233. **Yang, C. T., L. You, C. C. Yeh, J. W. Chang, F. Zhang, F. McCormick, and D. M. Jablons.** 2000. Adenovirus-mediated p14(ARF) gene transfer in human mesothelioma cells. J Natl Cancer Inst **92:**636-41.

234. **Yang, Y., L. Mou, N. Liu, and M. S. Tsao.** 1999. Autotaxin expression in non-small-cell lung cancer. Am J Respir Cell Mol Biol **21:**216-22.

236. **Zhang, C., D. L. Baker, S. Yasuda, N. Makarova, L. Balazs, L. R. Johnson, G. K. Marathe, T. M. McIntyre, Y. Xu, G. D. Prestwich, H. S. Byun, R. Bittman, and G. Tigyi.** 2004. Lysophosphatidic acid induces neointima formation through PPARgamma activation. J Exp Med **199:**763-74.

237. **Zhang, G., Z. Zhao, S. Xu, L. Ni, and X. Wang.** 1999. Expression of autotaxin mRNA in human hepatocellular carcinoma. Chin Med J (Engl) **112:**330-2.

238. **Zhang, Q., D. Cox, C. C. Tseng, J. G. Donaldson, and S. Greenberg.** 1998. A requirement for ARF6 in Fcgamma receptor-mediated phagocytosis in macrophages. J Biol Chem **273:**19977-81.

239. **Zhang, Y., and Y. Xiong.** 2001. A p53 amino-terminal nuclear export signal inhibited by DNA damage-induced phosphorylation. Science **292:**1910-5.

240. **Zuo, Z., N. M. Dean, and R. E. Honkanen.** 1998. Serine/threonine protein phosphatase type 5 acts upstream of p53 to regulate the induction of p21(WAF1/Cip1) and mediate growth arrest. J Biol Chem **273:**12250-8.